University of Notre Dame

2017 - 2018

Notre Dame Rocketry Team

Preliminary Design Report

NASA Student Launch 2018

Deployable Rover and Air Braking System Payloads

Submitted November 3, 2017

365 Fitzpatrick Hall of Engineering

Notre Dame, IN 46556

Table of Contents

List of Figures

List of Tables

1 Summary of PDR Report

1.1 Team Summary

Team Name: Notre Dame Rocketry Team

365 Fitzpatrick Hall of Engineering

Notre Dame, IN 46556

NAR Mentor: Dave Brunsting, NAR/TAR Level 2

dacsmema@gmail.com or (269) 838 - 4275

NAR/TRA Section: TRA #12340, Michiana Rocketry

1.2 Launch Vehicle Summary

The design of this rocket is significantly different than previous years. This year's design incorporates a transition from a larger diameter body tube to a smaller body tube. The forward section has a diameter of 7.5 in, which transitions over a 4 in section to a 5.5 in diameter tube. The larger diameter section is 20 in in length, and the overall length of the rocket is 124.5 in. This, along with the rocket's weight of 37.5 lbs without a motor, are two of the most important characteristics when it comes to evaluating the stability and projected apogee. The motors currently being considered are the Cesaroni L1685-SS and L1395-BS. Both of these motors met the minimum requirement for off-rail velocity, and give a desirable apogee of approximately 5400 ft.

The recovery system will ensure the reusability of the launch vehicle by safely recovering the vehicle through an automated two-stage parachute deployment procedure. The parachutes are

deployed using charges controlled by commercially available digital altimeters. The recovery system separates the vehicle into three sections, tethered with nylon shock cords.

1.3 Payload Summary

The deployable rover will contain an autonomously driven rover that is deployed via a ground station upon safe landing. The rover will detect the sections of the rocket and any other obstacles via a LiDAR sensor. The rover will drive at least five feet away from the rocket and deploy two sets of folded solar panels. The solar panels will be actuated via a servomotor. During the flight of the rocket, the rover will be secured to prevent any motion that could alter the flight path of the rocket.

The air braking system will use drag tabs to induce an additional, controllable drag force that will control the deceleration of the rocket and bring it to an apogee of 5280 ft. The tabs will be controlled using a servo-powered crank-slider mechanism and a control code.

2 Changes Made Since Proposal

2.1 Vehicle Criteria

There have been no significant changes to the launch vehicle since the Proposal. All materials researched for the main structure have remained the top choices for the final vehicle, and the motor choices have also remained the same. It is unlikely that the material selection for the rocket will change due to its strength and availability from vendors. However, it is possible that the motor choice could change depending on weight changes in the payload and recovery systems. In this case, the motor choice will be adapted so that a desirable apogee is attained.

2.2 Recovery Criteria

Since the Proposal was submitted, no major changes have been made to the Recovery Subsystem design. However, various design and material decisions have been finalized in the meantime. Most notably, the CRAM v4 will feature a screw-to-lock mechanism reminiscent of previous years, but with improved accessibility. Furthermore, the recovery bulkheads will be constructed from robust 0.25” acrylic instead of the deteriorating plywood used in the past.

2.3 Deployable Rover Criteria

Since the proposal the method of deploying the rover payload has been changed from compressed air to ejection charges. This was seen as a more reliable form of removing the nose cone. The team has history with using the proposed ejection charge system and will utilize those

past experiences in the design of this deployment system. The details of the ejection charge system is detailed in Section 5.1.4.

2.4 Air Braking System Criteria

Since proposal, the most significant change has been the selection of the mechanism design. It was decided that the crank-slider mechanism would be more effective than the rack and pinion mechanism. Other than this choice, the plan for the system has remained the same. PID control will still be used to control the servomotor, and both an accelerometer and barometer will be used to determine the flight path of the rocket. Additionally, the tabs will still extend directly outwards from the center of the rocket.

2.5 Project Plan

There have been minor changes to the project plan since the proposal. In terms of the development schedule, the subscale test flight has been changed from October 28 to November 19 due to the availability of launching with the Michiana Rocketry Team. One addition to our criteria for the project plan is the requirement to perform wind tunnel testing, which will occur during the week of November 6. Other than those, criteria has remained unchanged for the schedule. There have been no significant changes thus far in the budget and funding plan.

3 Vehicle Criteria

3.1 Selection, Design and Verification of Mission Success Criteria

3.1.1 Mission Statement

The team intends to design, construct, and launch a rocket to an altitude of exactly 5,280 ft above ground level with the aid of an air braking system, consisting of four drag tabs variably extended with changing altitude depending on flight conditions. The rocket will also carrying a rover that will deploy upon landing. As part of the flight plan, the vehicle will separate into 3 distinct sections and deploy both a drogue and main parachute for recovery purposes. The vehicle and its payloads must be reusable on the same day without need for repairs or modifications. The team also seeks to make an impact on the South Bend and Notre Dame communities through educational events and an active social media and local media presence.

3.1.2 Mission Success Criteria

Several conditions must be met for the mission to be considered a success. The following criteria are the team's main design drivers throughout this process and will be considered in all future design changes and verification methods.

The dominant criteria for a successful mission are:

1. *Altitude*: The vehicle must reach an apogee of as close to 5280 ft as possible. Success of this criterion will be determined based on readings from an altimeter onboard the rocket. A desirable altitude range is 5280 ± 100ft, or 5180-5380 ft.
2. *Stability*: The rocket must maintain an acceptable degree of stability for the duration of its flight. Stability is determined theoretically with OpenRocket and RockSim models.
3. *Structural Integrity*: The vehicle must remain intact for the duration of its flight. Each component of the rocket from the motor retention and the internal bulkheads to the drag tabs on the air braking system and the onboard rover must survive the flight without compromise.
4. *Recovery*: The vehicle must be reusable upon recovery without requiring repairs. Success in recoverability is predicted by the kinetic energy of each section upon landing based on simulation data. Recoverability of the rocket will be determined based on the condition of each component after the rocket lands.
5. *Rover Payload*: The rover payload must safely deploy from the internal structure of the launch vehicle when remotely triggered after landing, move 5 ft away from all rocket components, and deploy a set of foldable solar cell panels. Success of the rover payload is determined by GPS coordinates before and after movement and by the level of solar charge on the panels.
6. *Air Braking System*: The air braking system must successfully deploy its four drag tabs based on conditions of flight in order to slow the rocket to reach the goal apogee. Success of the air braking system will be determined based on the difference between the apogee of the rocket and the onboard computers logging servo motor actions.

3.1.3 System Level Design Review

3.1.3.1 Vehicle Description

The launch vehicle will have the capability of carrying two experimental payloads to an altitude of 5380 ± 100 ft. This exceeds the mission requirement of 5280 ft because one of the experimental payloads consists is an Air Braking System that is designed to reduce the rocket's apogee by up to 200 ft through the use of flat plates protruding from the body tube. The vehicle will separate into two tethered sections at apogee and one of those sections will separate into an additional two sections at an altitude of approximately 650 feet. The other aforementioned payload will be a Rover that will deploy from the nose cone section after landing. At this time, the launch vehicle will be propelled by a Cesaroni L1395 solid fuel motor.

3.1.3.2 Overview of Vehicle Design

The launch vehicle will incorporate a variable diameter main body tube in order to provide more room for the Rover Payload. The nose cone section will have a diameter of 7.5 in, which will taper down to 5.5 in for the rest of the body. These diameters were chosen because they provide ample room for the Rover Payload while still having body tube diameters that fit with commercially available nose cones. This eliminates the errors and risks of constructing a nose cone for diameters larger than 7.5 in. The launch vehicle will have total length of 124.5 in and an estimated weight of 799 oz with the motor and 646 oz without. A more detailed description of the dimensions can be found in Table 1.

Table 1. Vehicle Dimensions and Characteristics.

Property	Dimension
Length of Rocket (in)	124.5
Fore Diameter of Rocket (in)	7.5
Aft Diameter of Rocket (in)	5.5
Transition Length (in)	4
Number of Fins	4
Root Chord (in)	7
Tip Chord (in)	7
Sweep Angle (°)	31.6
Fin Height (in)	7.2
CG Position from Nose Cone (with motor) (in)	75.49
CP Position from Nose Cone (in)	98.5

Weight without Motor (lbs)	40.4
Weight with Motor (lbs)	49.9
Estimated Stability Margin without Motor	4.23
Estimated Stability Margin with Motor	3.07

The rocket will consist of 6 components: the Nose Cone, the Rover Payload Bay, the Transition Section, the Parachute Bay, the Air Braking System Bay, and the Fin Can. Each of these components are grouped into three separate sections that will we be tethered together by shock cords during descent. A more detailed description of the sections and components are given in Table 2 and is illustrated in Figure 1. The dimensions of the various components are then given in Table 3 and a 3D drawing can be found in Appendix C.

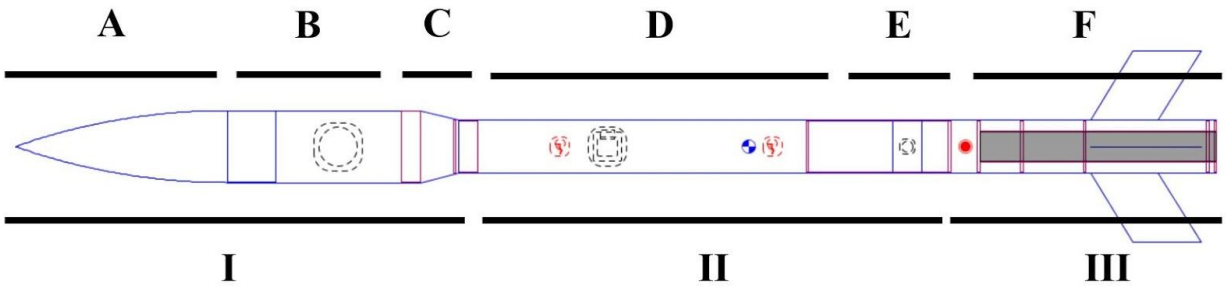

Figure 1. Vehicle Design Layout (Side View Shown).

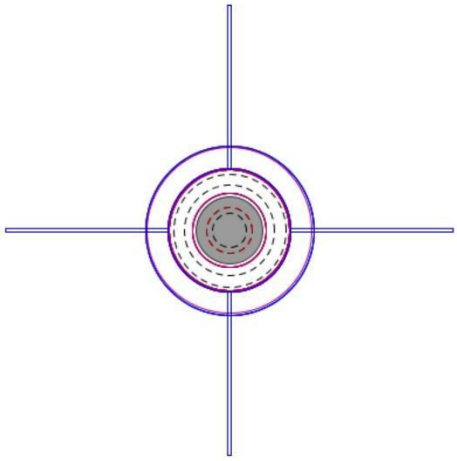

Figure 2. Vehicle Design Layout (Back View Shown).

Table 2. Vehicle Design Layout.

Section	Sub-Section	Label	Components	Description
I	Nose Cone	A	Hollow ogive shaped nose cone made of PVC	Connected to the rover payload bay (B) and measures 22 in - in length and 7.5 in - in diameter
	Rover Payload Bay	B	Fiberglass body tube	Contains rover payload and attaches to body tube transition coupler
	Transition Tube	C	Fiberglass transition	Transition piece and couplers measuring 4 in long to go from a 7.5 in diameter body tube to 5.5 in
II	Parachute Bay	D	Carbon Fiber Body Tube	Holds CRAM (Compact Removable Avionics Module), as well as a main and drogue parachute
III	Air Braking Payload Bay	E	Carbon fiber body tube and coupler	Secures 3 inch body tube piece to coupler connected to D and F, contains the air braking payload

	Fin Can and Motor Mount	F	Carbon fiber body tube and fins	Secures motor mount, motor, and fins to launch vehicle

Table 3. Dimensions of Various Components.

Component	Length (in)
Nose Cone	22 * (5 in shoulder)
Rover Payload Bay	20 *
Transition	4 * (2 in couplers)
Recovery Tube	45 *
Air Braking System Bay	3 *
Air Braking System Coupler	15
Fin Can	30.5 *
Motor Mount	24.5
Total *	124.5
* indicates the lengths that are measured for total length	

The launch vehicle is designed to reach an altitude of 5280 ft through the use of the Air Braking System. The system is designed to overshoot the altitude so that the system can deploy braking tabs after burnout to increase the drag forces acting on the rocket. The system and its effects will be discussed further in Section 5.2. The payload will be located just forward of the fin can and at the center of pressure after burnout. In the case where the Air Braking System is not verified by competition, the team will use additional ballast to maintain the design stability and bring the apogee down to 5280 ft.

The launch vehicle will also contain a Rover Payload located in the larger diameter body tube just aft of the nose cone. After a successful landing, the rover will be deployed from the nose cone and drive away from the rocket.

The recovery system of the rocket will consist of a drogue parachute that deploys at apogee and a main parachute to deploy approximately 650 ft to ensure a low kinetic energy at landing. Both the recovery system and the experimental payloads will be discussed in subsequent sections.

3.1.3.2.1 Design Selection: Nose Cone

For the full scale launch vehicle, a polypropylene nose cone will be used. The team has successfully used polypropylene nose cones for many years in the past. Polypropylene is lightweight and strong enough to withstand any forces during flight. The nose cone will be bought from Apogee Rockets. The outer diameter of the shoulder of the nose cone will be 7.5 in to match the inner diameter of the body tube section that houses the rover payload. Other materials were considered, as was building a nose cone. Carbon fiber and fiberglass nose cones were considered, but because the material properties of the nose cone does not have much influence on the rocket's ability to withstand forces during flight, the increased cost and lack of options made carbon fiber and fiberglass a poor choice. Building a nose cone was briefly considered, but offered no benefits to the team while dramatically increasing the likelihood of a manufacturing error. The nose cone bought from Apogee Rockets satisfies the team's criteria for a nose cone, namely that it is lightweight and reliable. Material properties of polypropylene will be discussed later in Section 3.1.4.3.

The shape of the nose cone is ogive. Ogive nose cones are easy to construct, which is why they are so common in hobby rocketry applications. Options for nose cones at the right diameter were limited, so no other shapes were considered. However, the team has used ogive nose cones in the past with success. The nose cone dimensions are shown below in Table 4.

Table 4. Dimensions of Nose Cone.

Characteristic	Dimension
Length (in)	22
Shoulder Length (in)	5
Weight (oz)	30.66
Outer Diameter (in)	7.675
Inner Diameter (in)	7.51

3.1.3.2.2 Design Selection: Airframe

The airframe of the launch vehicle will consist of both carbon fiber and fiberglass body tubes. Carbon fiber tubing was used the previous year and was shown to be a versatile material. Despite the cost and difficulties in manufacturing, carbon fiber is able to provide additional structural support compared to materials such as phenolic, while not sacrificing weight.

However, carbon fiber shields radio frequencies, and since the Rover Payload will need to communicate with a ground station after the flight, it cannot be contained in a carbon fiber tube. For this reason, the Rover Payload Bay and the Transition section (Section I) will be constructed out of fiberglass tubing to allow the transmission of signals to reach the rover without the need of an external antenna. The increased diameter was chosen so that there would be more space to fully develop a deployable rover, while the rest of the main body does not need the extra space.

The transition section of the body tube will consist of the tapered portion as well as two fiberglass couplers for the two different body tube diameters. This section is commercially available and will allow for a smooth reduction of 2 in of body tube diameter. In order to ensure that the Air Braking System would still be able to function properly, preliminary analysis of the flow field was conducted using ANSYS Fluent. Based on preliminary estimates for the maximum velocity (200 m/s) it was determined that even a transition from 8 in down to 5.5 in would not cause significant boundary layer growth or flow separation. This ensures that the Air Braking System tabs will be able to fully extend into the freestream flow path to increase the overall drag and will not extend into turbulent flow.

The integrity of the airframe will be verified ultimately by full scale testing. This test will involve the construction of the rocket that will be flown at the competition. However, prior to this, OpenRocket and RockSim will be used to estimate how the launch vehicle will perform for different configurations and flight conditions. These simulations will focus largely on the effects that ballast, airframe material finish, and locations of the center of pressure and center of mass have on the apogee of the rocket. After a full scale test launch, these prediction softwares can be verified and the team can see how well the carbon fiber and fiberglass airframe supported the rocket during flight. This will include looking for cracks or deformation of any of the components that can affect the structural integrity of or change the drag on the rocket.

Additionally, the team plans to utilize finite element method (FEM) analysis as well as additional computational fluid dynamics (CFD) tools to better understand the effects of forces on the rocket predicted by OpenRocket and RockSim during flight. ANSYS will be used to study components that are prone to failure as well as the integrity of the body tubes. These analyses have yet to start but are planned to be completed by CDR. The primary areas of concern are the airframe, bulkheads, and Air Braking System tabs.

3.1.3.2.3 Design Selection: Fins

In order to maintain flight in the vertical direction, a parallelogram fin shape was chosen because at low Reynolds numbers, it is highly effective in maximizing stability and minimizing drag - therefore it also maximizes apogee. Moreover, since all of the fins have the same airfoil shape, there is no drag caused by asymmetry in fin shapes. These fins provide the best stability of the launch vehicle at the speeds it will operate. Apart from the structural advantages of the

parallelogram shaped fin, such shape is easy and convenient to make, replicate, carry and assemble. The dimensions are shown in Figure 3 and Table 5.

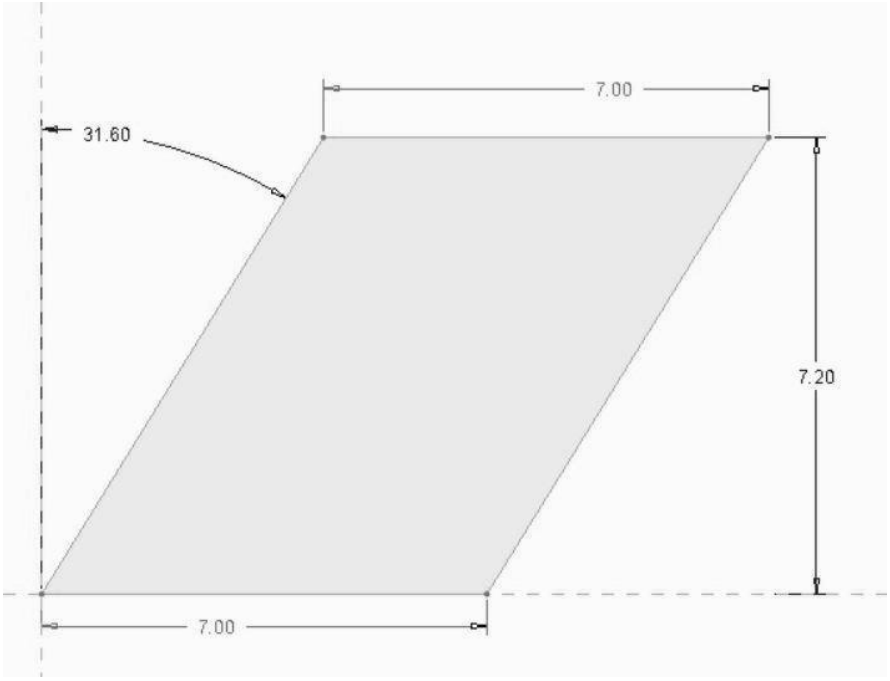

Figure 3. Swept fin dimensions.

Table 5. Fin Dimensions.

Property	Dimension
Number	4
Root Chord (in)	7
Tip Chord (in)	7
Thickness (in)	.125
Sweep Length (in)	4.4
Height (in)	7.2
Sweep Angle (deg)	31.6
Position Relative to end of vehicle (in)	6

In the past, plywood fins were used due to their low cost and their versatility for construction and attachment to the rocket. This year, like last year, carbon fiber fins will be used. Carbon fiber is a durable, lightweight material that maximizes structural robustness. Carbon fiber fins will aid in the rocket's ability to reach apogee. Both the fins and a significant portion of the lower half of the rocket will be composed of carbon fiber. This will aid in the integration process. The team considered constructing the fins in house using carbon fiber sheets and resin. However, the team realized that the purchase of solid carbon fiber plates will be more precise and more efficient. A summary of advantages and disadvantages is in Table 6.

Table 6. Advantages and Disadvantages of Fin Options.

	Advantages	**Disadvantages**
House Made Fins	- Less expensive - More experience in customizing fins	- May require more human resources than the team has at hand - May have variable mass - Precision not guaranteed
Purchased Fins	- Consistent mass - Guaranteed precision - Ease of structural analysis	-Must sand to achieve airfoil-like characteristics -More expensive

Though the more expensive route, the team has decided to purchase fins. The team will order large resin plates and order them to be cut to exact dimensions. The team must err on the side of caution with this mode of fin creation because once the exact dimensions are cut and shipped, they cannot be altered.

The fin strength will be verified by through FEM analysis as well as full scale tests. FEM analysis using ADINA is scheduled to begin the first week of November and the first full scale launch is scheduled for January 2018.

Fin alignment will be performed using the alignment mechanism used in years past. The mechanism consists of two circular plywood plates that are laser cut so the fin holes are exactly 90 degrees from one another. During construction, the plates are placed at each end of the fins for stabilization while the epoxy dries. The laser cutting process ensures perfect angles so that misalignment will be avoided. However, other options are being considered, and a decision on the alignment mechanism has not been finalized.

3.1.3.2.4 Design Selection: Couplers

In order for parachute and rover deployment to be successful, the rocket must at some point allow access to the individual bays. One option considered was access doors, but this would disturb the flow regime of the rocket, as well as limit the versatility of the rocket during flight. Instead, it was decided that couplers would be used to connect the individual bays of the rocket. This allows for weight reduction, as the longer body tube can be narrower than the rover tube if transitions and couplers are used. In addition, couplers allow for easy access to all parts of the rocket, and deployment of the parachute.

The transition section of the rocket from the rover tube to the body tube will be produced by the manufacturer with built-in couplers in order to minimize potential errors in fabrication, as well as reduce overall cost. These couplers will be made of fiberglass, as per recommendation of the manufacturer. There will also be an additional couplers connecting the body tube to the Air Braking Payload, as well as the engine mount.

Kraft Phenolic tubing and carbon fiber were both considered for construction of the couplers. Both are lightweight, and sturdy enough to withstand the stresses caused by normal operation. Carbon fiber was finally decided on, due to the fact that it is stronger and interfaces better with the rest of the rocket than Phenolic tubing. The couplers will be designed such that their outer diameter is as close as possible to the inner diameter of the body tubes. This will allow for a tight fit, and add to the overall stability of the rocket.

3.1.3.3 Materials

3.1.3.3.1 Full Scale

Material selection plays an important part in the design of the launch vehicle. Decisions on which material to use were made based on material properties, cost, and availability from vendors. All of the materials being used for the current launch vehicle have been used successfully in the past. Material will be bought commercially and, if necessary, cut utilizing Notre Dame facilities. Material properties for materials used are found below in Tables 7 and 8.

The nose cone of the launch vehicle will be made of polypropylene. Polypropylene is a rugged plastic used in many hobby rockets. The nose cone will be bought from Apogee Components at a set diameter in order to fit the inner diameter of the top section of the body tube. Other options for the nose cone were considered, namely fiberglass, but options were limited based on availability of professionally made nosecones. The team also explored building a nosecone, but decided against it as it offered little to no benefits over readily available polypropylene nosecones. Polypropylene is lightweight and structurally sound, but is inferior to both carbon fiber and fiberglass in terms of material properties. Given the lack of importance of the nosecone material in terms of material strength, polypropylene was chosen due to ease of availability and cost.

For the body of the launch vehicle, two materials are being used. These are carbon fiber and fiberglass, both of which have been used in the past by the Notre Dame Rocket Team. Some other options were considered, namely phenolic and Blue Tube 2.0. Phenolic had been used for a majority of the launch vehicle for many years and hard performed well. However, given that it has inferior material properties to all three other materials mentioned and vendors are readily available to cut custom pieces, phenolic is no longer being used for the launch vehicle in any capacity. As discussed later in the section, phenolic will be used heavily in the sub scale launch vehicle, where materials are of little importance due to its cheap cost and ease of use.

Blue Tube 2.0 was also considered for much of the body. Blue Tube 2.0 has material properties that are superior to phenolic, but in general inferior to carbon fiber and fiberglass. Blue Tube 2.0 is denser than phenolic, yet lighter than fiberglass. It is also cheaper than both carbon fiber and fiberglass, though more expensive than phenolic. Given that Blue Tube 2.0 was overall weaker than carbon fiber and fiberglass, and less cost effective than phenolic, the team decided against using Blue Tube 2.0 and opted for carbon fiber and fiberglass for different components of the launch vehicle body.

Both fiberglass and carbon have excellent material properties for a launch vehicle, given that they are incredibly lightweight and structurally strong. They both offer dramatic improvements over phenolic and Blue Tube. The disadvantages of these materials are the high cost and the difficulty associated with construction. Last year, the team had the vendors cut the materials to size for the body tubes. The carbon fiber fins were cut on Notre Dame's campus by the AME Machine Shop in Cushing Hall, run by Leon Hochtla. The fins were sanded by the team following proper safety protocol. Due to the sponsorship the team acquired, the high cost was worth the benefits that carbon fiber and fiberglass provide. For this reason, both materials will be used again as they provide superior material properties to phenolic and Blue Tube at a cost that the team can afford.

Carbon fiber will be used for sections of the thinner section of the body tube, the fins, and couplers. Fiberglass will be used for the top section of the body tube, bulkheads, centering rings, and the transition section of the body tube.

The bulkheads and centering rings are made from fiberglass not only for their material properties, but because they can be cut by the team using a CNC router to the desired shape. The team has had success with this method in the past. Strength of the bulkheads is critical as bulkheads have previously been a point of failure for the team when made of plywood. The upper section of the body tube is made of fiberglass rather than carbon fiber despite the lighter weight of carbon fiber primarily because of the need of the Deployable Rover Payload to have wireless communication through the walls of the body tube. Carbon fiber fins have been used in the past with success, and the team has experience working with them. The lower section of the body tube is also carbon fiber, which is the same as last year's launch vehicle. Carbon fiber is also going to be used for the motor mount. It is capable of handling the high temperatures that it will be exposed to during motor burn.

The materials used for the full scale prioritize quality over cost effectiveness and ease of construction.

3.1.3.3.2 Sub-Scale

The sub scale launch vehicle focuses less on building the optimal design and more on building a cost effective and easy to construct design that still represents that full scale launch vehicle adequately. For this reason, the materials being used to construct the full scale will not be used in the sub scale with the exception of a polypropylene nosecone. Instead, like previous years, the sub scale will be constructed using phenolic and birch plywood. The body tube, couplers, transition section, and motor mount will all be made of phenolic. The centering rings, bulkheads, and fins will be made of birch plywood. The fins for the air braking payload will be 3-D printed by the team. The material used has been used by the team in the past, and has provided sufficient strength during flight. The reason for 3-D printing is that it allows the fin shape to be more precise as opposed to working with plywood and laser cutters. Overall, the materials used in the subscale were chosen because they are easy to work with and are inexpensive, while still representing the full scale model accurately.

Table 7. Material Properties of Considered Materials.

Material	Component Use	Density (lb/in^3)	Tensile Strength (ksi)	Tensile Modulus (msi)	Shear Modulus (msi)	Com-pressive Strength (ksi)	Com-pressive Modulus (msi)	Specific Weight (lb/in^3)
Carbon Fiber	Body Tube, Fins	0.0578	300-350	15-30	0.6-.0725	82-120	18.5	0.065
Fiberglass	Body Tube, Bulkheads, Centering Rings	0.055	250-300	0.8-1.4	4.351	140-350		0.063
Phenolic Paper	Body Tube		12-15			32		0.049

Table 8. Material Properties for Polypropylene Plastic.

Property	Dimension
Density (lb/in^3)	0.0342
Tensile Strength (psi)	5800
Compressive Strength (psi)	5800
Young's Modulus (msi)	217-290

3.1.3.4 Integration

3.1.3.4.1 Deployable Rover Payload

The proper integration of the rover payload into the vehicle is essential for both the flight of the rocket, and the deployment of the rover. The rover must be able to fit inside of the vehicle's rover tube, which has an overall length of 20 in and an internal diameter of 7.515 in. The rover is not expected to be the exact length or width of the rover tube, and must be secured to prevent movement during flight. This prevention of motion is essential so as not to affect the flight pattern of the rocket, or to damage the rover itself. In order to do this, a track system will be installed into the entire length of the rover tube of the vehicle (20 in). This system will provide a platform on which the rover wheels will rest, and small vertical pieces that will stabilize the wheels from moving horizontally. It was determined that making the supports out of aluminum would be best. The rail system will also include a set of triangular supports, made out of aluminum, which will function as the connection between the tracks and the body of the rocket. These supports will be adhered using RocketPoxy, as it provides a high-strength bond when joining fiberglass and carbon fiber. A diagram of this system is shown in Figure 4. During flight, the rover will be housed directly in between the nose cone and the transition piece to the rest of the body. Once the rocket lands, the rover will exit through the nose cone. The nose cone will be removed using black powder charges. It is also important that the rover be designed and housed in such a way that it can exit the rocket no matter the orientation it lands. For this reason, the rover will be designed with large wheels so that it can potentially drive in an inverted orientation. The rover will be able to drive out of the rover tube on the rails of the pin and rail system which will secure the rover. This feature, along with the oversized rover wheels will ensure that the rover can exit the rocket.

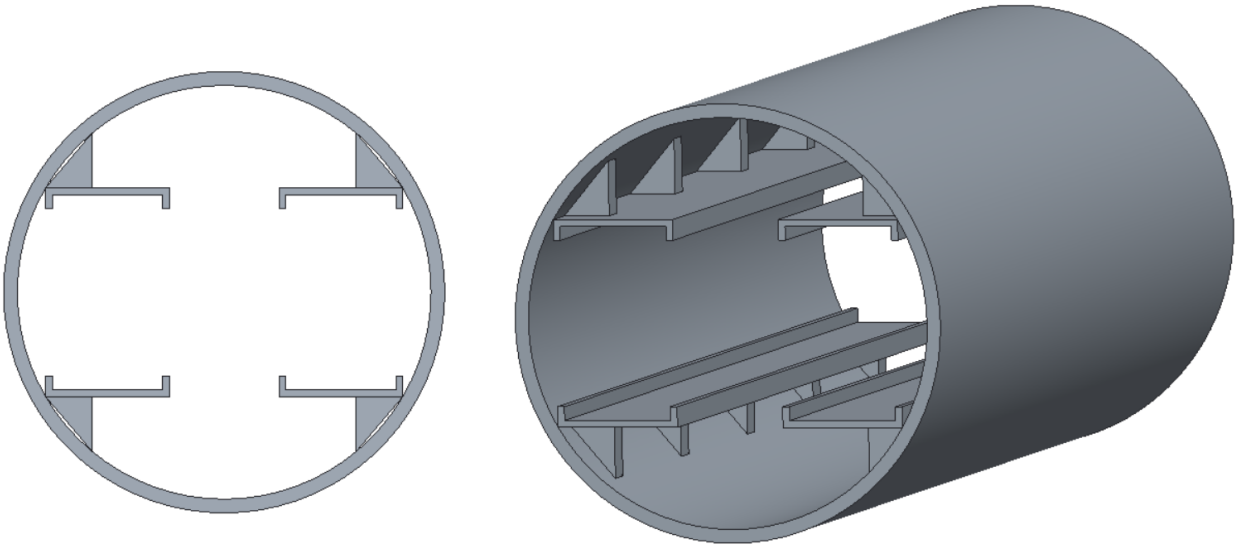

Figure 4. Track system design concept for rover payload interface with rocket body.

3.1.3.4.2 Air Braking System

The air braking system will be contained in a 15 in long coupler located just fore of the fin can section. The actual air braking tabs will protrude from a 3 in section of body tube connected 3 in above the aft end of the coupler. These are located close to the post burnout location of the center of pressure to ensure that the moment arms created by the additional aerodynamic forces are smaller and their effects will not induce any spikes in airframe stresses or instabilities.

In order to properly secure the coupler to the rest of the launch vehicle, a series of four steel rods will protrude from the motor mount bulkhead in the fin can and pass all the way through the Air Braking System coupler. The coupler will be capped by two fiberglass bulkheads. The aft bulkhead will have nuts epoxied to the rods so that coupler will not be able to slide into the fin can and induce higher stresses on the payload components. The fore bulkhead will have a series of locknuts attached to the rods to secure the contents of the payload in the coupler. The components that make up the system will be discussed in more detail in Section 5.2. This type of system was used in previous years and has proven to be successful. It gives the team access to the components in the coupler while securing the payload into the entire launch vehicle. Additionally, the fore bulkhead will be connected to an eyebolt with a shock cord connected to the main parachute. The fore section of the coupler will also incorporate shear pin holes that will keep the parachute body tube and fin can secured until main deployment.

3.1.3.4.3 Recovery System

The recovery payload will be located in the recovery section (section 2) of the rocket. Couplers will connect the recovery section to sections 1 and 3 of the rocket. Shear pins will hold the sections together until the ignition of ejection charges in the avionics module causes the desired sections to separate for deployment of the drogue or main parachute. The recovery section will house the drogue and main parachutes in addition to the Compact Removable Avionics Module (CRAM). The CRAM will be located in the middle of the section with the drogue parachute on one side and the main parachute on the other. Both parachutes will be attached via shock cord to a 1500lb-rated eye bolt on either side of the CRAM. The quick links connecting the shock cords to the parachutes are rated for 2000lb. These specifications have been used successfully in past years. The CRAM itself will attach to the rocket by screwing into a 3D printed coupling inside of the recovery section of the rocket. Additionally, the CRAM will be held in place via a screw perpendicular to the rocket body so as to prevent spinning and/or detachment of the CRAM from the airframe. The Recovery System is discussed more in Section 3.3.

3.1.3.4.4 Motor

The integration of the propulsion system is crucial for the success of the launch. The current motors being considered are both Cesaroni motors with 2.95 in (75 mm) diameters. While the two motors vary in length, one length will have to be chosen before CDR so that a motor casing can be purchased. Cesaroni sells custom motor casings with outer diameters of 2.965 in and varying lengths. For safety and consistency of design, a Cesaroni motor casing will be used.

The motor and its casing must be perfectly centered inside the main body tube so as to not add any pitching moments during flight. Slight misalignment either before or during flight could lead to a gimbaled thrust system during burnout, which describes the phenomena where an uneven motor can cause a torque about the rocket's center of gravity. This requires very careful motor mount construction and measurements.

Multiple motor mount system options were considered to ensure the centering of the motor. A few options included "legs," or bracing beams, moving either straight out from the motor outward to the body tube or creating a star pattern of triangles around the motor. While these options would require less material, their complexity eventually led to the decision of using a more traditional motor mount system. Ultimately, based on past years of success, it was decided that the chosen motor and motor casing would be held in place by a carbon fiber 3 in inner diameter and 3.125 in outer diameter body tube surrounded by a set of centering rings and bulkheads. The motor mount system will be attached to the rocket's final body tube (furthest aft) so as to leave the most possible room in the rocket for the other payloads. As has been described in other portions of this report, this body tube (also known as the fin can), will also be made of

carbon fiber due to the structural integrity of this material and the importance of this portion of the launch vehicle. The centering rings will be placed strategically along the inner carbon fiber ring to not interfere with the fins being inserted into the main fin can body tube around the same region and the foremost region of the aircraft being capped with a bulkhead to separate the fin can/motor mount from the rest of the launch vehicle. This capping prevents the motor from flying through the center of the rocket. To reserve weight but keep the strong structure of the motor mount, the centering rings and bulkheads will all be made of 0.25 in thick fiberglass. The centering rings will have inner and outer diameters of 3.126 in and 5.394 in respectively, while the bulkheads will simply have an outer diameter of 5.394 in. These dimensions were chosen to properly fit the motor mount inner body tube and the main fin can body tube. The last centering ring will be a mere 0.5 in from the aft end of the motor mount to account for the positive motor retention system, which will be described further in Section 3.1.3.6.2. Both the centering rings and bulkheads will be attached to the motor mount and fin can body tube using JB Weld epoxy that will keep all the components in place during flight. JB Weld is used rather than regular epoxy because it is better equipped to handle the intense heat generated from burnout.

3.1.3.5 Launch Pad and Rail

The launch pad will consist of a 12 ft long 1.5 in wide launch rail and platform provided by NASA for the competition. This will allow the rocket to attain an off rail velocity of 77.3 ft per second using the Cesaroni L1395-BS. The body tube will be attached to the rail by 1.25 in rail buttons, which will be located on the fin can of the rocket. Since a variable diameter is used, the rail buttons will have to protrude enough so that the rail is not in contact with the larger section at the nose cone.

The rail buttons will be located 45 degrees offside the fins and will be secured to the body tube with screws driven into wooden blocks on the inside of the body tube. In order to achieve the additional 1 in needed for the variable diameter, the current idea is to attach small wooden blocks to the outside of the body tube as well and sand them down to reduce any effects on drag. One rail button will be positioned 1 inch away from the aft end of the fin can, and the other will be placed 26 in away from the aft end. Since the Air Braking System is not activated until after burnout, the drag tabs are still inside of the body and are not at risk of deploying into contact with the launch rail.

3.1.3.6 Propulsion

3.1.3.6.1 Motor Choices and Description

The height of apogee of the launch vehicle will primarily be determined by motor selection. To make this selection, a number of motor configurations were simulated on a preliminary model of the launch vehicle created in the simulation software OpenRocket. This

initial motor selection process focused mainly on estimated apogee. To estimate the altitude at apogee, OpenRocket takes into account many parameters, including the vehicle shape, material finish, and weight. For this initial design, liberal weights were chosen for the various rocket components that will be updated as the vehicle design is finalized, specifically the weights of the air braking system and the rover payload. Due to the presence of the air braking system, motors were selected with an estimated apogee range between 5400 and 5600 ft with the expectation that the air braking payload will be used to decrease the apogee altitude ultimately achieved by the rocket.

After many simulations with a number of Cesaroni, Loki Research, and Aerotech motors, the two motors selected for the current configuration are the Cesaroni L1685-SS and the Cesaroni L1395-BS. Both motors have off-rail velocities greater than 52 ft/s, and do not cause the launch vehicle to exceed Mach 1. Both of these conditions satisfy the Student Launch constraints. Table 9 shows the individual characteristics of the two motors.

Table 9. Motor Characteristics for Cesaroni L1685-SS and Cesaroni L1395-BS.

Motor Classification	Cesaroni L1685-SS	Cesaroni L1395-BS
Diameter (in)	2.95	2.95
Length (in)	29.80	24.45
Total Weight (lb)	13.34	9.53
Propellant Weight (lb)	8.32	5.21
Average Thrust (lbf)	379.0	313.8
Max Thrust (lbf)	577.7	400.1
Total Impulse (lbf*s)	1139.6	1100.5
Burn Time (s)	3.01	3.51
Thrust to Weight Ratio	11.57	8.10

Figures 5 and 6 show thrust curves for both motors.

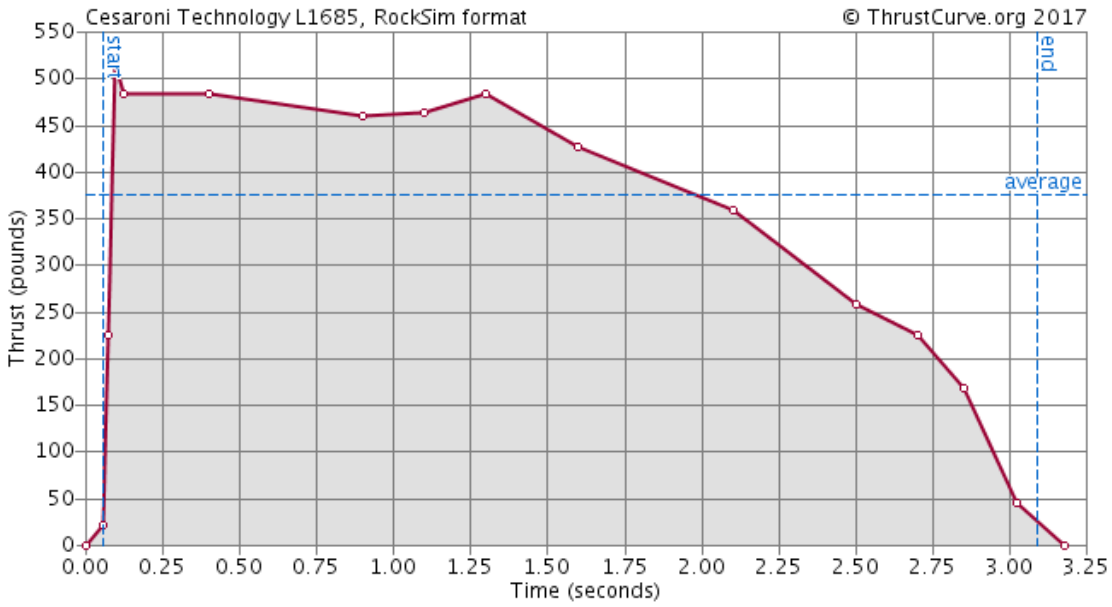

Figure 5. Thrust curve for Cesaroni L1685-SS.

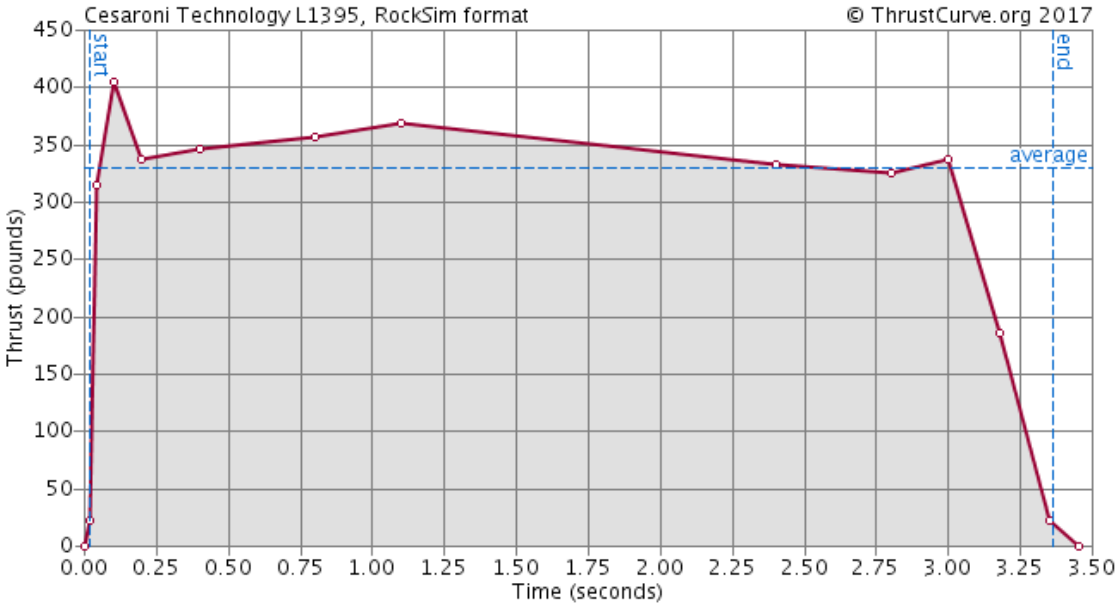

Figure 6. Thrust curve for Cesaroni L1395-BS.

As previously described, simulations were run in OpenRocket in order to predict performances from the two motors. These simulations were done using 5 mph winds with a standard deviation of 0.5 mph and a rail length of 12 ft. The results are seen in Table 10. As shown, the results are almost identical, with the Cesaroni L1685-SS traveling slightly higher, while coming off the rail at a slightly lower velocity. In addition, both motors were predicted to take the vehicle higher than the target altitude, to apogees around 5400 ft. This accounts for the

ability of the Air Braking System to slow the vehicle mid-flight, thus resulting in an altitude closer to 5280 ft. It was also noted in this selection that the flight ceiling for the competition is at 5600 ft. Initial verification of these results was already done by comparing the thrust curves shown above with those found in OpenRocket. As expected, the thrust curves were nearly identical. Live motor performance will be verified by comparing data from these simulations with that from full-scale test launches. Necessary adjustments will be made based upon results of the test launches. Motors will be launched multiple times to ensure reliability.

Table 10. OpenRocket Simulation Results for Cesaroni L1685-SS and Cesaroni L1395-BS.

Motor Classification	Cesaroni L1685-SS	Cesaroni L1395-BS
Altitude (ft)	5421	5406
Off Rail Velocity (ft/s)	74.8	68.4
Max Velocity (ft/s)	612	612
Flight Time (s)	189	190
Time to Apogee (s)	18.8	19

Based on *wildmanrocketry.com*, the CTI L1685-SS would cost $299.95, while the CTI L1395-BS would cost $246.95. As was stated in the motor integration section, 3.1.4.4.4, the use of CTI motors will require the team to also purchase a new motor casing. The CTI L1685-SS requires a 5-Grain 75 mm casing, while the CTI L1395-BS requires a 4-Grain 75 mm casing. Once again based on pricing from wildmanrocketry.com, a casing and corresponding closure set will together cost $309.95 for the 4-Grain casing and $359.95 for the 5-Grain casing. The team does own a motor casing that would fit a Loki 2.95” diameter motor, which would greatly decrease costs. However, the team has been unable to find a suitable Loki motor for the initial design weight and size that will meet the team’s altitude requirements without passing the 5600 ft flight ceiling. Given this information, the current primary motor selection is the CTI L1395-BS as it provides similar flight characteristics to the CTI L1685-SS, but requires a cheaper casing and is cheaper overall. If the Air Braking System works properly, the specifics of the propulsion system will not need to be as exact as a simpler launch vehicle without a system controlling the apogee.

3.1.3.6.2 Motor Retention

As described in Section 3.1.3.6, the propulsion system will be held in place by the motor mount, which will be located within the fin can. The main goal of the motor mount is to keep the motor and motor casing aligned with the launch vehicle and prevent pitching moments/gimbaled thrust, which could lead to destabilizing flight. While the motor mount controls alignment with the central axis of the body tube, an additional motor retention system is necessary to keep the motor inside the launch vehicle during flight. A typical motor retention system consists of both a burnout retention system and a descending retention system. The former protects the motor from shooting up through the rocket due to the thrust produced during burnout, while the latter keeps the motor from falling out the rocket during the remaining duration of flight after burnout.

As described previously in Section 3.1.3.3, a 0.25" thick fiberglass bulkhead will cap the motor mount to create the burnout retention system. This will be attached to the motor mount tube and the fin can using JB Weld Epoxy.

The other half of the motor retention system allows for more freedom in the design selection. The team has considered many options including handmade systems and commercially available kits. One simple design used in past years consists of two washers offset by 180° and attached to two screws protruding from the aft-most centering ring of the motor mount. The washers were tightened to the screws using nuts and the screws were held in place on the centering ring using JB Weld epoxy. While this system was cheap, the risks are high. The heat and thrust force from burnout could deform the washers or loosen the nuts holding them in place, causing them to be unable to support the motor. This past design is shown in Figure 7.

Figure 7. Screw and Washer Motor Retention.

Another option is to use either a glue on or a bolt on quick-change motor retainer that is commercially available. These retainers are available online from LOC Precision Rocketry and

Aero Pack Incorporated for 75 mm or 3 in diameter rocket motors. They cost around $45 and are made out of lightweight aluminum (6061-T6 aluminum). The glue on version includes an adaptor that is epoxied to the aft end of the motor mount and a cap that is then screwed onto the secured adaptor. The assembly of this type of motor retention is shown in Figure 8, taken from Aero Pack's website.

Figure 8. Glue on Bolt Motor Retainer.

A slightly more expensive version of the quick change motor retainer is the bolt on version that is shown in Figure 9, also taken from Aero Pack's website. These cost around $50 and are available from the same retailers as the glue on motor retainers. Instead of epoxying an adaptor, these retainers include an aluminum cap that is bolted into the aft most centering ring of the rocket. The quick-change motor retainer offers a more expensive way of securing the motor in the launch vehicle. The glue on version requires a new adaptor for each vehicle and relies on the use of JB Weld epoxy to be attached, while the bolt on version can be used for multiple rockets. It does, however, leave more room for manufacturing error. As seen in Figure 9, it is necessary to get all of the holes made in the correct location for the system to be installed properly, but unlike the team's old design, allows for failure in one or two screws without compromising the entire system.

Figure 9. Bolt-On Motor Retention with Cap.

A more middle of the road option is to use a clamp system for motor retention instead of a washer system. The principle is the same, to drive two screws offset by 180 degrees into the aft most centering ring, however, instead of using washers, the system uses two stainless steel clamps to hold the motor in place as shown in Figure 10 taken from Giant Leap Rocketry's website. This set is available online from Giant Leap Rocketry for around $10. This design is cheaper than the quick-change motor retainers and secures the motor more effectively than the washers.

Figure 10. Clamp-On Motor Retention.

Despite the pros and cons of all the designs considered, the leading design is the glue on bolt design shown in Figure 8. It is the simpler design of the two quick change retainer options for construction and the easiest of all designs for use on launch days. While the Clamp-On system would be a cheaper design, this system would be harder to align and to ensure tightness

when preparing the motor for launch. While the team is confident that the simplicity and robustness of this system will lead to success in the launch vehicle, the effectiveness of the system will be further verified through materials analysis and successful test flights.

3.1.3.7 Mass Statement

Mass is one of the primary driving factors of apogee and performance, and is therefore important to track in the design of the launch vehicle. For this reason, Table 11 shows the weight of each component of the vehicle.

Table 11. Weight of Various Rocket Components.

Component	Mass (oz)
Nose Cone	30.7
Rover Payload Bay	
Rover Tube	39.3
Transition Tube and Coupler	13.7
Payload Equipment	130
Bulkhead	6.33
Parachute Bay	
Parachute Bay Body Tube	62.1
Main Parachute	53.7
Drogue Parachute	18
CRAM	54
Air Braking Payload Bay	
Bulkheads (2)	11.28
Payload Equipment	110
Payload Coupler	110

Fin Can	
Fin Can Body Tube	42.1
Motor Mount Tube	5.11
Bulkhead	6
Centering Rings (3)	11.1
Motor	153
Fins (4)	25.4
Motor Retainer	3.4
Total	799

The above estimates are based on past experience with certain materials, as well as with manufacturers' specifications. The OpenRocket simulation of the rocket has the center of gravity at 75.49 in aft of the tip of the nose cone. Based on rockets in previous years, the mass of the rocket is not expected to increase more than 20% over the course of the design phase. Data from earlier rocket designs has allowed this is improvement over the 25% to 30% increase which is normally projected. While the weight of the rocket does affect motor choice, the mass would have to increase by around 5% before another motor would be considered.

If necessary, ballast can be added to move the center of gravity in order to increase stability and if the Air Braking System cannot be verified by competition, ballast can be added to decrease apogee to meet the mission requirement of 5280 ft. The ballast will be in the form of sand measured to an appropriate mass and will be contained in a bag within its own coupler in the body tube. This coupler would be capped by two bulkheads clamped together and screwed into the main body tube to ensure it does not shift during flight.

3.1.3.8 Risk Mitigation

The team understands engineering projects often run into problems such as scarcity of time, budget, resources, etc. The team uses the following mitigation techniques to ensure that the project is not derailed.

Table 12. Risks and Mitigations.

Risk	Likelihood/Impact	Mitigation Technique
Budget	Low likelihood/Low Impact	The Vehicles Sub-team has developed a budget within whose bounds it always tried to stay. There is material left over from previous years. This material is used to perform tests or to test out ideas, particularly in form of payload integration. The budget for the Vehicles Sub-team is shown in Appendix O. The team estimates that the budget can only go down because it shot high to start choosing expensive material (such as Carbon Fiber and Fiberglass) that may not end up being needed. This covers the oversights. The only foreseeable budget problems lie in integration material, such as screws and nuts, but these items are not overly costly and the University workshops keep them.
Time	High Likelihood/Medium Impact	The Vehicles Sub-team is organized in such a way as to help members stay on top of their work while not being affected by those who may be behind. Members own certain sections and work on these throughout the design and construction process. For example, the owner of Roll Control Payload integration works with the Vehicles Lead and the Roll Control Sub-team to design the structural aspect of the payload. During construction time, he leads the integration. All members are aware of launch dates and deadlines and work with an internal deadline of 1 week before the NASA SL or launch deadline. In cases of testing, scheduling is done in the month of November for December test dates, results of which are included in the CDR.
Resources	Low Likelihood/High Impact	It is unlikely that the team runs out of physical resources, as plans will be made for any needed resources and they will be ordered before they are required, but using up all available resources and not planning will slow the project. Material for construction of full scale is ordered in December for January launches so that any missed material can be ordered in time. In terms of human resources, the Vehicles Sub-team has a member who “owns” a sub-

		system, but there is usually a secondary person who is somewhat familiar with the sub-system and who can take over should the primary owner not be available.
Functionality	Medium Likelihood/High Impact	Functionality of the rocket is a top priority for the team. Testing, computer models, and subscale models will help the team determine what steps need to be taken to ensure the final product meets project goals. The Sub-team emphasizes the need for robust verification methods to ensure that what has been designed meets the requirements. Functionality goes hand in hand with time, because whatever doesn't work as intended must go through a redesign process. Resources also play a role because resources must be moved around so that certain functionalities can be perfected. Functionalities that directly affect flight are prioritized.
Safety	Low Likelihood/High Impact	Dangerous materials (rocket motors and carbon fiber) and tools will be used to construct the rocket. Ensuring safety through proper protective equipment and communication with the team's safety officer will mitigate risk to team members. The motors are handled by the mentor; therefore, this is not a concern. The Carbon fiber may be a bit tricky since the team has not used it before to this scale, but workshops exist on campus with construction experts that are willing to help the team with ventilation.

3.1.4 Mission Performance Prediction

3.1.4.1 PPF: Performance Prediction Program

In previous years, the team has depended on commercially available predictive software to estimate the performance of the launch vehicle. This year, the team is developing several ways to verify this software, including a program in python that will estimate the rocket's performance based on physical equations for the vehicle.

This program accepts inputs such as the mass of the rocket, mass of engine, mass of propellant, coefficients of drag, thrust, burnout motor time, etc. The masses are important because the altitudes will partially depend on this. The mass of the rocket changes during flight because the propellant disappears.

The coefficients of drag are important. This is because the launch vehicle will go through several flight phases. While the motor is burning, the velocity will be increasing and thus the drag will increase; therefore, the team needs a reliable coefficient of drag at different points of velocity. After burnout, the launch vehicle coasts for a little bit, before air breaks will be deployed. These will be able to be modeled in the performance prediction program after wind tunnel tests.

There are three distinct rocket phases: the thrust phase, the air breaking phase, and the coast phase. OpenRocket does not allow us to deploy air breaks in the middle of a simulation and this is the most important reasoning for the necessity of an independent program. However, the team can still use OpenRocket to guide the design of the program. Which of these simulations is proven to be superior can only be found out after the full scale launch. The MATLAB code used for the model can be found in Appendix B.

3.1.4.2 OpenRocket and RockSim Simulations

Both OpenRocket and RockSim were used in order to predict the vehicle's flight. These two simulation programs are being used to cross reference with flight data in order to verify their accuracy in predicting apogee, velocity, and acceleration. The software is also being used to verify the accuracy of the Performance Prediction Program to provide additional redundancy in performance prediction. After the sub-scale launch, OpenRocket and RockSim simulations will be run for the weather conditions at the launch site and their results will be compared with the flight data. The results will then be applied to full scale simulations to determine uncertainties in both programs.

3.1.4.2.1 OpenRocket Predictions

Table 13. OpenRocket Predictions with Cesaroni L1395 Motor.

Wind Speed	0 mph	5 mph	10 mph	15 mph	20 mph
Apogee (ft)	5419	5355	5187	5121	5158
Max Velocity (ft/s)	612	611	608	605	601
Max Acceleration (ft/s^2)	227	227	227	227	227
Flight Time (s)	187	189	185	186	186
Time to Apogee (s)	19.1	19	18.6	18.5	18.6

CG Location from nose (in)	75.49	75.49	75.49	75.49	75.49
CP Location from nose (in)	98.529	98.529	98.529	98.529	98.529
Stability Margin with motor	3.07	3.07	3.07	3.07	3.07

Table 14. OpenRocket Predictions with Cesaroni L1685 Motor

Wind Speed	0 mph	5 mph	10 mph	15 mph	20 mph
Apogee (ft)	5432	5383	5283	5163	5125
Max Velocity (ft/s)	612	611	609	605	602
Max Acceleration (ft/s^2)	274	274	276	276	277
Flight Time (s)	192	187	187	185	186
Time to Apogee (s)	18.8	18.7	18.6	18.3	18.2
CG Location from nose (in)	77.433	77.433	77.433	77.433	77.433
CP Location from nose (in)	98.529	98.529	98.529	98.529	98.529
Stability Margin with motor	2.81	2.81	2.81	2.81	2.81

3.1.4.2.2 RockSim Predictions

Table 15. RockSim Predictions with Cesaroni L1395 Motor

Wind Speed	0 mph	5 mph	10 mph	15 mph	20 mph
Apogee (ft)	5553	5535	5480	5387	5259
Max Velocity (ft/s)	611	611	610	610	609
Max Acceleration (ft/s^2)	1125	1118	1126	1143	1126
Flight Time (s)	151.9	165.33	190.26	241.54	18.84
Time to Apogee (s)	19.36	19.33	19.23	19.07	189.84

CG Location from nose (in)	75.29	75.29	75.29	75.29	75.29
CP Location from nose (in)	98.28	98.28	98.28	98.28	98.28
Stability Margin with motor	3.07	3.07	3.07	3.07	3.07

Table 16. RockSim Predictions with Cesaroni L1685 Motor.

Wind Speed	0 mph	5 mph	10 mph	15 mph	20 mph
Apogee (ft)	5572	5561	5525	5465	5382
Max Velocity (ft/s)	612	612	611	611	610
Max Acceleration (ft/s^2)	1125	1125	1125	1141	1102
Flight Time (s)	193.42	191.90	192.47	240.12	194
Time to Apogee (s)	19.13	19.11	19.04	18.94	18.79
CG Location from nose (in)	77.24	77.24	77.24	77.24	77.24
CP Location from nose (in)	98.28	98.28	98.28	98.28	98.28
Stability Margin with motor	2.81	2.81	2.81	2.81	2.81

3.1.4.3 Kinetic Energy Calculations Summary

The kinetic energy at landing for each rocket section is a function of the descent velocity and the mass of the section in question. Specifically, the kinetic energy equation is shown below in Equation 1.

$$KE = 12\, m\, v^2, \qquad \textbf{Eq. 1}$$

where *KE* is the kinetic energy, *m* is the mass, and *v* is the velocity. For ease of calculation, quantities are often converted to SI units for use in this equation. Table 17 below shows some various relationships which were used to find the desired values.

Table 17. Useful units conversions for KE calculation.

SI Unit	Imperial Equivalent
1 Joule (J)	0.7376 ft-lbf
1 kilogram (kg)	35.274 oz
1 meter per second (m/s)	3.28 ft/s

The parachute sizing calculations recommended a 12 ft diameter main parachute to produce a final descent velocity of 12.57 ft/s. The speed can be used in conjunction with the estimated masses of the rocket section to find their kinetic energies. Table 18 below shows the predicted final KE of each section of the rocket upon landing.

Table 18. KE at landing for rocket sections.

Rocket Section	Mass (oz)	Kinetic Energy (ft-lbf)
Nose cone	213	32.61
Recovery tube	161	24.65
Fin can	375	57.41

Clearly all the final kinetic energies are within the 75 ft-lbf limit of the competition. There is also plenty of leeway in case a section of the rocket such as the fin can ends up considerably heavier than expected.

3.1.4.4 Drift Calculations Summary

To calculate the wind drift, the primary method the team employs is a legacy Matlab code which utilizes the 4th Order Runge-Kutta method to simulate the descent of the rocket for various environmental conditions. The relevant inputs are the rocket weight and the size of the main and drogue parachutes. The output of the code is diverse as it can calculate the velocity descent path, the horizontal descent path, accelerations experienced throughout the flight, and even the kinetic energies of the segments at various times. For the purposes of this section however, only the horizontal path is shown, as seen in Figure 11 below.

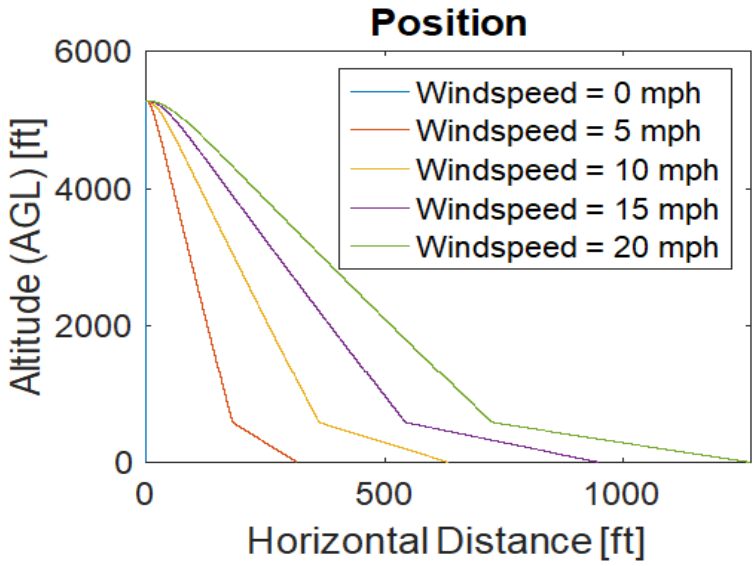

Figure 11. Horizontal flight profile under various wind conditions.

The second method used to calculate drift is through OpenRocket simulation. All the launch vehicle specifications are entered into the program, and it produces data for a wide variety of desired outputs. Figure 12 below graphically displays the simulation data under various wind conditions.

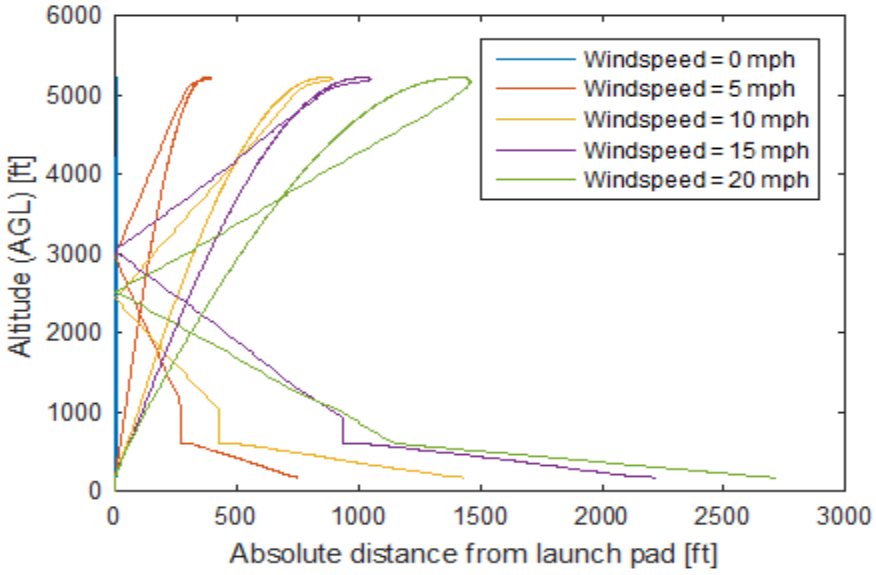

Figure 12. Predicted wind drift from OpenRocket simulation

Some key differences are apparent between the Matlab program and the OpenRocket simulation. Perhaps most notably, OpenRocket takes into account more launch conditions such as the launch rail angle, wind direction relative to it, and the lateral distance data is taken as an absolute value. This accounts for the looped and backtracking shape of the OpenRocket graphs because the rocket first travels away from the launch pad into the wind, but then passes directly back over the pad during flight due to the wind's influence on the parachutes. Another notable difference is the predicted range of the drift. OpenRocket predicts a much further lateral distance than Matlab. The team has not used OpenRocket for drift simulation in the past and the Matlab program has always been satisfactorily accurate.This means the OpenRocket simulation is most likely in need of further work because its predictions are almost certainly overestimates according to past experience. However, going forward the two methods will be refined and averaged to produce the most accurate possible prediction.

3.1.5 Launch Vehicle Checklist

A complete checklist of launch vehicle procedures can be found in Appendix XX. The checklists are divided up for the various stages of a launch day as well as for each of the four subsystems.

3.2 Comparison between Subscale and Full Scale

A subscale vehicle is being constructed in order to verify the simulations that are being run in Openrocket as well as simulations going to be run using RockSim and in-house physics models. The subscale is also being built in order to verify the altimeters being used for the full scale. The simulation software will give estimates of the center of mass, stability, and flight performance of the subscale rocket, and the subscale flight will determine whether or not these simulations are reliable for predicting the performance of the full scale rocket. Additionally, the subscale vehicle will be used in order to measure the performance of the air braking system. This will be done with subscale wind tunnel testing as well as the subscale test flight, more information on these can be found in section 3.1.5: Vehicle Design Verifications.

The subscale rocket being built is designed to be 40% the size of the full scale rocket. The airframe design of the subscale greatly resembles that of the full scale, however, the internal structure is much different. The altimeters will be placed on a removable slide in the forward section of the rocket in place of the Rover Payload. The transition section will be created in-house using methods found through Apogee Components. Furthermore, the subscale rocket will be composed of only two separate sections. A model of the subscale rocket can be found in Figure 13 and the dimensions and masses for the model can be found in Table 19.

Table 19. Subscale Vehicle Dimensions and Characteristics.

Property	Dimension
Length of Rocket (in)	52.25
Fore Diameter of Rocket (in)	3.14
Aft Diameter of Rocket (in)	2.27
Transition Length (in)	1.6
Number of Fins	4
Fin Root Chord (in)	2.8
Fin Tip Chord (in)	2.8
Fin Sweep Angle (°)	31.6
Fin Height (in)	1.77
CG Position from Nose Cone (with motor) (in)	31.83
Weight without Motor (oz)	54
Weight with Motor (oz)	58.5
Estimated Stability Margin without Motor	3.42
Estimated Stability Margin with Motor	2.95

These internal differences were decided on for a variety of reasons. First, the rocket is only two sections because of its simpler design that does not require an additional avionics bay. A motor can be purchased that has a built in ejection charge that deploys the parachute a

specified time after motor burnout, eliminating the need for the teams designed Compact Removable Avionics Module (CRAM). Second, the altimeters were placed in the forward section because there is no rover payload on the subscale. They are also to be placed here in order to keep them safe from the ejection charges in the main body tube. Finally, the transition section is going to be made in-house due to the fact that a section with the dimensions needed is not commercially available.

The materials being used for subscale are also different than those used for the full scale. The main structure of the subscale rocket will utilize phenolic and birch plywood, whereas the full scale will use carbon fiber and fiberglass. This is being done mainly due to budget constraints, as well as the ease of working with the materials during construction. This difference in material is being taken into account in the computer simulations in order to minimize error. For wind tunnel testing, it is critical that the subscale has a smooth finish, as this is what the full scale will have.

In order to simulate the Air Braking System tabs, the separation point of the rocket will be near the center of pressure, and a coupler with 3D printed, scaled tabs will be placed here. This coupler will be removable in order to simulate flight with and without tabs deployed, and will be secured to ensure that it does not become separated during descent. The two subscale models can be seen in Figure 13 and Figure 14.

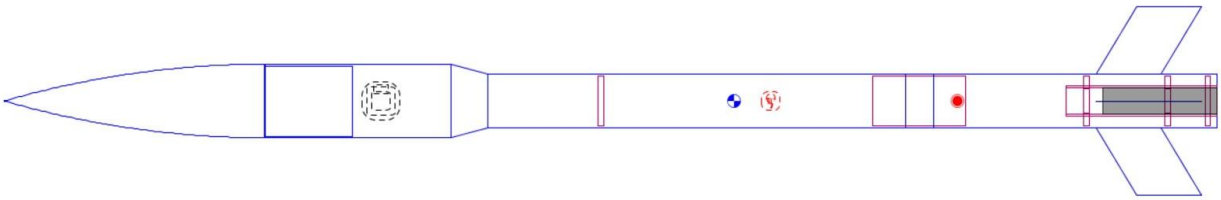

Figure 13. Subscale model without tabs deployed.

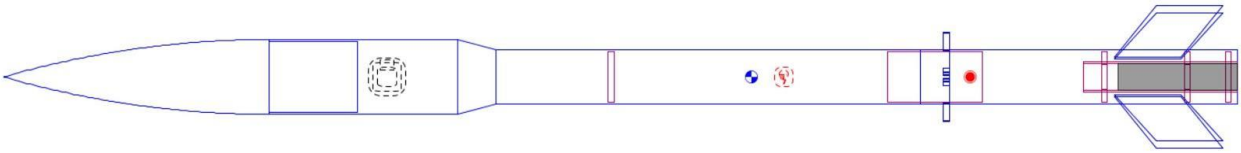

Figure 14. Subscale model with tabs deployed.

The motor being used for the subscale was decided as the Aerotech G78-7G. This motor gives a desirable altitude of 790 ft with no wind, and has a similar thrust curve to the motors being considered for the full scale rocket. The thrust curve for the G78-7G can be found in Figure 15, and the curves for the full scale motors can be found in Section 3.1.3.6. Additionally, the properties of the motor can be found in Table 20.

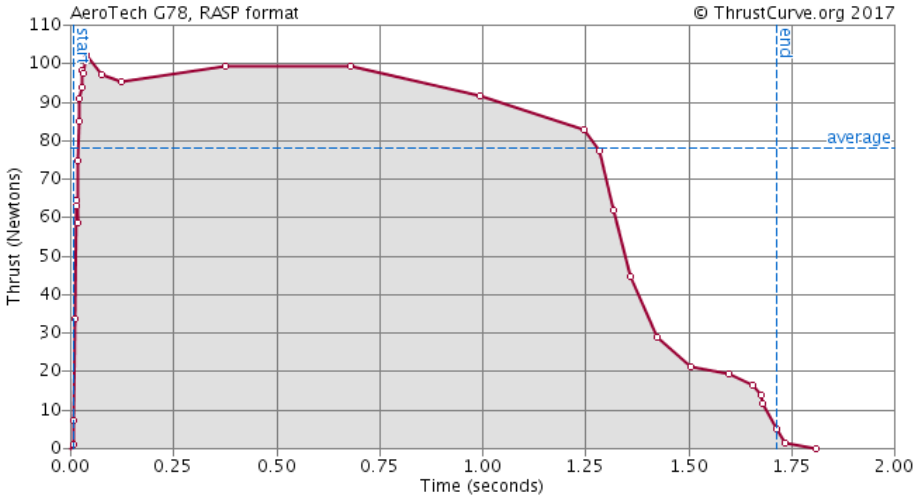

Figure 15. Thrust Curve of the Aerotech G78-7G.

Table 20. Properties of the G78-7.

Motor Classification	AeroTech G78-7G
Diameter (in)	1.14
Length (in)	4.88
Average Thrust (lbf)	17.96
Maximum Thrust (lbf)	22.91
Total Impulse (lbf*s)	24.70
Burn Time (s)	1.4
Total Weight (lb)	0.28
Propellant Weight (lb)	0.13

The stability margin for both the subscale with and without tabs are 2.88 and 2.95, respectively. Both of these values are above the minimum requirement of 2.0, and below the ceiling of 3.0. The launch predictions for the subscale with and without tabs deployed can be found in Table 21 and Table 22, respectively. These predictions were found using OpenRocket, and were run for wind speeds of 0 mph, 5 mph, 10 mph, 15 mph, and 20 mph. These simulations will be verified using RockSim.

Table 21. Subscale predictions without tabs deployed.

Wind Speed	0 mph	5 mph	10 mph	15 mph	20 mph
Apogee (ft)	790	786	777	760	753
Max Velocity (ft/s)	212	211	211	209	208
Max Acceleration (ft/s^2)	174	174	174	174	174
Flight Time (s)	154	140	141	137	136
Time to Apogee (s)	7.49	7.44	7.42	7.41	7.34

Table 22. Subscale predictions with tabs deployed.

Wind Speed	0 mph	5 mph	10 mph	15 mph	20 mph
Apogee (ft)	698	694	683	671	661
Max Velocity (ft/s)	204	204	203	202	200
Max Acceleration (ft/s^2)	173	173	173	173	173
Flight Time (s)	119	121	120	116	114
Time to Apogee (s)	6.94	6.95	6.92	6.87	8.82

3.3 Recovery System

3.3.1 Overview

In general, the Recovery Subsystem for this year's vehicle can be considered an iteration from previous years' systems. It will feature dual-stage parachute ejection capability, controlled

from a centralized unit - the Compact Removeable Avionics Module (CRAM). The reason this system can only be considered an iteration "in general" is because some things have stayed the same, while other important differences will be implemented. Constants from previous years include: shock cords tethering all rocket sections together and to the parachutes, Quicklink connectors between shock cords and bulkhead eyebolts, Nomex fire retardant cloth, black powder ejection charges controlled by altimeter barometric sensors, and a screw-to-lock mechanism which secures the CRAM to a complimentary mount inside the rocket. Notable changes taking effect this year include: *triple* redundant parachute ejection systems, acrylic bulkheads at the top and bottom of the CRAM, commercial battery boxes for battery containment and wiring, removal of custom circuit board in favor of direct wiring between components, and removal of screw terminals in favor of semi-permanent 'clip' terminals at all critical junctures. All these features and the reasons for their selection is spelled out in length in following sections.

Considerable design work on the recovery subsystem - and on the CRAM in particular - has continued since the Proposal. A nearly complete virtual model and preliminary prototypes have been created to help inform the construction of the system going forward. Figure 16 and Figure 17 below show side and isometric views (respectively) of the current design as it will appear before a launch, ready to enter its respective body tube section. Only the connecting bolts running the length of the CRAM body and protruding on each side have been omitted, for the sake of visual clarity. Figure 18 shows an overview of the component order and layout within the launch vehicle. Table 23 provides the part identification for the component layout diagram.

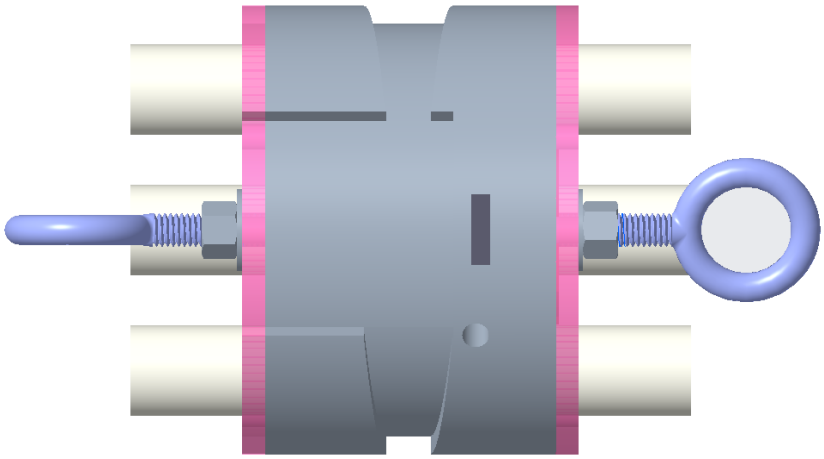

Figure 16. Side view of fully assembled CRAM v4.

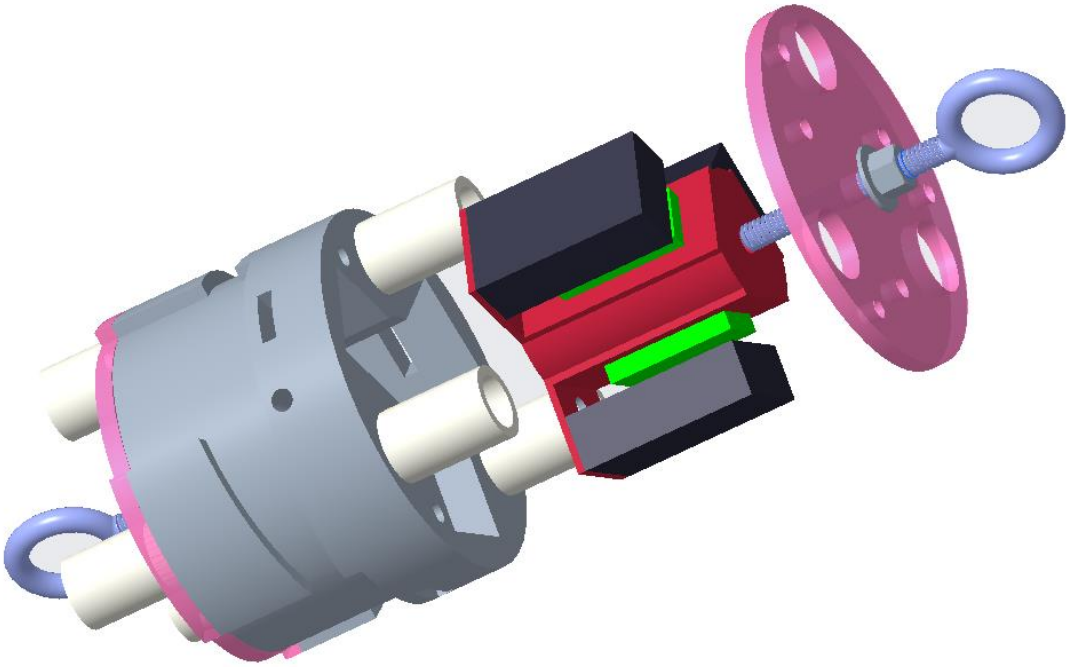

Figure 17. Exploded view of CRAM v4.

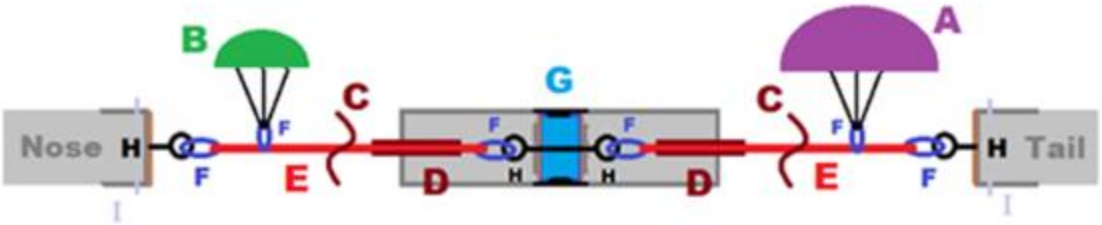

Figure 18. Component view of the recovery subsystem.

Table 23. Recovery System Components and Layout.

Component	Location on Figure 3.
Main parachute	A
Drogue parachute	B
Nomex cloth	C
Nomex shock cord protectors	D

Shock cords	E
Quicklinks	F
CRAM v4	G
Eyebolts	H

3.3.2 Component Review

3.3.2.1 Altimeters

The altimeter for the recovery system is an absolutely critical choice because the accuracy and reliability of the component will ultimately determine the success or failure of the entire system. The team has always used *Featherweight* brand altimeters in the past because of the simplicity, reliability, and functionality they provide. For this reason, the *Featherweight Parrot 2* and *Raven 3* were the top contenders for this year's altimeter and they are seen below in Figure 19. Since the candidate that will best fit our system's needs is not readily obvious, Table 24 below shows a pro/con list for each of these in order to assist with the decision-making process.

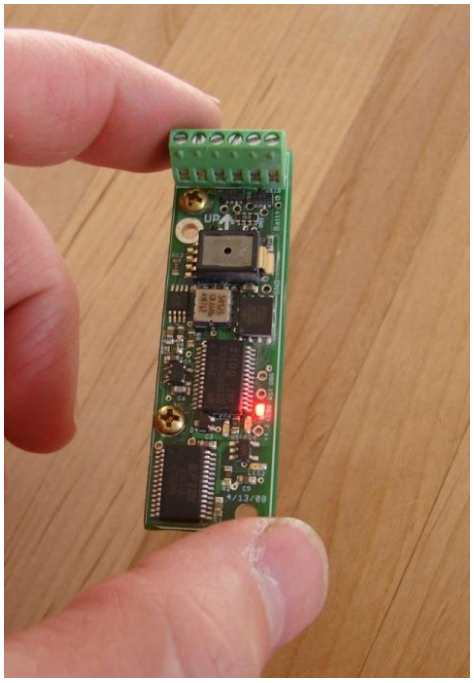

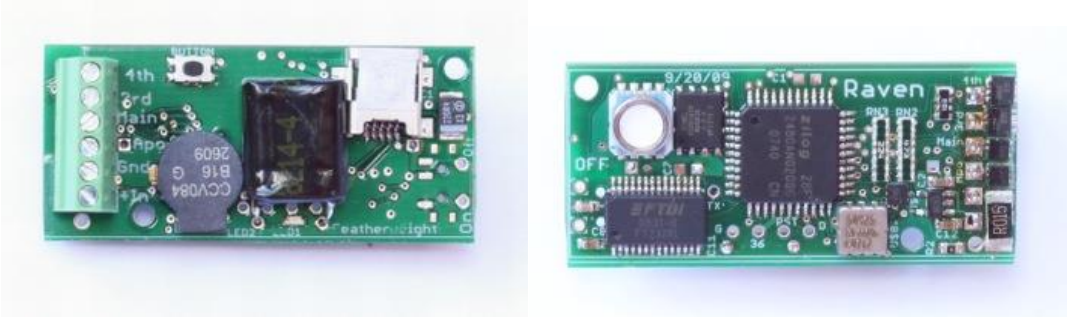

Figure 19. Parrot 2 (left) and Raven 3 (right) altimeter choices for recovery system.

Table 24. Pro/con chart for altimeter choice.

Parrot 2		***Raven 3***	
Pros	**Cons**	**Pros**	**Cons**
3 programmable ports	Bulky	Small and light	Low Hz sensor readings: 20 Hz
Isolated arming screw switch	Long lead-time on order	Previous team experience	
Functional with either end up		Simulation support	

3.3.2.2 Battery Box

In this design, battery boxes will be used to contain and connect the 9V batteries to the altimeters rather than clip connectors. There are many reasons as to why these battery boxes are more advantageous than clip connectors, which the team used last year. Last year the team used clip connectors because they were relatively simple and reliable, and they were an easy way to connect the batteries to the altimeters. This year, the team realized that battery boxes are safer and even more reliable, and they greatly lessen the chance of any errors. Pictured below in Figure 20 is a battery switch box compared to a connector clip, which is are two of the possible options. There are many pros and cons to these two options, and they are described in Table 25 below.

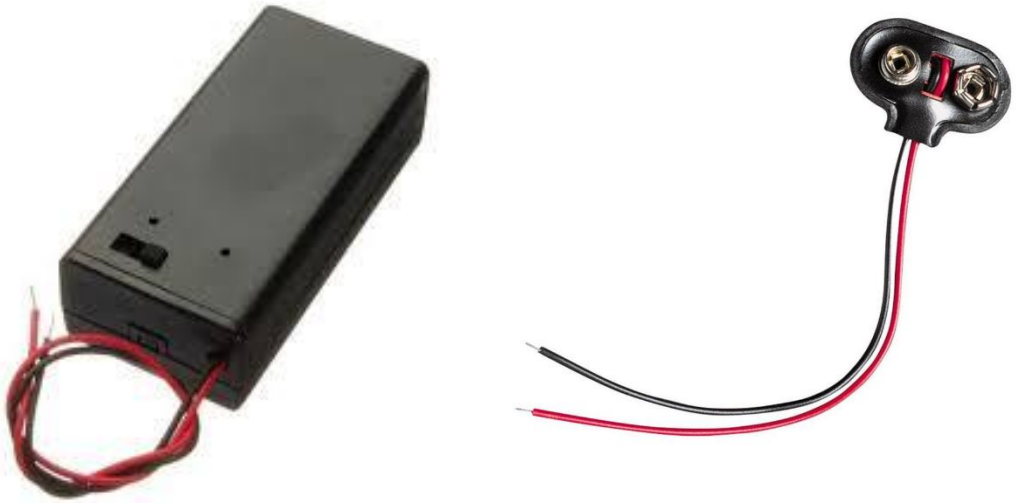

Figure 20. Battery box (left) versus battery clip (right).

Table 25. Pro/con chart for battery connector selection.

Battery Box		***Clip Connectors***	
Pros	**Cons**	**Pros**	**Cons**
Contains the battery and prevents it from interfering with the rest of the system	Is more expensive than clip connectors	Is very simple and trustworthy	Can leave the battery out in the open and exposed to the rest of the system
Allows the battery to be connected to the altimeter with ease		Allows the battery to be connected to the altimeter with ease	Can fall off the battery/become dislodged
Ensures that the battery is not dislodged from the wires Fits into the design very easily		Is cheaper than battery boxes	Creates the need to find a way to attach the battery to the rest of the design

As can be seen from Table 25, the pros for the battery box far outweigh the cons; on the other hand, the clip connectors have much more negative effects on the design. Using this

decision-making process, the team has determined that battery boxes are definitely the safer and more effective option, even though they may be slightly more expensive.

3.3.2.3 Eyebolts and Connector Nuts

The eye bolts and connector nuts used in the construction of the rocket recovery system are vital in ensuring that the drogue parachute and main parachute stay connected to the rocket all the way from deployment to landing. For the eyebolts used in the recovery system, we will used a forged bolt construction instead of a bent wire construction. Forged bolts provide a much stronger connection, up to the tensile strength of the material used to construct them, while eye bolts made with the bent wire construction method are only suitable for lighter applications, due to the chance that the eyebolt will reopen. The material of the eyebolt is also a significant consideration, as the maximum loads can vary widely from material to material. The most common material for eyebolts in normal applications is galvanized steel, while other options include stainless steel. Table 26 shows some of the benefits and drawbacks to each material type.

Table 26. Pro/con chart for hardware selection.

Galvanized Steel		***Stainless Steel Alloy***	
Pros	**Cons**	**Pros**	**Cons**
Cost: Galvanized steel is significantly cheaper than most alternatives (Approximately $10 for a 3 inch eyebolt)	Strength: Galvanized steel tends to be weaker than other steel alloys	Strength: Stainless steel is typically stronger than galvanized steel	Cost: Stainless steel is expensive, especially in comparison to galvanized steel (Approximately $20 for a 3 inch eyebolt)
Corrosion Resistance: Galvanized steel is resistant to rust and other forms of corrosion	Weight: Galvanized steel tends to weigh more than stainless steel	Weight: Stainless steel tends to weigh less than galvanized steel	
		Corrosion Resistance:	

		Stainless steel is resistant to corrosion such as rust.	

At the moment, forged, stainless steel eye bolts will be the best choice for our recovery system. Despite the increased cost, forged, stainless steel eye bolts will be significantly stronger and more reliable than comparable forged galvanized steel eye bolts or any bent construction eyebolt.

The connector nut used to couple the eyebolts together is of similar importance. If the coupling nut is not strong enough, the parachutes may separate from the CRAM upon deployment. Therefore, despite the cost increase, the best choice of material for our recovery system is an eyebolt created from Grade 2H steel, which despite being among the most expensive material options, has a higher load strength than nuts made from any other grade of steel.

3.3.2.4 Bulkheads

Secured to each side of the CRAM is a layer of material known as the CRAM bulkhead whose purpose is to protect the 3D printed body of the CRAM from the harsh conditions of launch, especially the black powder ejection charges. In years past, this material has been plywood, but other materials may be more suited for the demands of the system this year (namely the triple redundant charges which will be experienced during each launch). The top choices for the CRAM bulkhead are plywood, acrylic, and steel. These are compared in Table 27 which highlights the various positive and negative qualities of each material choice.

Table 27. Pro/con chart for bulkhead material selection.

Plywood (1/4 in)		***Acrylic (1/4 in)***		***Steel (1/16 in)***	
Pros	**Cons**	**Pros**	**Cons**	**Pros**	**Cons**
Lightweight: 1 ppsf	Vulnerable to deformation from explosions	High compressive strength: 95 MPa	Could shatter if dropped	Complete protection for CRAM	Heavy

Easy to manufacture	splinters	Resistant to wear and charring	Expensive: $7.00 psf		Expensive
Cheap: $1.75 psf	unsightly	Machinable with CNC mill	Heavy: 1.424 ppsf		Near impossible to machine and affix to CRAM

3.3.2.5 Quicklinks

In this design, the team is utilizing Quicklinks in order to connect the eyebolts to the shock cords. Quicklinks are a clip that uses a screw mechanism rather than a spring mechanism in order to shut, and it is a very reliable way of connecting two things. Figure 21 depicts a screw-lock Quicklink and high-end clip carabiner, which are two of the possibilities for the team's design. Some other options the team had were carabiners, which use the aforementioned spring mechanism, or tying the shock cord directly to the eyebolt. Quicklinks are the most secure way of tying these two components together, and they also make it much more convenient to separate the CRAM from the shock cords. If the team chose to tie the shock cords directly to the CRAM, then it would take a significant amount of time to separate the CRAM from the shock cords when it was necessary. A carabiner would provide the ease of access that is necessary, but it would not provide the security and sturdiness that is required when developing a recovery system. Quicklinks are the only solution that provides both the ease of access and the sturdiness that is required by our team. The pros and cons of each of these options are outlined in Table 28.

Figure 21. Screw-lock Quicklink versus high-end clip carabiner.

Table 28. Pro/con chart for connector hardware selection.

Quicklinks		***Carabiners***		***Tying Directly***	
Pros	**Cons**	**Pros**	**Cons**	**Pros**	**Cons**
Ease of access	More expensive	Easiest to take on/off	Not as durable as quicklinks	No cost	Unreliable
Very sturdy		Cheaper than quicklinks		Can be very sturdy	Very difficult to disconnect CRAM from shock cords

3.3.3 Leading Components Choices

3.3.3.1 Altimeters

Based on the specifications of the altimeters, the *Raven 3* is the leading choice for the recovery systems altimeter. The *Raven 3* is smaller and lighter, which will allow it to fit comfortably into the team's current design and more likely to fit into any future design changes.

3.3.3.2 Battery Connector

Based on the needs of the recovery system and desire for greater reliability, the battery box is the leading choice for battery connector. This method has the added benefit of containing a convenient arming switch for the independent avionics systems.

3.3.3.3 Eyebolts and Connector Nuts

Since reliability and robustness is the most important aspect for the recovery system components, the stainless steel eyebolt and coupling nut are the leading contenders.

3.3.3.4 Bulkhead

With the possible need for repeated manufacture and, but also for resistance to wear under use, acrylic is the leading material for the recovery bulkheads as it stands.

3.3.3.5 Hardware Connector

Since accessible and rapid securing is of importance to this part of the recovery design, the choice between clip and screw carabiner is not immediately obvious. However, the added reliability of the screw connector Quicklinks makes them the leading contender.

3.3.4 Parachute Sizing

When sizing parachutes, essentially a two-variable optimization is at play. The first factor is the speed of descent and the second is the wind drift. These factors are in direct opposition because a slower descent speed will correspondingly lead to a greater horizontal drift. The goal then, is to choose the smallest possible parachute that will meet the maximum allowable descent velocity. The maximum allowable descent velocity is a function of the mass of the heaviest rocket section and the maximum allowable kinetic energy of 75 ft-lbf. According to preliminary estimates, the heaviest section of the rocket while be the fin can and it will weigh 375 oz. The total estimated weight of the rocket is 749 oz. Therefore, the maximum allowable descent velocity is 14.36 ft/s. For added safety and to ensure the actual landing energy is within bounds, the maximum landing velocity going forward will be held between 12 ft/s and 13 ft/s.

With a desired descent velocity and total rocket mass in hand, simulations can be utilized to find the appropriate main parachute size. The rule of thumb for descent velocity under drogue is between 70 and 80 ft/s, so choose 75 ft/s the same simulations can be used to find the required drogue size as well. The two simulations used by the team toward this end are (1) Custom Matlab code which takes velocity and mass as inputs, incorporates drag coefficient and air density, and produces recommended parachute diameter. (2) Online graphical calculator from *FruityChutes* manufacturer which assists in parachute selection.

When provided the weight of the rocket and the desired descent velocity, the Matlab code produced a recommended parachute diameter of 12.57 ft. This result was confirmed when the *FruityChutes* descent calculator found that a parachute of diameter 12.5 ft would land at 12.26 ft/s. Since most parachute manufacturers produce in 2 ft diameter increments, it will be considerably more cost effective to get a **12 ft diameter main parachute** than to attempt increase it slightly toward the aim of hitting the 12 ft/s mark exactly. Since the predictions both confirm it will land at under 13 ft/s with a 12 ft diameter, the team can be confident in the result going forward. The same process was repeated to find the drogue parachute size required for a 75 ft/s descent speed. Both the Matlab code and *FruityChutes* simulator produced the same result. A **2 ft diameter drogue** will provide the desired descent velocity.

3.3.5 Redundancy

Emphasis on redundancy is one the main hallmarks of this year's recovery subsystem design. In light of less than favorable results during the final flight of last year's launch vehicle, exceptional care has been devoted to this year's design to ensure perfect reliability. Most notably, the entire system is *triple* redundant. Three independent power sources energize three independent altimeters which control three independent ejection charges for each parachute. Furthermore, each ejection charge will be primed with two electronic matches connected in parallel in case one of them proves faulty upon receiving the power signal from the altimeters. This redundancy can be seen below in Figure 22 where the independent (redundant) systems are clearly labeled (1), (2), and (3).

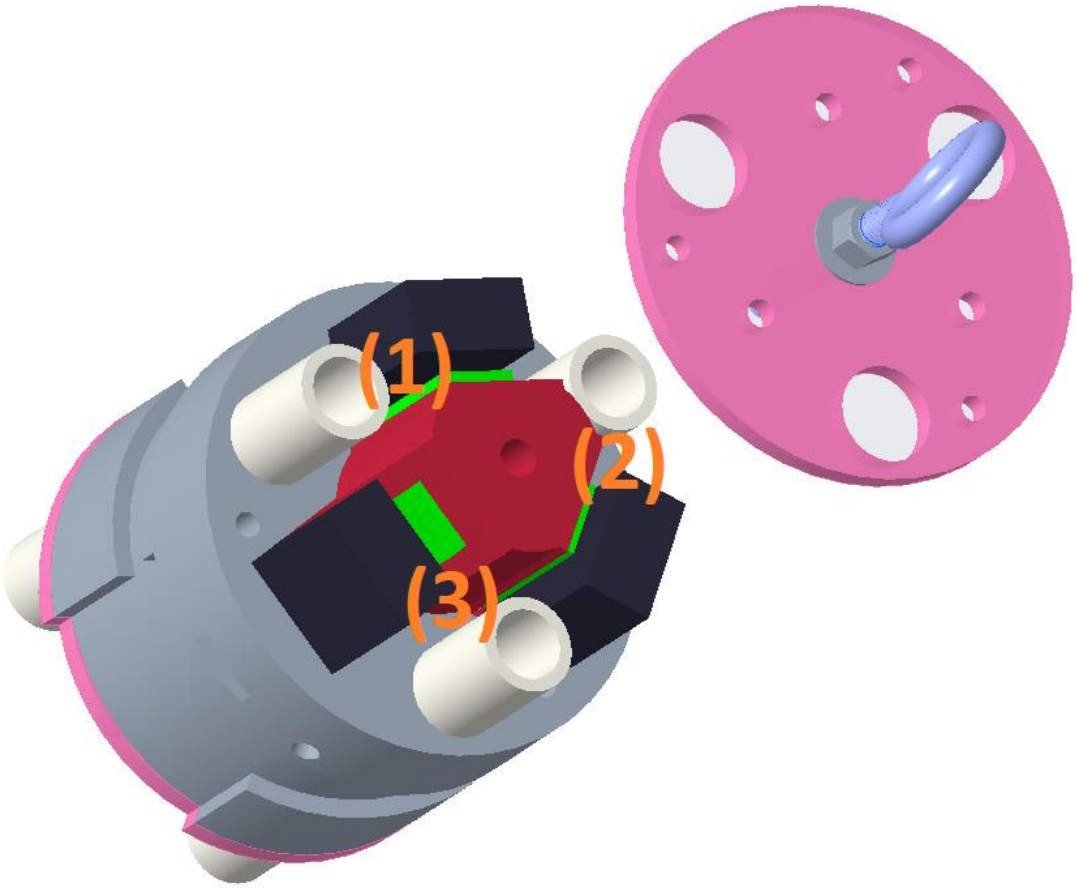

Figure 22. View of CRAM v4 with core partially inserted showing triple redundancy.

3.4 Safety and Risk Mitigation

An in-depth analysis of the risks of the vehicle can be found in Appendices D through I. These include a FMEA table for the vehicle, as well as risk assessments for many different aspects of this competition.

4 Safety

4.1 Checklist of Final Assembly and Launch Procedures

A detailed pre-launch checklist will guide the final assembly process for the rocket with step-by-step instructions. A repeatable launch procedure will also be developed to mitigate risk of failure at the launch site, and a post-launch procedure will ensure the all personnel retrieve the rocket in a manner that is safe for both the personnel and the rocket. These steps must be followed precisely to ensure successful execution of the project. These procedures can be found in Appendix D.

4.2 Preliminary Personnel Hazard Analysis

The Notre Dame Rocketry Team understands that the construction, testing, and launch of the rocket pose several potential hazards to team members. The table below explores the personnel hazards that may occur during different phases of constructing or testing the launch vehicle and its subsystems. Similar to the FMEA table, a severity, likelihood, and overall risk level was assigned to each hazard to better understand what mitigations are necessary. The risks and likelihoods were assessed assuming that all team members have been properly trained, are following the correct procedures, and are wearing the proper personal protective equipment (PPE). By recognizing these hazards now, the team can be better prepared to mitigate them and to take the proper actions in the event that an accident occurs. This table can be found in Appendix E.

4.3 Preliminary Failure Modes and Effects Analysis (FMEA)

A Failure Modes and Effects Analysis (FMEA) table was developed to identify the potential technical failures of the vehicle. For each failure, the effects and causes were identified, as well as their likelihood of happening, and the severity of their occurrence. The last two parameters were used to assess the risk of each failure through the Risk Assessment Codes (RACs) suggested in the handbook for the competition. The risk matrix used, based on the one shown in the handbook's appendix, is shown in Figure 23.

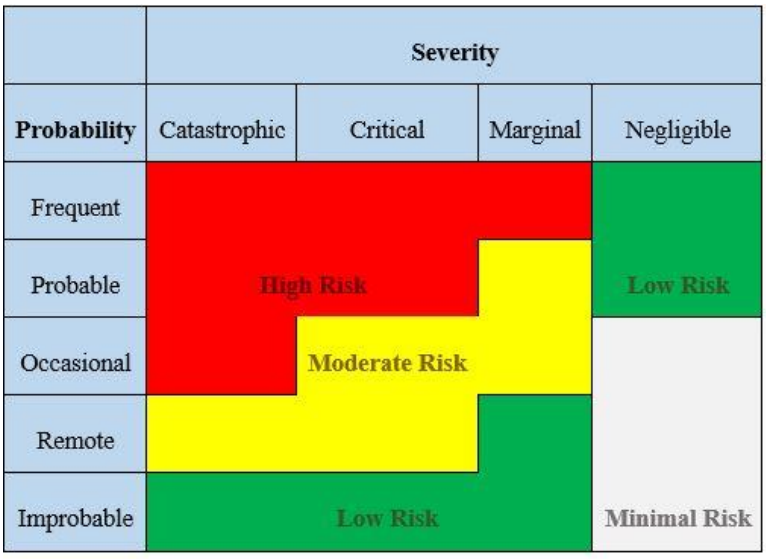

Figure 23. Risk Assessment Matrix.

After classifying the risk of each failure mode, mitigations and controls to prevent said failures were developed. It is important to note the importance of first determining the level of risk of each failure as to implement appropriate mitigation levels. Figure 24 depicts how the failure modes were divided into six categories: Structural, Recovers, Propulsion, Stability, and relating to the specific payloads. The FMEA table for all possible failure modes the launch vehicle and its subsystems may experience can be found in Appendix F.

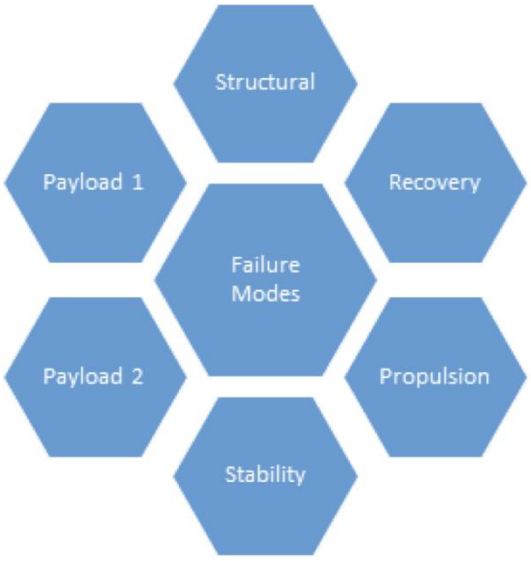

Figure 24. Failure Mode Classification.

4.4 Environmental Concerns

The environment in which the rocket will be operated also poses a certain amount of risk. Specific problems related to inclement weather at the launch and landing sites have been identified and solutions have been devised to decrease the negative effects of the environment on the rocket. Additionally, many of the materials used in the construction of the rocket pose a significant hazard to the environment if they are improperly handled. By considering these things, one can ensure that the rocket is able to adequately perform and not be negatively affected by the environment. Failure modes tables have been constructed for both the environmental effects on the rocket and the rocket's effect on the environment. These tables can be found in Appendix G and Appendix H respectively.

4.5 Project Risks

There is the possibility of encountering a number of roadblocks throughout the rocket design and launch process. Each of these risks has been identified and categorized in terms of their potential impact on the project and the likelihood of that specific problem occurring. Risk is minimized with specific mitigation plans for each scenario. Failure to mitigate these risks will result in significant time delays for the project, which in turn lowers the chance of success on launch day. A table has been constructed outlining potential risks associated with the project, their likelihood, their impact on the project, and how they will be mitigated. This table can be found in Appendix I.

5 Payload Criteria

5.1 Deployable Rover - Selection, Design and Rationale

5.1.1 Overall Design Statement

The objective of the Deployable Rover Payload is to remotely deploy a small rover from the main body of the rocket upon safe landing. Once the rover is deployed it will move five feet away from all points of the rocket and unfold two sets of solar panels.

These rover will be remotely deployed via a ground station that makes use of radio frequency to communicate with the deployment system and the rover. The rover is located in the top of the rocket directly below the nose cone. The nose cone will be removed with ejection charges allowing the rover to drive out and into the field. The rover has the capability to drive inverted if the rocket lands in such orientation. Using a Lidar sensor, the rover will detect objects in the field and move away from the rest of the rocket. Once the rover is safely away from the rest of the rocket, two sets of solar panels will unfold. The rover will be machined from aluminum to allow for customization.

This experimental payload will be deemed successful if all the following criteria are met:

1. Autonomously drives five feet away from the rocket
2. Solar panels unfold and provide power to the rover
3. The rover will be reusable within the same launch day

5.1.2 Subsystems

5.1.2.1 Rover Body

The body of the rover will be machined out of standardized aluminum alloy. This lightweight material ensures that the body of the rover is durable and is easily altered within the design process. From a design development standpoint, using a modular type of material is simpler to track and adjust necessary dimensions which will affect the performance of the rover. Machining the body allows for true customization and the ability to make modifications later in the design process. This makes our design of the rover adaptable, effective, and inexpensive in terms of time and cost.

An alternative method of creating the body of the rover was to purchase modular body parts from online robotics websites. However, this would limit the design of the rover to parts that are commercially produced and would allow for little change to the pre-made design. 3-D printing was also another viable solution since it is readily available to engineering students for model assembly and final design. The downside to 3-D printing is polymers, such as plastic, could break under bending, torsion, and vibrations during the flight and landing of the rocket. This would increase the risk of cracks and fractures in the body of the rover which would lead to catastrophic failure. A material that would benefit the design of the rover body is titanium. While being stronger and more lightweight than aluminum, titanium was very expensive and difficult to not only manufacture within the design specification but also highly resistant to change. The body of the rover is seen in Figure 25.

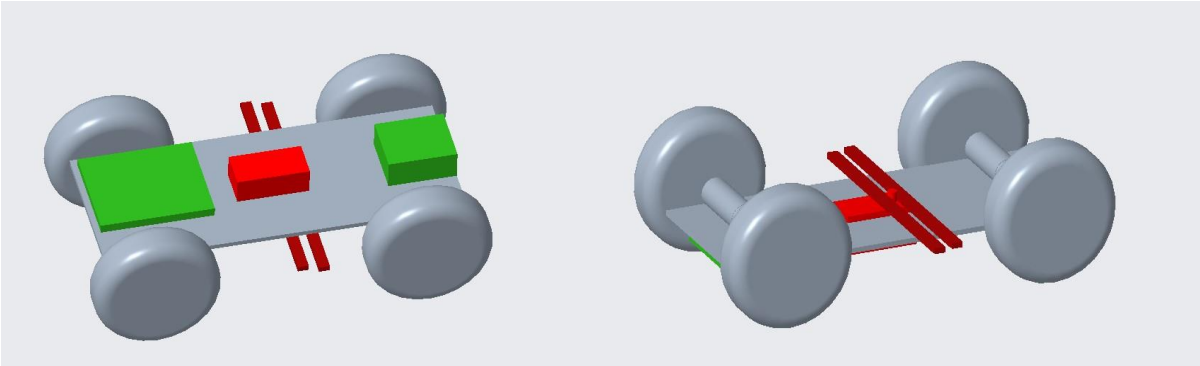

Figure 25. CAD rendering of the deployable rover body.

5.1.2.2 Solar Panels

5.1.2.2.1 Extension Mechanism

The deployable solar panels need to be extended after the rover exits the fuselage. This will be controlled by a rack-and-pinion mechanism. At the center of the rover body will be a single servo motor with 2 parallel gear racks on either side. Attached to one end will be a folded solar array. The opposite end will extend beyond the rover to aid in-flight security. When the rocket has landed, the servo will spin and pull the racks over the profile of the rover to allow exit. Once the rover has exited the rocket, the servo will spin further to extend the folding array. The folding array mechanism will begin in the folded position, and will extend to cover 3 times the initial area. The folding array can be seen in Figure 26. The solar panels will be mounted on the flat surfaces and extended via a servo motor.

Figure 26. CAD rendering of the solar panel folding mechanism.

5.1.2.2.2 Solar Cells

The solar cells used will be 2.08 x 1.81 in. Because of their small size, several will fit on each panel of the folding array. This means there will not be folding of the individual cells. The cells will line both the top and the bottom of the folding array, so once extended the vehicle can be powered in either the upright or inverted orientation. The solar panels used are seen in Figure 27.

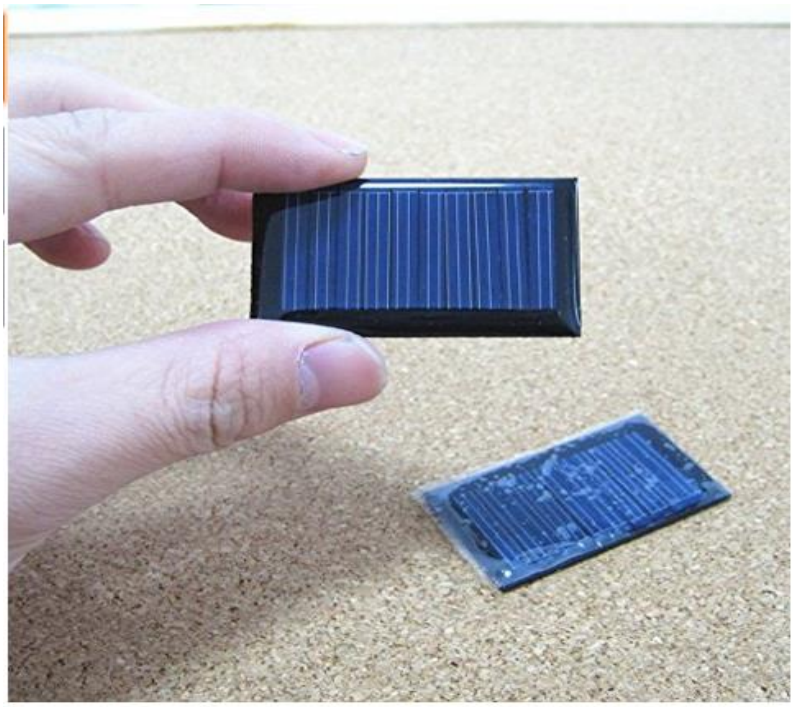

Figure 27. The solar panel structure will be constructed out of multiple small panels shown above.

5.1.2.3 Wheels

The rover payload design must also feature a mechanism for vehicle propulsion on the ground. This ground may consist of uneven clumps of dirt, small shoots of corn, rocks, twigs, and other moderately-sized obstacles. To resolve this challenge, the team first considered arming the Rover with continuous treads. Treads are generally used to overcome uneven terrain. They command excellent traction for a wide range of surfaces, allowing the vehicle to overcome a variety of obstacles, especially on inclines, which may be encountered. Also, treads have a smaller ground impact than wheels, thus avoiding the chance of the rover sinking into mud on a rainy day.

However, treads have a high likelihood of becoming stuck when twigs and brambles enter the rotational area. On the small building scale of the Rover, this would result in the track becoming broken or dislodged. Furthermore, treads provide inefficient maneuverability when turning or moving in multiple directions, an important part of the Rover's objective, as it must navigate in any direction. Because of these liabilities, the team chose to build the Rover with wheels. Wheels are lightweight, minimizing payload weight. They provide excellent maneuverability and well as simplicity–less moving parts to get damaged. They are also inexpensive and secure.

The team decided four Goolsky FY-CL01 RC Tires, seen below in Figure 28, were an optimal fit for the project. These wheels provide a sizeable rubber tire with deep tire treads, retaining some of the traction the continuous treads would have given. The four wheels will be oversized, making it easier for the Rover to climb obstacles as well as providing protection for

the Rover body, which will be situated in the center of their large circumference. The wheels are composed of ABS (Acrylonitrile butadiene styrene) and TPR (ThermoPlastic Rubber). The wheel diameter is 1.77in with an outer tire diameter of 3.54in, the tire width is 1.18in, and each wheel has a weight of 0.145lb; all four wheels equate to a combined weight of 0.578lb.

Figure 28. Goolsky FY-CL01 RC Tires will be used on the rover.

5.1.2.4 Motor

The powertrain of the rover starts with four DC brushless motors that are equipped with sensors. The rotational power is then passed from a pinion to a spur gear out to each wheel. The team chose Turnigy TrackStar 17.5T Sensored Brushless Motor 2270KV size 540 motors (177g) since these are a readily available standard size in the remote control vehicles world. The motors chosen can be seen in Figure 29. Brushless motors, though more expensive, are more powerful than brushed motors. They also come with encoders so it will be possible to measure the distance that the rover travels from them.

Each wheel will be powered individually in order to simplify the gearing so that no differential, drive shaft etc. is required. While the motors should have plenty of torque directly, they will be geared down to save power since in general the less torque a motor supplies the more efficient it is. It also allows for a multiplication of torque in the event the robot needs to climb over an obstacle.

Figure 29. The rover will feature four Turnigy TrackStar 17.5T Sensored Brushless Motor 2270KV.

5.1.3 Securing System

While the rocket is in motion, it will be essential to prevent any movement of the rover, which could potentially damage the rover itself as well as unpredictably alter the rocket's flight path. The two shafts attached to the rover that hold the solar panels will be extended into 0.25-inch cube-shaped extensions on the walls of the interior rocket body, the pressure of which will prevent movement in the X-direction. The walls of the cube-shaped extensions will also prevent movement in the Y- and Z-direction. The tire tracks will provide backup restriction in the Y-direction. This coordinate system can be seen in Figure 30 along with the overall securing system.

Other methods of securing the rover were considered, including a sliding rail system and a spring-loaded pin. However, these methods were determined to be too bulky and would add too much weight to the interior of the rocket compared to the team's chosen method discussed above. The "cube and pin" method will be relatively lightweight due to limited added material which also reduces the space needed for the system.

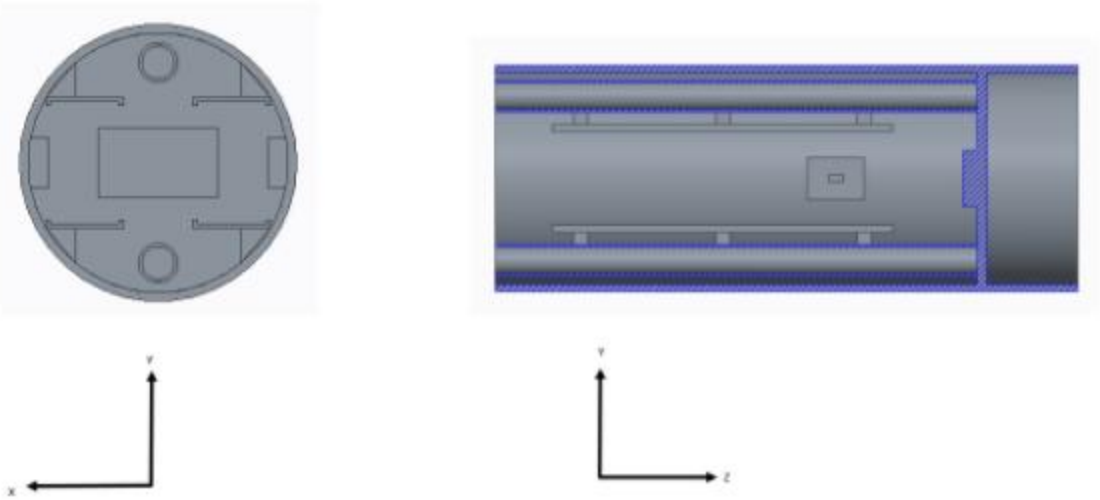

Figure 30. CAD rendering of the securing system, the local coordinate system is listed below each view.

5.1.4 Deployment System

Upon safe landing, the ground station will signal the ejection of the nose cone allowing the rover to exit from the top of the body tube. Deployment will be facilitated by two charges of 6g of black power to separate the nose cone from the payload bay. Charges will be housed in two long PVC tubes that run above and below the rover. The second tube serves as a redundant system for the first. The tubes will run through slots in one bulkhead at the base of the nosecone and end before reaching a second bulkhead closer to the top of the nose cone. The front of the tire tracks will also slide through this bulkhead. The use of these two bulkheads protects the payload bay from the black powder charges so that the only space exposed to the heat and forces of ignition is the void between bulkheads. The charges will be lit via electronic matches that run along the PVC pipes to ignite at the front (top) of the black powder section when they receive a signal from the ground station. The electronics receiving this signal to ignite the matches will be mounted on a bulkhead at the base of the payload bay. Originally, pneumatics were considered instead of black power charges, but black powder charges were chosen because they are more space effective and reliable for providing enough force to successfully remove the nose cone. A diagram of this system can be seen in Figure 31.

Once the nose cone is removed, the rover will drive out of the payload bay on two of the four rails that run parallel to the roll axis and include wells to keep the wheels on track. Systems to forcefully eject or throw the rover out of the payload bay were considered, but using the power of the rover's own drive system was selected because it makes use of actuators already in the payload bay (the rover's motors) thus requiring less additional technology within the payload. The second set of rails run just above the top of the rover's wheels and serves as both a

redundant system in case the payload lands upside down and as a way to minimize motion of the rover during flight.

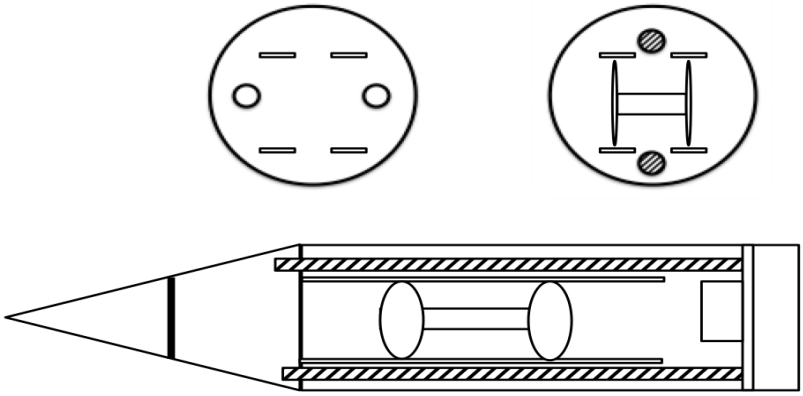

Figure 31. Diagram of the deployment system.

The hash marks represent where the black powder will be located. The top left section is the bulkhead that the PVC pipes and driving rails will slide through into the nose cone. The top right section is a cross section view of the inside of the payload. The bottom view shows the entire system. The electronics is located on the bulkhead at the back of the payload.

5.1.5 Electronic Control System

In order to integrate the various electronic components, the following control system will be implemented. A microcontroller will be used to interface between each of the sections of the rocket to attain the important goals of the rocket: communicate the distance traveled, object avoidance for the rover, and communication of altitude, acceleration, and orientation of the rover to the ground station. The following flow diagram, Figure 32, will be used to control the rocket.

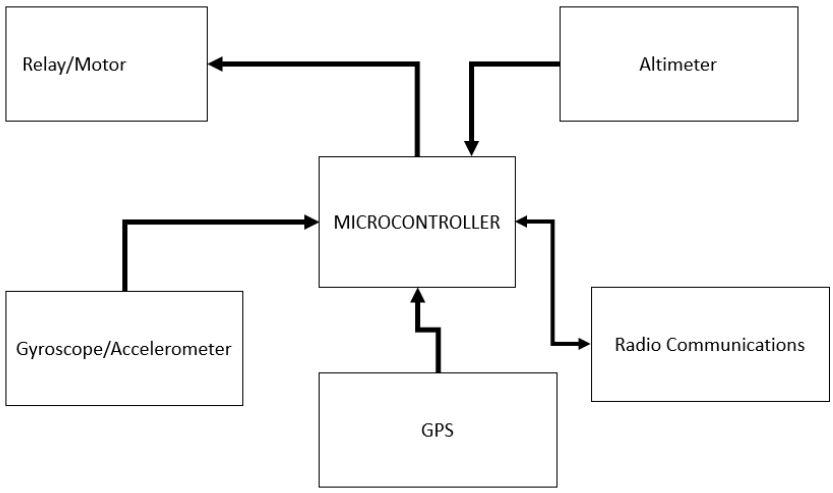

Figure 32. Flow diagram for the electronic control system, arrows point in direction of communication.

5.1.5.1 Microcontroller

For the processor, a PIC32MX795 microcontroller will be used as the control unit for the rover and rocket as a whole. The PIC will be used to complete the major goals of the rover: object avoidance, autonomous movement from the rocket, and communication of important parameters to the ground station. The PIC will be connected as in Figure 33 below.

The PIC was chosen due to the convenience of the IDE, as well as its comparatively low cost and larger number of remappable pins and greater options for customizations. The PIC32MX795 was chosen over other types of PIC's for its large data memory, 128 KB, and program memory 512 KB. A PIC24 was considered, however some of the sensors require 8 byte data streams, therefore the PIC32 was necessary.

For object avoidance, the PIC will have interface with the LiDAR sensor using I^2C. This comes with a JST 6 pin connector, and will be used to reliably connect to the board. In addition, the microcontroller will interface with the other sensors (GPS, altimeter, gyroscope) using SPI. On the first board, I^2C communications will be used in the interest of using fewer wires and simpler troubleshooting; however, in the final printed board, SPI communications will be used wherever possible due to much lower power consumption and easier programming. Using a series of relays and the built in i/o ports, the PIC will also interface with the motors and control the motion of the rover.

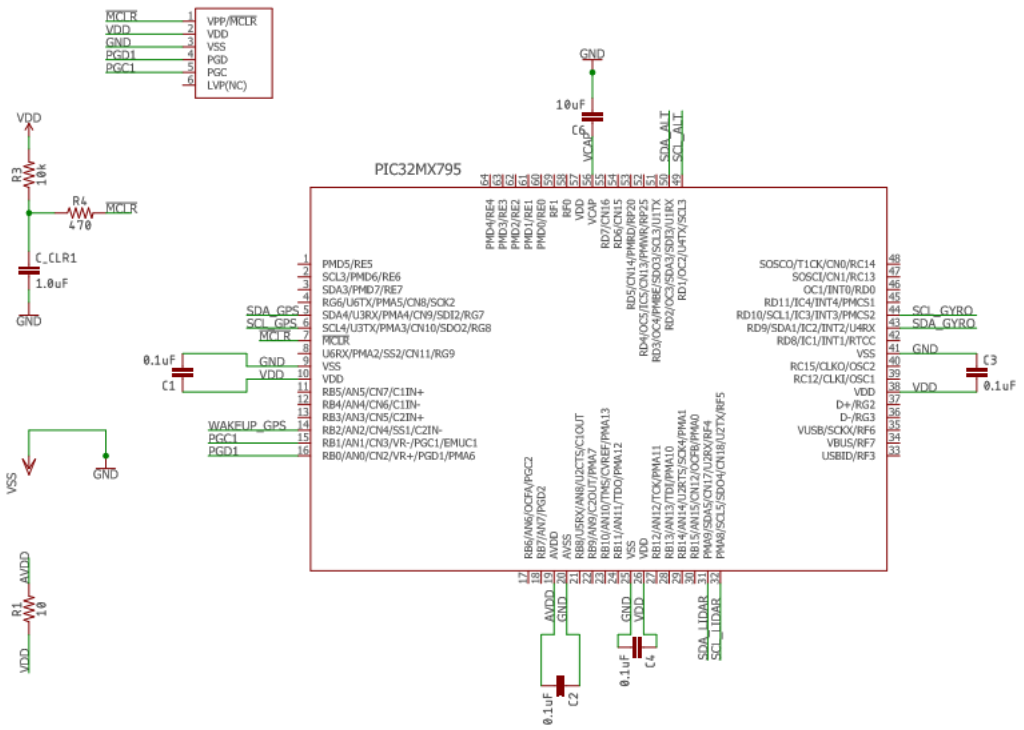

Figure 33. PIC32 power supply and programming.

For the rover, a number of sensors will be necessary to attain the goals of the rover. A section for each of these sensors can be found below. The schematic for the sensor connections can be found in Figure 34 below.

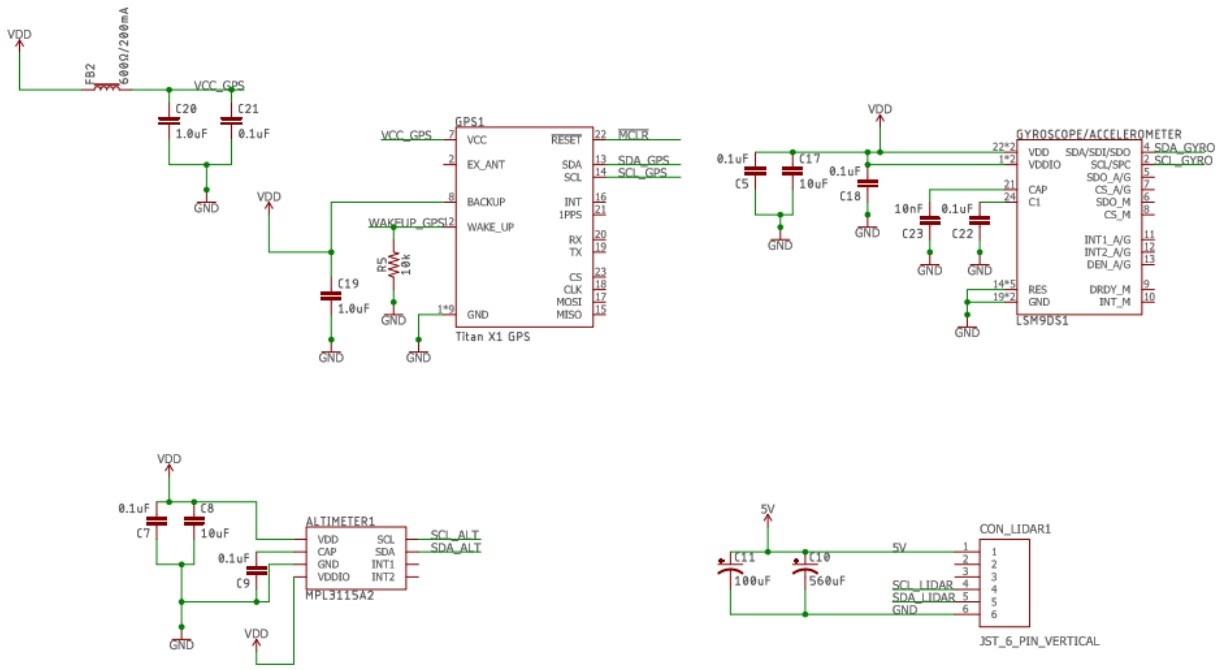

Figure 34. Sensor Schematic for the LiDAR Sensor.

In order for the rover to be able to sense and avoid obstacles while moving autonomously after it is deployed, a LiDAR sensor will be used. The LiDAR sensor will measure the distance and location of any objects by sending out a pulsed laser light that will reflect off any objects and then measuring the reflected pulses. A LiDAR sensor was chosen for obstacle avoidance rather than a sensor such as ultrasonic sensor because LiDAR sensors do not have the same problems with noise interference or adverse conditions that ultrasonic sensors do. Since the conditions during the launch could vary, an ultrasonic sensor whose data could be affected by external noise, wind, rain, fog, or other conditions would not be as robust as a LiDAR sensor.

The LiDAR sensor that will be used is a LiDAR Lite v3 manufactured by Garmin. The dimensions for the sensor are 20 x 48 x 40 mm. This sensor has a range of up to 40 m and a resolution of +/- 1 cm, which will allow for the recognition of many obstacles that could impede the motion of the rover. The LiDAR Lite v3 is powered by a 5 Vdc supply and weighs 22 g.

5.1.5.2 Gyroscope and Accelerometer

In order for the orientation of the rover to be determined once the rocket lands, a gyroscope will be used. This gyroscope will also include a built-in accelerometer that will be able to continuously relay data to the ground station concerning the motion of the rover and, thus, the rocket. The data from the accelerometer will be used to determine when the rocket has landed and come to a complete stop so that the rover can be deployed. Meanwhile, the data from the gyroscope will be used to determine whether the rover is oriented right-side-up or upside-

down as it prepares to exit the rocket. The orientation of the rover needs to be known so that the wheels will rotate in the correct direction (clockwise or counterclockwise) for the rover to exit the rocket and then move autonomously away from the rocket before deploying its solar panels.

The gyroscope/accelerometer package that will be used is an LSM9DS1 manufactured by STMicroelectronics which combines a 3D accelerometer, a 3D gyroscope, and a 3D magnometer. This sensor utilizes an analog supply voltage of 1.9 to 3.6 V and has SPI and I^2C serial interfaces that will be used for communicating data.

5.1.5.3 Altimeter

The altimeter will be used to communicate the current altitude of the rocket to the ground station. The data from the altimeter will be used to check the whether the correct altitude has been attained, and whether the rocket has reached the ground again.

The rocket will use the altimeter MPL3115A2, which was chosen due to its wide operating range, from 20kPa to 110kPa, its high acquisition rate, up to once per second, and its easy I^2C interface.

5.1.5.4 GPS

Each section of the rocket will have an integrated GPS chip in order to check that the rover has moved an adequate distance from the body of the rocket. For the GPS tracking chip, the titan X1 GPS module will be used. It was chosen for its high sensitivity, up to -165dBm. This will allow for very precise location measurements for each of the sections of the rocket. The GPS module will communicate with the microcontroller via a SPI interface.

5.1.5.5 Radio Communications [LoRa™ Modem Network]

The rover deployment will need to be remotely activated. To achieve this, the rover will be equipped with a Microchip RN2483 LoRa™ Modem operating at 868 MHz. An RN2483 in the base station (located at the launch site) will communicate with the RN2483 in the rover, commencing deployment operations. The RN2483 in the rover will then be able to continuously update the ground crew at the base station on the rover's status as it autonomously exits the cargo tube and moves away from the landing site to where it will deploy the solar panels.

5.1.6 Power Control System

The Power Control System is the subsystem that powers the rover. It needs to provide enough voltage and current to drive the four motors and the microcontroller. The motors selected have a max voltage rating of 8V. The microcontroller requires a voltage between 3.3 and

5V. All the sensors used have similar voltage ranges. The LiDAR sensor requires 5V, the Gyroscope and Accelerometer needs between 1.9 to 3.6V, the GPS module requires 3.3V, the Altimeter needs between 1.6 and 3.6V, and the LoRa Modem requires 3.3V.

In addition to supplying the necessary power, this subsystem also has to meet other design parameters such as size, weight, durability, and safety requirements. The system should also be transportable so batteries are an obvious choice. The battery system should be compact, lightweight, and robust enough to withstand vibrations and pressure from the rocket launch.

To meet all these requirements, the Tracer 12V 8Ah Lithium Polymer Battery Pack was selected. This battery has dimensions of 80 x 153 x 49 mm which is well within the size for the rover. The pack weighs only 600 grams and will be able to supply power to the rover for over two hours. The pack comes in a hard shell that protects it from impact. Another nice feature of this battery pack is that it comes with a built in fuel gauge to check the remaining power level. And, more importantly, the pack is UN38.3 certified safe which includes several safety features such as overcharge and over-discharge protection, thermal, protection, over current and short circuit protection.

5.1.7 Base Station

The base station will consist of a Microchip PIC32 and RN2483 (operating at 868 MHz), which will communicate P2P with the RN2483 in the rover and communicate via serial connection with the base station PIC32. The PIC32 will communicate via serial connection with a laptop for easy display of the rover's status as well as a location where the command to the rover to begin deployment can be entered.

5.1.8 Interface

In order to integrate the rover payload into the vehicle, a track system will be implemented. This track system is intended to provide a platform for the rover wheels, restricting any radial and tangential motion relative to the rocket body. It is crucial that the track system is integrated into the rocket body effectively to prevent any undesired displacement of the rover payload during flight. A diagram of this concept can be found below in Figure 35. The system includes a set of tracks for each wheel and triangular supports. The tracks will extend 12 inches, along the length of the rover tube. The triangular supports will serve as the mating connector between the tracks and the rocket body. To adhere the triangular supports to the tracks and the rocket body, RocketPoxy will be used. The epoxy provides high strength bonds for joining the fiberglass and carbon fiber materials of the rocket body to that of the triangular supports, resulting in a robust integration between the rover payload and the rocket body.

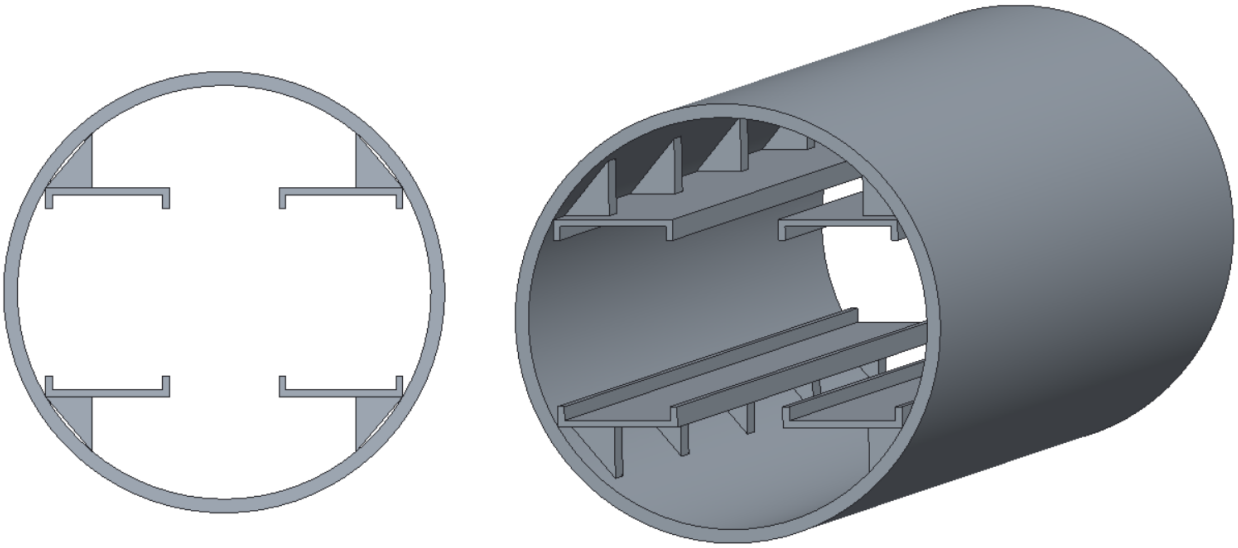

Figure 35. Track system design concept for rover payload interface with rocket body.

5.1.9 Scientific Value

In the current age of space exploration, the rover payload models many of the current aspects of space innovation. A key function of the rover is deploying a set of solar panels. This models the advantages of utilizing solar energy for power during a space mission. Solar power is not only a cost-effective, but also weight effective alternative to traditional fuels, and a highly renewable resource in outer space. As solar technology continues to improve, the applications in space also grow. Solar power has many applications across the space industry from satellites to rovers.

The rover also employs autonomous driving and remote activation. As space exploration continues there will be many circumstances where the human is taken out of the loop. Autonomous driving and remote activation allows for more dangerous missions and extends the range of these missions. As space exploration moving further into the solar system the importance of smart rovers increases. With autonomous rovers, the communication time delay between the rover and Earth is greatly reduced.

5.2 Air Braking System – Selection, Design and Rationale

5.2.1 Overall Design Statement

The purpose of the air braking system is to assist the rocket in reaching its primary goal of an apogee of 5280 ft. To achieve this a control code will use data from sensors to measure altitude and velocity and project a flight path for the rocket. Then a PID controller will determine

the amount of drag force needed to alter the flight of the rocket to an ideal flight path with an apogee of 5280 ft. The controller will then activate a servo motor, which will be connected to a crank-slider mechanism. This mechanism will extend four drag tabs out of the rocket into the airflow, which will be the control surfaces that will induce the drag necessary to reach the target apogee. This system will activate after motor burnout and will run continuously until the rocket reaches apogee. The total system is shown in Figure 36.

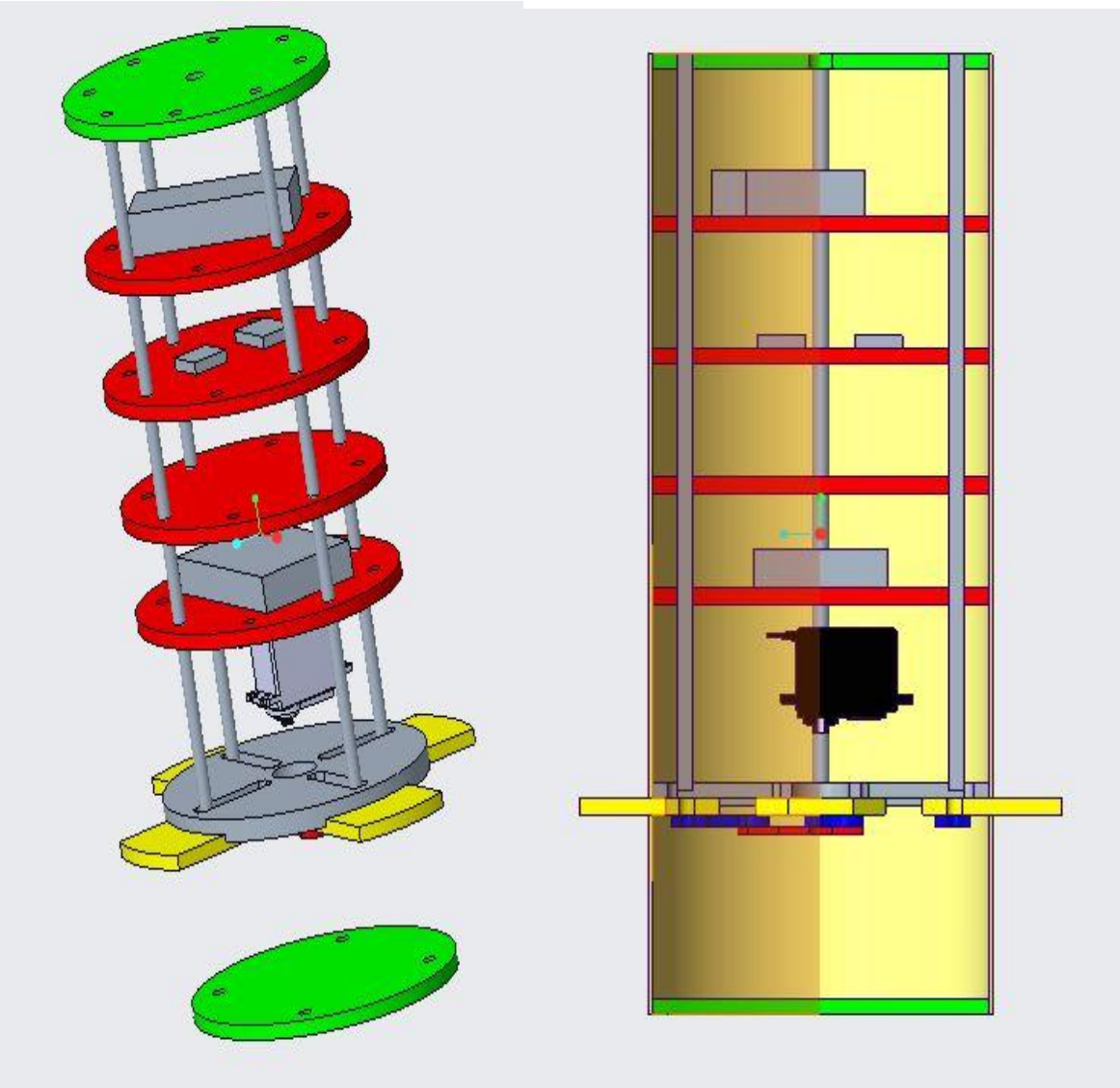

Figure 36. Isometric and cross-sectional views of the air braking system.

The team will design a system that will brake the rocket, placing apogee at 5280 feet. The following is a set of criteria for the system:

1. The system must not create additional moments or instabilities on the rocket.
2. The system must not generate additional thrust along the direction of flight.
3. The system must use a control surface to induce drag.
4. The control surfaces must be aft of the post-burnout center of gravity.
5. The system must not operate during motor burn.
6. The system must be controlled by an onboard flight computer.

5.2.2 Aerodynamics

5.2.2.1 Approximation of Drag Tab Size

Each drag tab area was calculated to be 2 in^2. This value was obtained using the fact that the tabs would be deployed at full extension after motor burnout. This fact allowed for the calculation of the largest tab size needed to stop the rocket at the target apogee of 5280 ft. The calculation was performed using the force balance for the rocket shown in Equation 2.

$$m_{rocket}a = F_{drag,rocket} + F_{gravity} + F_{drag,tabs} \quad \text{Eq. 2}$$

where m_{rocket} is the mass of the rocket, a is the deceleration of the rocket needed to reach the target apogee that was obtained from simulation, $F_{drag,rocket}$ is the drag force due to the rocket itself, $F_{gravity}$ is the force due to gravity, and $F_{drag,tabs}$ is the drag force due to the tabs. The drag forces on the rocket were calculated using the drag equation, Equation 3,

$$F_{drag} = \frac{1}{2}\,\rho\, v^2 C_D, \quad \text{Eq. 3}$$

where ρ is the density of air, v is the rocket velocity, A is the cross sectional area, and C_D is the drag coefficient. To find the drag coefficients, the tabs were approximated as a flat plate and the rocket was approximated as a bullet. According to NASA (footnote here), these approximations This led to the optimum design of four tabs, each with a surface area of 2 in^2 to be positioned axisymmetrically about the rocket.

Because of changes in the density of air, velocity, and other perturbations, the full deployment of the tabs is not necessary throughout the entire time period in which the system will be active. Therefore, a control system will be implemented that will continuously calculate the drag necessary during flight to reach apogee and will adequately change the extension of the tabs, therefore changing the cross-sectional area. The tab was shaped to sit flush with the body tube of the rocket when fully retracted, as shown in the CAD model in Figure 37, which shows the area of the tab the airflow will see.

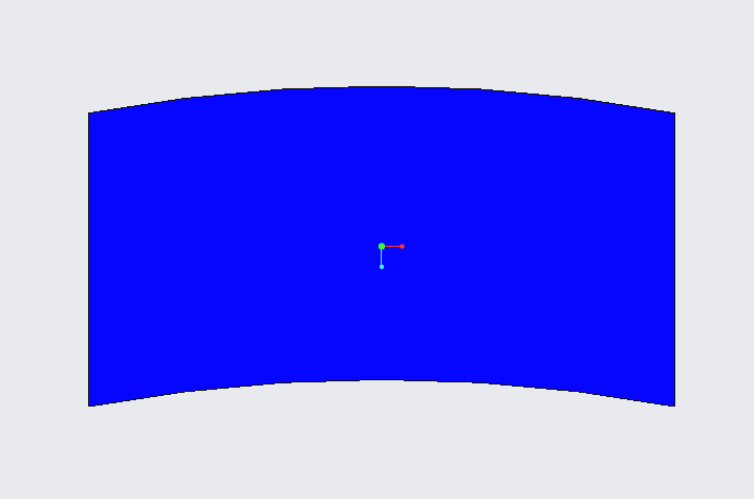

Figure 37. Top view of the area of the drag tab that the flow will see.

5.2.2.2 Drag Tab Materials

Considering an estimated tab area of 2 in^2, the maximum force on each tab was calculated to be approximately 15 lbs per tab, meaning each tab will experience a compressive stress of 7.5 psi. Since this force was nominal in comparison with the yield stress of most typical materials, the choice of tab materials will be decided using factors other than strength. Primarily, these factors consist of machinability, density, friction when in contact with aluminum, and the cost to purchase the necessary quantity. All considered materials and their properties can be seen below, in Table 29.

Table 29. Material Options for Drag Tabs.

Material	Machinability	Density (g/cm^3)	Friction (Static/kinetic)	Yield Stress (psi)	Cost
Aluminum	Very easy	2.7	0.3-1.1	40000	$27.53
Carbon Fiber	Difficult, especially hard to interface (tap holes	~1.6	0.23-0.68 [Friction occurs to splintering from friction]	40000	$95.00
HDPE	Very easy	0.93-0.97	~0.075 [HDPE on steel]	4000	$2.06

Titanium	Easy	4.51	0.41	120000	$157.16

Because of the large density of titanium, the degenerate tendencies of carbon fiber, and the high cost of these materials, both of these options were eliminated. Currently, the team is deciding between aluminum and HDPE tabs, however, in the interest of cost overshoot, the more expensive option (aluminum) will be placed in the budget.

5.2.3 Mechanical System

5.2.3.1 Mechanical Design

Mechanically, the air braking system will consist of four drag tabs deployed by a crank-slider type mechanism. The tabs will be extended and retracted in sync, using the mechanism shown in Figure 38. Pictured in the CAD model, the drag tabs are shown in yellow. The red crosspiece will be driven by the servo motors, and push the tie rods, drawn in blue, which will extend or retract the tabs. The tabs will slide in the slots in the lower plate, drawn in gray. The CAD model omits two of the tabs and tie rods to more clearly show the geometry of the slots, and also omits another top plate that holds down the back edge of the tabs to prevent them from rocking, in order to more clearly show the mechanism.

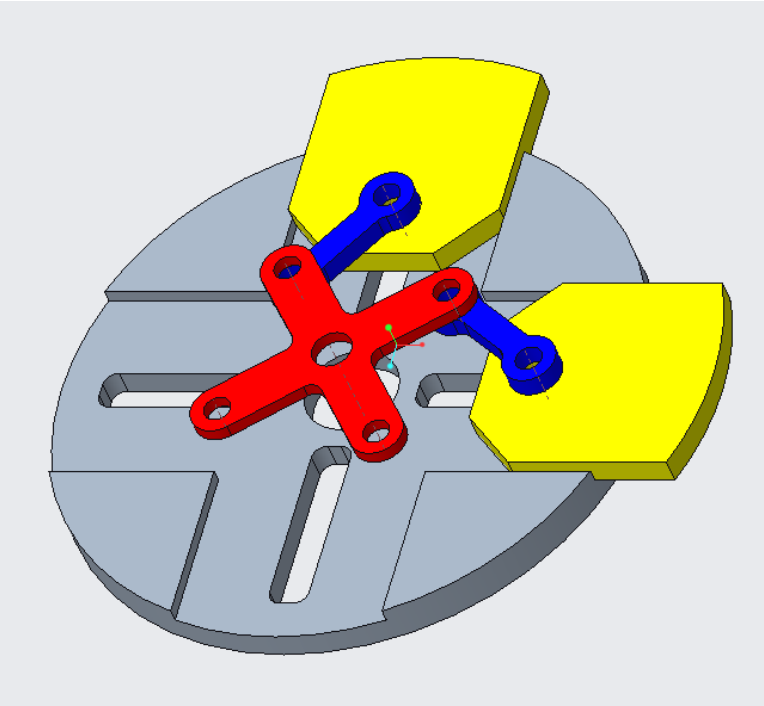

Figure 38. Image of the mechanism prototype.

The team also considered a mechanism using a rack and pinion gear system, powered by a central servo that drove a gear that engaged gear racks on all four tabs. However, that design was ruled out because the tolerances involved in getting the gears to mesh properly would make for a slot that could be too tight to slide the tabs, and because of the number of precise, small parts that would be involved in fitting four rack and pinion pairs into the small space, especially when the tie rod system is mechanically simpler.

5.2.3.2 Dynamic Analysis

To determine the required torque, a dynamic analysis of the system was performed. First, the team analyzed the mechanism using the Vector Loop Method, as described in *Mechanisms and Machines: Kinematics, Dynamics, and Synthesis* by Dr. Michael M. Stanisic. Using this method, the relationship between the servo rotation angle and the tab extension was found in closed form. This relationship is plotted in Figure 39, where zero degrees is the fully extended tab position, and the servo is rotated counter clockwise to retract the tab.

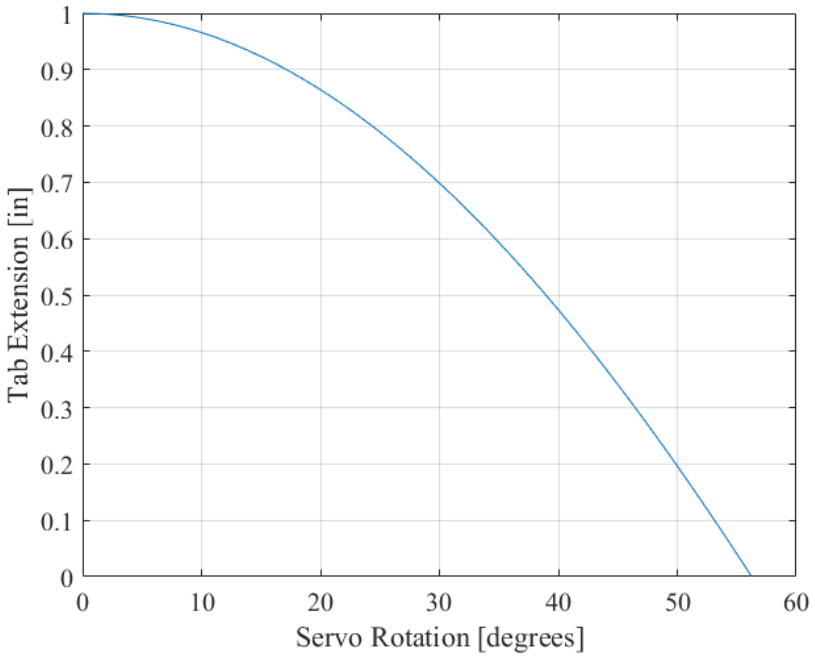

Figure 39. Servo rotation vs. tab extension for the air braking system.

This analysis used a 1.125 in center-center distance (link length) for both the servo arm (the red driven component in Figure 1) and the tie rod.

Calculating the torque required is a complex problem, because the mechanical advantage of the servo moving the tab changes as the system rotates, while the drag force on the tab also changes as the tab extends. Adding additional complexity is the fact that the tabs will cock in the

slot, meaning that the main load, friction, will act on two points on the tab, one of which will move as the tab extends.

Figure 40 shows the forces acting on the drag tabs, from a side view. The wind load varies linearly as the tab extends. Note that this ignores a third friction component caused by the part of the tie rod force that acts along the side of the tab when it is pushed into the slot wall. Also note that as the tab moves, the distance between Normal Force 1 and the rocket exterior change, which was also accounted for in the model. The Tie Rod Force drawn is the component that lies in the plane of the drawing, but in reality the force acts along the tie rod, which is treated as a two-force member. The model assumes simple point contact friction, using a coefficient of friction of 1.2, for dry aluminum-on-aluminum friction.

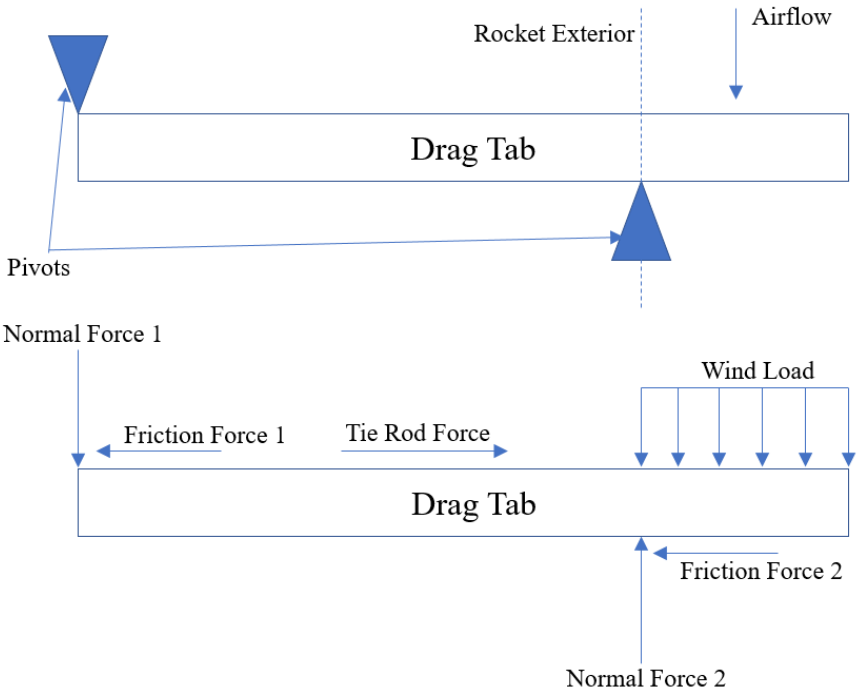

Figure 40. Drag tab free body diagram, side view.

Figure 41 describes the behavior of this friction model. The wind load in Figure 3 is expressed as the drag force, and is treated as acting halfway out on the extended portion of the tab. The friction force is the sum of the two friction forces that act on the top and bottom of the tab, and the tie rod force is the force that acts along the two-force member tie rod, which includes the previously described third friction force from the slot wall. This tie rod force is the force necessary to overcome static friction in the system, so it is the required force to be exerted on the tie rod by the driven crosspiece.

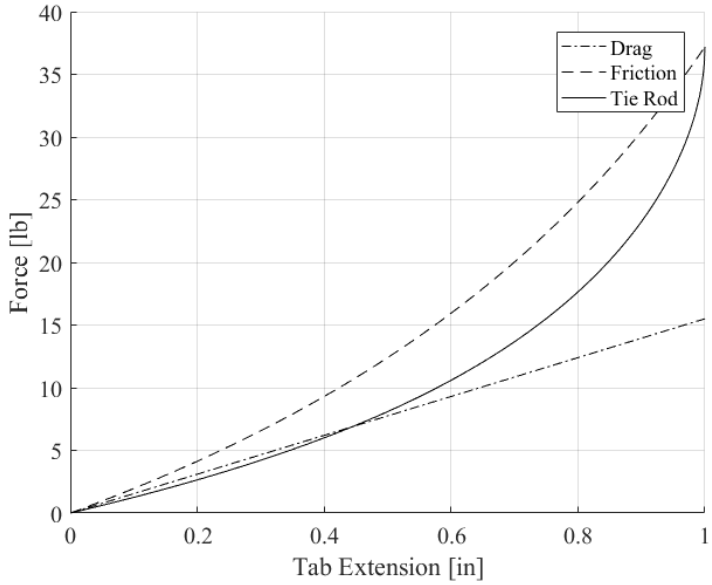

Figure 41. Drag, friction, and tie rod forces as a function of tab extension.

The tie rod force will be created by the torque exerted on the cross piece. Figure 42 shows the relationship between required torque and tab extension. This model assumes the worst case scenario (ie. maximum rocket velocity) and is for a single tab. The system behaves as expected. As the tab extends, the static friction force increases from an initial value of zero, while the rotation changes the position of the system and increases mechanical advantage. As the extension, and therefore drag force, increases, so does the required torque, until the extension approaches its maximum value. Towards this maximum, the mechanism approaches infinite mechanical advantage, such that at max extension it can, in theory, overcome an infinite static friction force, which is why the required torque drops back to zero.

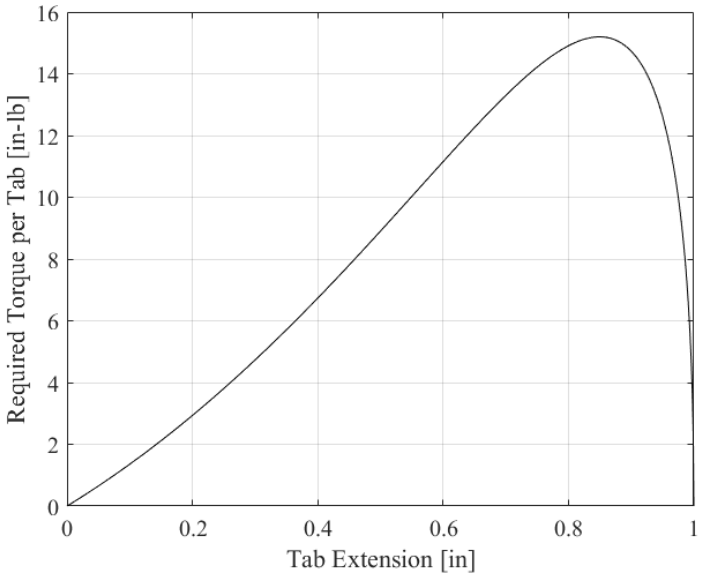

Figure 42. Required torque as a function of tab extension.

The final result from this analysis shows that the system will require a maximum torque of 15.5 in-lbs at the worst case to still be able to function, for a single tab. Multiplying by four tabs and converting to a servo catalog-friendly unit, the system overall needs to be able to provide at least 992 oz-in of torque in the worst case. After final component selection, the system will be able to provide this much torque plus some extra overhead for safety. Note that this value will significantly decrease if the payload is lubricated, but dry friction was considered as a worst-case scenario just in case. This analysis will be expanded upon following PDR, pending component selection and more specific mechanism design.

5.2.3.3 Mechanism Components and Materials

The success of the overall mechanism is dependent on the materials chosen for each part, including the servo horn, tie rods, and lower plate.

Servo horn options are typically limited to HDPE and aluminum, and sometimes horns are included with purchased servos. As the correct extension of the tab is critical to achieving the correct apogee, it is desirable that the horn flex very little while supplying the force to the tabs. To this end the group will use an aluminum servo horn in hopes of maximum extension accuracy. With respect to sourcing, the team could either machine a horn to exact size, or purchase a premade horn. While an in house fabrication would provide the exact desired dimensions for the team, it would also cost more overall. Oppositely, a commercial horn will provide a lower cost but possibly undesirable dimensions, therefore, the team is still considering both options.

The team has decided to purchase a commercially available tie rod product because they are cheaper overall and will provide less friction than machined tie rods. Although tie rods do not present a host of materials choices, they do present options with respect to configuration. The various tie rod types include: fixed length, threaded variable length, and tie ends. Fixed length tie ends provide the most in flight security, but similar to the commercial servo horns, could result in undesirable dimensions in the overall. Threaded tie rods offer somewhat less security due to vibration, which could lead to uneven extension and an unpredicted flight path. Finally, tie ends, if unthreaded, allow for very precise lengths to be cut, and can be almost as secure as fixed length rods if secured properly by welding or another process.

The lower plate, for the same reasons as discussed in the drag tab discussion will likely be made out of either aluminum or HDPE with aluminum again being the more expensive option. Because multiple options are being considered for the servo horn, tie rods, or lower plate, therefore the budget will reflect the most expensive combination of these choices.

5.2.4 Electronics

5.2.4.1 Servo Motor

The primary concerns in selecting a servo motor will be torque output, power needs, speed, and the weight. The maximum torque that the motor will need to provide is approximately 1000 oz-in. The servo's power needs must stay in a range that can be accommodated by a power supply inside the rocket when producing this max torque. Closely related, the servo must be small enough and light enough to be incorporated into the rocket itself. The servo's speed will directly affect the efficacy of the control algorithm, so this criterion must also be taken into account. The team is considering using gearing to increase the motor torque. However, increasing the gear ratio will cause slower drag-tab movement.

Due to budgetary constraints, the team is also considering using two servo motors operating in tandem. This will allow us to meet the torque requirements at a much lower price.

In general, digital servo motors provide greater accuracy and greater torque than do analog motors. Therefore, only digital motors will be considered. Three servos have been selected for consideration. Table 30 lists their relevant specifications.

Table 30. Comparison of different servo motor options.

Motor	Stall Torque (oz-in)	Operating Voltage (V)	Current at Stall Torque (A)	Speed (sec/60°)	Size (in)	Weight (g)	Cost ($)
FEETECH FT5335 (use 2)	550	7.4	9	0.18	2.47 x 1.28 x 2.20	180	$40.00
Power HD 1235MG (use 2)	560	7.4	9	0.18	2.34 x 1.16 x 2.14	170	$60.00
Hitec HS-1005SGT (use 1)	1167	11.1	6.5	0.19-0.26	2.52 x 1.3 x 2.87	363	$400.00

The FT5335 and 1235MG motors are almost identical. The main difference is the FT5335 has bushings supporting the output shaft while the 1235MG output shaft is supported by ball-bearings. Both feature metal gear trains which are more durable than the plastic gears often found in small servos. Both of these options will require two identical motors working together to produce enough torque. The third option, the HS-1005SGT, can produce enough torque on its own, however, it is much more expensive than the other two options. For this reason, the team is leaning toward either the FT5335 or the 1235MG.

5.2.4.2 Sensors

As this system is concerned with the rocket's velocity, altitude, and acceleration, the primary sensors that will be utilized are a barometer and an accelerometer. Data from these sensors will be used by the control algorithm to determine the necessary extension in the drag tabs. Therefore, sensor range, precision, and output rate were the key factors used to determine the best sensor options. For accelerometers, the ADXL345 meets these requirements. Its range of ±16g is greater than the maximum of 7-13gs which has been recorded in previous years during engine burn, its resolution is approximately 0.004 gs, and it has a maximum output data rate of 3200 Hz. Since the rocket is using a more powerful engine this year with a greater potential peak acceleration, the ADXL 377 is also under consideration due to its ±200g measurement range.

Overall, however, the ADXL 345 is more favorable for this application because of its greater precision. These results and other relevant information are summarized in Table 31.

Table 31. Comparison of different accelerometer options.

Sensor	Range (±g)	Resolution (g)	Output Rate (Hz)	Weight (g)	Size (mm)	Cost
ADXL 345	16	0.004	3200	1.27	25x19	$17.50
ADXL 377	200	0.1	1300	1.27	19x19	$24.95

In terms of barometers, the BMP 280 is the primary model currently under consideration. It has an output rate of 157 Hz, a resolution of 1.3 cm, and a noise level of 11 cm. Most importantly, it performs onboard pressure to altitude conversion, which saves significant data processing time for the control algorithm. Another model which fulfills the basic requirements is the MPL3115A2, which contains onboard altitude calculation along with an output rate of 100 Hz, a resolution of 30 cm, and a noise level of 30 cm. This data is summarized, along with other information, in Table 32.

Table 32. Comparison of different barometer options.

Sensor	Resolution (cm)	Noise level (cm)	Output Rate (Hz)	Weight (g)	Size (mm)	Cost
BMP280	1.3	11	157	1.3	19.2x18	$9.95
MPL3115A2	30	30	100	1.2	18x19	$9.95

Along with an onboard barometer and accelerometer, the team is exploring the possibility of running data lines from the Featherweight altimeters in the CRAM system to the Air Breaking System. This would allow the system's control algorithm to track and affect the rocket's altitude as measured by the same standard by which the rocket itself will be judged.

5.2.4.3 Circuit Board

The team will utilize a printed circuit board (PCB) to simplify wiring inside the body of the rocket. The board will consist of simple transistor circuit to control logic interface between the servo motor, power supply, and microcontroller. A PCB is desirable over point-to-point wiring all of the connections within the rocket because it is less likely connections will come loose during flight, landing, or transport when all connections are secured to the board. In addition to being a more robust design, creating a PCB reduces the risk of design errors in the final circuit compared to point-to-point wiring because everything is laid out on a digital schematic before actual components begin to be wired together.

While it is clear the PCB is the best choice for wiring components within the rocket, multiple options exist for how to procure the actual board. One option is to create a custom board in-house. This gives advantages of no lost time waiting for the board to ship, and the option to redesign a new board quickly if a required change is discovered. Ultimately these pros are outweighed by increase in the time it would take to devise a method of cutting the board with our current tools, as well as procuring the individual materials to construct the board. Additionally, there is a greater risk for a waste of materials due to errors in the amateur manufacturing process.

The better option is to order a custom PCB from a supplier. The key aspects of a good PCB manufacturer is a low minimum order quantity and domestic manufacturing to shorten the lead time. The most promising such manufacturer is OSH Park. The team has ordered from them in the past, and they have proven to be reliable and prompt due to their location within the United States (Oregon). Their minimum order quantity is 3 PBCs, so there will not be much waste, but some margin for an easy drop-in replacement in the case of bad soldering or broken board components. Another benefit of this company is that they will create the board based on an uploaded .brd board file from CADWROK's Eagle 7.70 software, among other file types. Eagle has been used successfully by this team in the past. A second option is 4PCB from Advanced Circuits. They also make their boards in the US and are hold an advantage over OSH Park with no minimum order quantity. However, two major downsides from 4PCB are that each order is price quoted individually, making budgeting difficult, and all designs must be finalized in special software approved by Advanced Circuits, requiring an additional learning curve over sticking with Eagle.

Space and other constraints and restrictions will be taken into account when designing the PCB. The pricing structure from OSH Park is by square inch so it is advantageous to keep the board small. A realistic design goal would be a board that is 2.5 in by 2.5 in. This would fit easily within the rocket while still having room for all the required components. The board will also make use of Molex connections between the larger components such as the servo motor, power supply, and microcontroller to eliminate the need to de-solder many of these connections to interchange a failing part. These Molex connectors and other various circuit components will need to be ordered separate from the PCB and incorporated into budgeting.

5.2.4.4 Microcontroller

We will use the circuit board to integrate information from sensors to identify the rocket's position in 3D space, along with other variables such as angle, speed, and acceleration. The microcontroller will be used to gather this information and calculate the appropriate actions needed to adjust the rocket's flight path. Finally, the microcontroller will control a servo to adjust the drag tabs to the appropriate positions. The choice of microcontroller is highly dependant on the needs of the software and algorithm design. All choices selected are compatible with arduino libraries to use in algorithm programming.

The primary concerns for circuit board choice are clock speed, SRAM, and Operating Voltage. 16 MHz is the preferred speed for faster processing. As for the SRAM, all the listed options in Table 33 should provide enough SRAM for the control algorithm. Preferred operating voltage is 5 Volts or above to decrease the amount of noise in the signals. All of the listed options should also provide enough I/O for sensors and servo motor control.

Table 33. Comparison of microcontroller options.

Name	Arduino Uno	Teensy 2.0	Teensy++ 2.0	Feather 32u4 Basic Proto
Price	$24.95	$15.95	$24.00	$19.95
Microcontroller	Atmega328	ATmega32u4	AT90USB1286	ATmega32u4
Clock Speed (MHz)	16	16	16	8
Memory (KB)	32	32	128	32
SRAM (KB)	2	2	8	2
Operating Voltage (V)	5	5	5	3.3
# Digital I/O pins	14	25	46	20
# Analog Input pins	6	12	8	10

# PWM output pins	6	7	9	7
Footprint (mm)	75.14 x 53.51 x 15.08	30.5 x 17.8	50.8 x 17.8	51 x 23 x 8

Currently the Arduino Uno and Teensy 2.0 are considered the favored options. The Arduino Uno provides sufficient specifications for a reasonable price, and provides the advantage of developing with the Arduino libraries directly with an Arduino board. However, the Teensy 2.0 is also under serious consideration due to its significantly lower cost and smaller physical footprint on the payload, despite having similarly powerful specifications, which may ultimately outweigh the advantages of the Arduino Uno. If higher memory capacity is desired depending on the algorithm design, a Teensy++ 2.0 would be a strong option.

5.2.4.5 Batteries

Batteries will be used to power the servo motors controlling the fins. A custom PCB is in consideration, and a switch will likely be used to control connection of two batteries to the two servo motors. Two batteries will be used to power the servo motors. The estimated power needed is for a 7.4 V battery capable of sustaining up to 9 A, providing approximately 140 W total per the specifications of the servos under consideration. Diodes will be needed to prevent any back Electromotive Force (EMF) from the servo motors. Also, a smaller capacity battery, such as a commercial battery holder with four AA batteries for 6 V, separate from the servo power supply will be used to power the microcontroller.

Seven options for batteries are listed in Table 34. A final decision has not yet been made, but preference is being given to the Tenergy 30C Li-ion battery. The Tenergy battery provides sufficient power specifications at 7.4 V and 2200 mAh with a max current of 66 A, which should be sufficient for the power needs of the servo motor. Its weight and physical dimensions are acceptable for the size of the rocket and its price is low. The smaller King Max Li-ion battery is also under serious consideration because of its lower weight and price, and smaller dimensions; however, its lower capacity may require multiple batteries, which offsets these benefits. Primary concerns going forward is to better determine a reliable company to serve as our battery supplier.

Table 34. Comparison of battery options.

Battery	Voltage (V)	Quantity	Capacity (mAh)	Max Current (A)	Weight (kg)	Dimensions (mm)	Cost Per Item
King Max Li-Ion	7.4	1	2200	66	0.206	138.5 x 47.5 x 24.5	$15.95
Tenergy LiPO	7.4	1	2700	27	0.113	105 x 34 x 16	$14.99
Tenergy LiPO w/Traxxas Connector	7.4	1	5200	312	0.293	139 x 47 x 23.9	$54.99
Zippy Flightmax	7.4	1	5200	156	0.314	137 x 46 x 25	$22.18
King Max Li-Ion (small)	7.4	1	1000	25	0.085	70 x 35 x 18	$9.95
Tenergy Li-ion	7.4	1	2200	4	0.099	72 x 38 x 19	$15.99
Tenergy 30C Li-ion	7.4	1	2200	66	.104	82 x 32 x 18	$14.99

5.2.5 Control Code

5.2.5.1 General Code Architecture

In order to reach a target altitude with the aid of an air-braking system, the drag tabs must be deployed in a predictable and controlled manner. To this end, onboard calculations will be run continuously to determine the necessary resistive force to be generated via the drag tabs to lower the rocket's speed, and subsequent commands will be issued to the servo to physically extend or retract the tabs accordingly. The calculations will be performed by the chosen microprocessor in real time and adjust the drag tabs accordingly. Only by performing these tasks quickly, reliably,

and accurately can the air-braking system hope to achieve its goal of lowering the projected altitude down to its target value.

The determination of the amount by which to extend the tabs is informed by measurements from instruments on the rocket, namely a barometer and/or accelerometer as discussed in the next section. These sensor readings allow for the control code to determine the rocket's current speed and thus predict the apogee given the current conditions. This prediction, combined with an estimate for the speed needed to reach the target altitude, enables the code to calculate how far to extend the tabs in order to decelerate the rocket as needed.

Although the tabs will not be extended until after burnout, the code will need to monitor the kinematics of the rocket beginning at launch. Thus, sensor readings (most likely from a barometer) will be monitored during powered ascent by the code, but commands to extend the tabs will not be issued until the coast phase of the flight. Once the recovery system deploys, the task of the air-braking system is complete, so the tabs will then retract fully into the rocket and the control code will cease operating. An overview of the control algorithm is shown in the flowchart Figure 43 below.

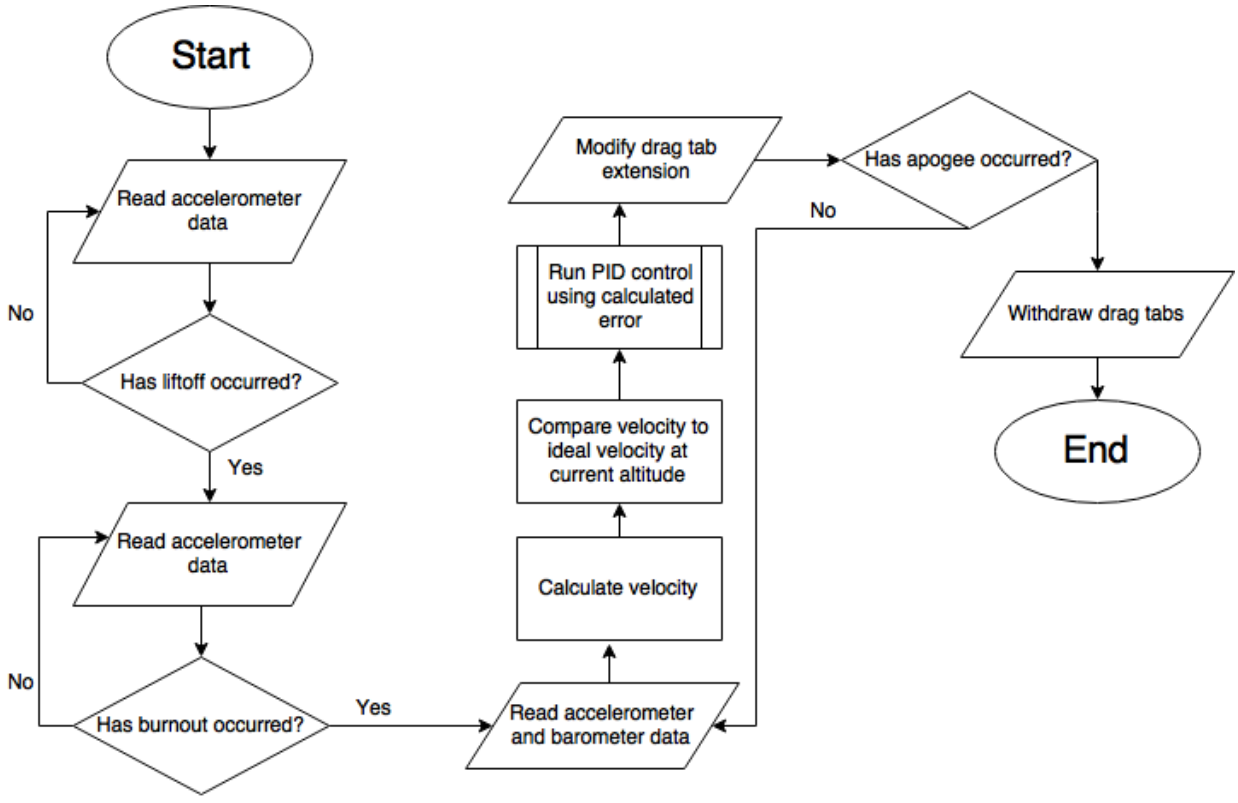

Figure 43. Flowchart describing the control code architecture.

5.2.5.2 Sensor Data Processing Algorithm

The error value which the PID controller will utilize is based on vertical velocity at a given altitude, since that is the measurement most directly related to the rocket's apogee. Therefore, the control algorithm will need to have highly precise information about the rocket's vertical velocity throughout the coast phase, which could be measured in several ways. The three options initially under consideration were integrating acceleration measurements from an accelerometer, differentiating altitude measurements from a barometer, or directly measuring airspeed using a pitot tube. The latter option, while providing the most direct measurements, is particularly prone to error due to the rocket's horizontal velocity, and would also have an impact on the rocket's aerodynamics. Therefore, the pitot tube method has been ruled out, although indirect methods with both an accelerometer and a barometer are still under consideration. Integrating an accelerometer would provide data at a faster rate, since the commercial accelerometers under consideration can output data at 3200 Hz, but this method is also more susceptible to long-term imprecision since each velocity calculation relies on the accuracy of the previously calculated velocity. Differentiating a barometer resolves this problem, since each calculated velocity is independent of previous calculations. However, the data output rate of the primary barometer under consideration is 157 Hz, and requires a multiple-point linear regression to offset the effects of sensor noise. Both methods have been tested using a control algorithm simulation, and under ideal conditions each reliably allows the rocket to get within 10 ft. of the target apogee. However, accelerometer-based calculations become inaccurate with a launch angle more than 8° from vertical, while barometer-based calculations are more generally susceptible to noise. Currently, the team's simulations have shown the most success and adaptability by initially calculating velocity based on barometric data, then switching to accelerometer-based calculations after burnout.

5.2.5.3 PID Control

The control algorithm will utilize a PID controller to determine the necessary drag tab extension throughout flight. The error measurements fed into this controller will be error in velocity at a particular altitude, since the rocket's velocity and altitude most directly predict its apogee after burnout. Therefore, the algorithm will have a pre-loaded buffer of “ideal” velocity and altitude data, which will be compared to the current sensor data in-flight to calculate error. The PID controller will then calculate the proportional, differential, and integral components of this error- the proportional component responds to current error, the differential component responds to predicted future error, and the integral component accounts for all previous error. These three terms are then summed to produce an output position for the servo motor. So far, the controller has been manually tuned using the results of a control algorithm simulation to have a proportional coefficient of 1.9, a differential coefficient of 0.1, and an integral coefficient of

0.001. These values will undergo more precise tuning when the algorithm is implemented on hardware and linked to the servo motor.

5.2.6 Integration

The air braking system will have four evenly-spaced threaded rods running all the way down the system, which will be attached to the forward bulkhead. Four low-strength steel threaded rods will be used, with a thread count of 10-32 and ordered at a length of 1 ft, to be cut to an appropriate size during construction. These rods will be used because the team does not want them to add significant weight to the rocket, but they need to be strong enough to hold their components. These rods will secure the batteries, circuit board, microcontroller, and the upper aluminum plate in place within the air braking system. The two servo motors will be connected to the upper aluminum plate, which will have a cutout in the center to accommodate the shafts. The aluminum plate will have a diameter of 5.255 inches. An 8 inch by 8 inch plate with a ¼ inch thickness will be cut to these dimensions. This size was chosen so various copies of the plate can be made in case of a mistake during construction; the thickness was chosen to ensure the plate is strong enough while saving weight. The team is also considering using a HDPE plate, but since aluminum is heavier and more expensive, our current assumption is that this will be our material. For each of the components, there will be a wooden disk with four holes cut around the outside, which the threaded rods will run through. The wooden disks will be secured to the steel rods with washers, and the components will be individually screwed onto the wooden disks. To secure the rods into the upper plate, we will tap a hole halfway through it and screw the rods in.

The total system itself will be integrated using a method that the team has had success with in the past. All of the components will fit inside of a coupler made of a 1/16” thick phenolic tube, which will be used because of it is an easy material to work with during construction. Two bulkheads will be epoxied to each end of the coupler to provide additional structural integrity to both the air braking system and the body tube. These bulkheads will be made of fiberglass, as it is very strong while minimizing weight, and will be 5.255 in in diameter and 0.25 in thick. The diameter is determined by the inner diameter of the coupler. The coupler, and therefore the system, will connect the section of the body tube carrying the parachute with the fin can. The body tube section carrying the parachute will attach to the coupler using plastic shear pins, which will hold the sections together until the ejection charges are fired, after which they will break and allow the sections to separate. The coupler will be mounted to the fin can using a different method. Four threaded rods, each 0.25 in in diameter, will be attached to a bulkhead in the fin can using nuts and epoxy. These rods will extend through the air braking system through the forward bulkhead. Both the forward and aft bulkheads will use nuts to secure the coupler and system in place on the rods.

5.2.7 Simulation and Testing

5.2.7.1 Control Algorithm Simulation

A simulation of the control algorithm was implemented, first in an Excel spreadsheet, and then as a code in C++. It initially only modeled the rocket's flight using kinematic equations and drag, and then expanded to include a PID controller which modified the CDA component of drag force given a comparison "ideal" flight. Further iterations of the simulation were developed to take into account sensor noise, launch angle, movement time in the drag tabs, and other factors which could impact the rocket in a real-world flight. These simulations allowed the team to visually track how the control algorithm would respond to potential perturbations, through output graphs such as Figure 44 below. This graph shows the control algorithm's response to an engine impulse larger than predicted. Over the course of the flight, the rocket re-approaches the ideal velocity curve in steps, and in this case reaches an apogee of 5271 ft.

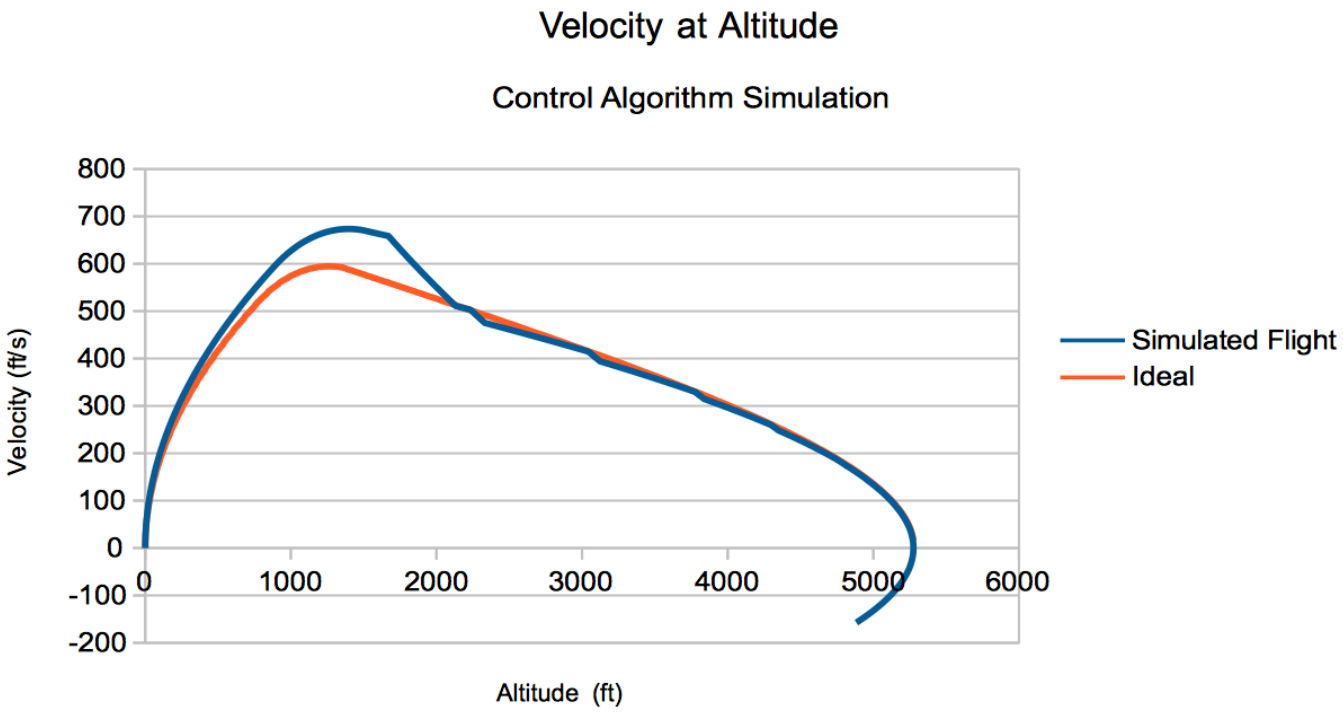

Figure 44. Control Algorithm Response to Engine Impulse Larger than Predicted.

These simulations have also been used to approximate the area of each drag tab and the maximum pressure on each tab, compare the reliability of different sensor data processing algorithms, and note the impact of various real-world conditions on the algorithm's precision. Most notably, these simulations have identified the drag tabs' movement time as the most significant factor of the algorithm's success, as even a 0.25 second propagation delay reduces the rocket's precision to within 100 ft. of a mile.

5.2.7.2 ANSYS Fluent Simulation

A flow simulation using ANSYS Fluent will be used as another method of determining the drag force due to the tabs and of modelling the behavior of the flow around the drag tabs and the rocket as a whole. This will be done be developing a grid around a 3D model of the rocket and using the velocity, acceleration, and other flight conditions predicted by OpenRocket simulations. This model should tell us information not only about the forces on the rocket, including the drag induced by the air braking system, but also about the behavior of the boundary layer and the separation of the flow as it passes over the tabs. The results of this simulation may alter the drag tab design and placement on the rocket.

5.2.7.3 Solid Mechanics/Finite Element Method Simulation

To ensure the stability of the aluminum tabs under loading conditions, a simple solid mechanics analysis was conducted. From the free-body diagram in Figure 45, shear diagrams were plotted to find the maximum shear stress for various tab extensions.

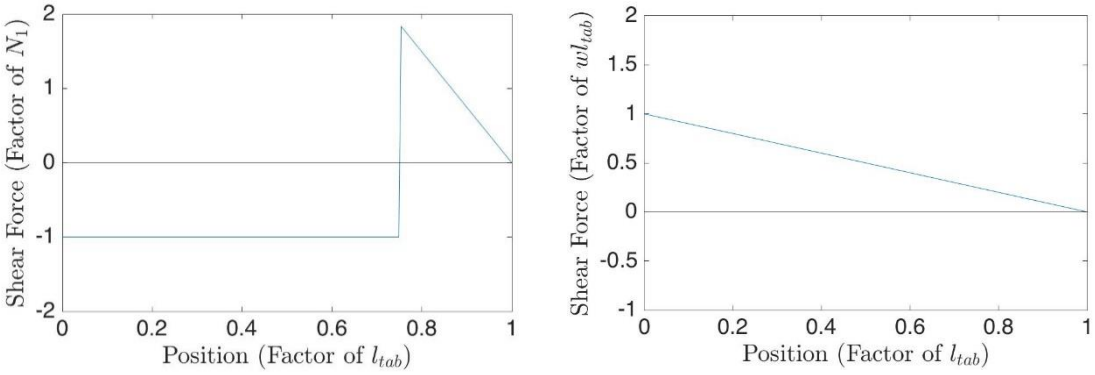

Figure 45: Left: Shear diagram for an arbitrary tab extension l_{out}. In this particular shear diagram, lout=0.25 l_{tab}. The shear force was calculated as a factor of Normal Force 1, N1. Right: Shear diagram for maximum tab extension $l_{out} = l_{tab}$.

The tab will be subject to the greatest external force and thus the greatest shear force when the tab is fully extended. From Figure 6, the maximum shear force will be wl_{tab}, where w is the wind force per unit length and l_{tab} is the length of the tab. Assuming the wind force to be 15 lbf per tab, l_{tab} = 1 in, thus w = 7.5 lbf/in, the maximum shear force will be 7.5 lbf. As the yield strength of aluminum is 4104psi and the Young's modulus is 10106psi, the elastic deformation will be negligible.

5.2.8 Subscale Testing

One of the primary factors in the efficacy of the air braking system is the drag coefficient of the drag tabs. In the calculations and designs above, they are being approximated as flat plates extended into the flow, which gives a drag coefficient of 1.28 according to NASA's website. To better determine the drag coefficient, wind tunnel testing will be performed on the subscale test rocket. The tabs will be scaled down by 40% and will be set on a ring with the same dimensions as the subscale body tube. This tab system, shown in Figure 46 will be 3D printed and placed into the body of the subscale rocket. The wind tunnel will be run once with the tabs on the subscale rocket and once when they are not. The subscale rocket will be attached to a force transducer which will measure the total drag force on the rocket in both states. By subtracting these two forces, the drag due to the tabs can be determined. Then using this force in the drag equation, and also knowing the area of the tabs, airspeed in the wind tunnel, and density of the air in the wind tunnel, a more precise drag coefficient for the designed tab shape can be determined.

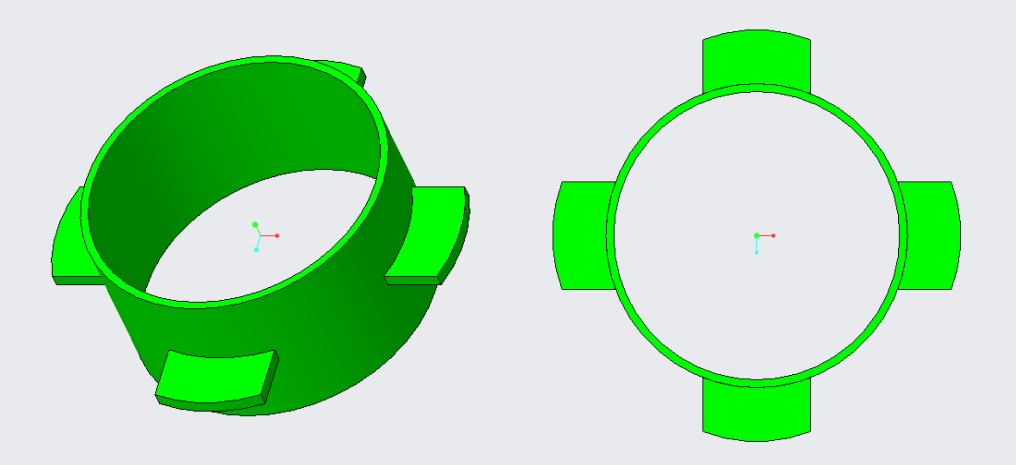

Figure 46. Subscale drag tab model to be 3D printed and used for wind tunnel testing.

6 Project Plan

6.1 Requirements Verification

A set of requirement verification charts for the general rocket and for each subsystem can be found in Appendices J through N. Each table states the requirement, the verification method and the status of the verification as of the PDR submittal.

6.2 Budget

Detailed line item budgets for each sub-team can be found in Appendix O. This includes the expected budgets for the four technical sub-teams as well as for the anticipated educational outreach events.

6.3 Funding Plan

Table 35 below summarizes the intended budget plan for the 2017 – 2018 competition year.

Table 35. Annual budget for each sub-team.

Allocation Group	Budget
Vehicle Design Sub-team	$ 4,000
Recovery Systems Sub-team	$ 800
Deployable Rover Sub-team	$ 1,200
Air Braking System Sub-team	$ 800
Rocket Subtotal	**$ 6,800**
Educational Outreach Events	$ 300
Miscellaneous	$ 300
Competition Travel	$ 5,000
GRAND TOTAL	**$ 12,400**

The costs shown in Table 35 can be accounted toward the following items:

Vehicle Construction and Propulsion: These costs account for all materials that will be used to build the launch vehicle as well as for the motors used in all launches.

Recovery System: The recovery costs include all parachutes, altimeters, 3D printed materials and all items necessary for a safe and robust integration into the vehicle.

Deployable Rover Payload: The costs associated with the experimental payload include all materials, wheels, solar cells, rover motors, all electronics and items needed to ensure a safe and successful integration.

Air Braking System: The costs for the extra payload account for all materials, electronics, servo motors and 3D printed items needed.

Educational Outreach: These funds are set for use during educational and community engagement events, and are planned to be used to purchase Estes rockets with kids.

Miscellaneous: In this category are costs for posters and other items associated with a professional team image and presentation.

Travel: All costs associated with traveling are included in this number including transportation, food and lodging.

Currently, all sub-teams are below their budget, which can allow more people to attend the competition as part of the travel budget. The Notre Dame Rocketry Team draws funding from two main sources. The first is from a general account dedicated to aerospace design projects at the University. Support for this fund comes from a wide variety of sources, including the College of Engineering, the Department of Aerospace and Mechanical Engineering and generous donors. The fund is replenished annually as deemed necessary by University faculty and staff.

The second source is from sponsorship by The Boeing Company. The team is working hard on securing corporate relations with different aerospace companies, and Boeing has been a pioneer with the Notre Dame Rocketry Team in this effort.

6.4 Timeline

Following a project schedule is crucial in any engineering design, test and building process. For this reason, the Notre Dame Rocketry Team is committed to abiding by the detailed schedule in Appendix P for the entire NASA Student Launch Competition.

Appendix A: Safety Agreement

(The following is the safety agreement that all team members have signed)

By signing below, I agree to abide by all regulations, standards and guidelines set forth by the National Association of Rocketry. I have read and understand the High-Powered Rocketry Safety Code and will follow all rules outlined within the code. I am cognizant of all local, state, and federal laws regarding the regulation of airspace and handling of explosive or controlled materials.

I understand that the Huntsville Area Rocketry Association will oversee the contest launch, and I will abide by all club rules at the launch. I acknowledge that the Notre Dame rocket will be subject to range safety inspections before flight, and I will comply with the determination of the safety inspection. The Range Safety Officer has the final say on all rocket safety issues, and failure to comply with safety requirements will prohibit the team from launching its rocket.

I agree to abide by all procedures outlined by the Safety Officer of the Notre Dame Rocket Team, Team Leader, and Team Advisor when working on the NASA Student Launch project. I will use laboratory equipment and tools only when properly trained or under appropriate supervision. I will follow all Material Safety Data Sheets for materials used in design, construction, launch, and conclusion of the project.

I understand that failure to comply with anything in this safety agreement can result in my removal from the Notre Dame Rocketry Team.

_____

(Team Member Name Printed)

_____

(Team Member Signature) (Date)

Appendix B: Performance Prediction Model

```
import math

def apogee(m_r, m_e, m_p, p, Cd_t, Cd_c, A, T, g, t):
    """
    m_r   : rocket mass [M]
    m_e   : engine mass [M]
    m_p   : propellant mass [M]
    p     : air density [M/L^3]
    Cd_t  : drag coefficient during thrust phase
    Cd_c : drag coefficient during first coasting phase
    A     : rocket cross sectional area [L^2]
    T     : thrust [F]
    g     : acceleration due to gravity [L/T^2]
    t     : burnout motor time [T]
    """
    # Cd_air_break = *to be measured in wind tunnel*

    k_t = .5 * p * Cd_t * A #aerodynamic drag coefficient [M/L] (thrust phase)
    k_r = .5 * p * Cd_r * A #aerodynamic drag coefficient [M/L] (roll phase)
    k_c = .5 * p * Cd_c * A #aerodynamic drag coefficient [M/L] (coast 1 phase)

    # thrust
    m_a = m_r + m_e - m_p/2 #average mass [M]
    q1 = math.sqrt((T - m_a*g) / k_t) #burnout velocity coefficient [L/T]
    x1 = (2 * k_t * q1) / m_a #burnout velocity decay coefficient [1/T]
    v1 = q1 * ((1-math.exp(-x1*t)/(1+math.exp(-x1*t)))) #burnout velocity [L/T]
    y1 = (-m_a/(2*k_t)) * math.log((T-m_a*g-k_t*v1**2)/(T-m_a*g)) #altitude burnout [L]

    # air break
    m_c = m_r + m_e - m_p #coasting mass [M]
    qr = math.sqrt((T - m_c*g) / k_r) #burnout velocity coefficient [L/T]
```

```
xr = (2 * k_r * q1) / m_c # burnout velocity decay coefficient [1/T]
vr = q1 * ((1-math.exp(-x1*t)/(1+math.exp(-x1*t)))) #burnout velocity [L/T]
yr = (-m_c/(2*k_r)) * math.log((T-m_c*g-k_r*v1**2)/(T-m_c*g)) #altitude burnout [L]
#print(yr000.)

# coast
qc = math.sqrt((T - m_c*g) / k_c) #burnout velocity coefficient [L/T]
xc = (2 * k_c * q1) / m_c #burnout velocity decay coefficient [1/T]
vc = q1 * ((1-math.exp(-x1*t)/(1+math.exp(-x1*t)))) #burnout velocity [L/T]
yc = (-m_c/(2*k_c)) * math.log((T-m_c*g-k_c*v1**2)/(T-m_c*g)) #altitude burnout [L]
```

Appendix C: Vehicle Design Drawings

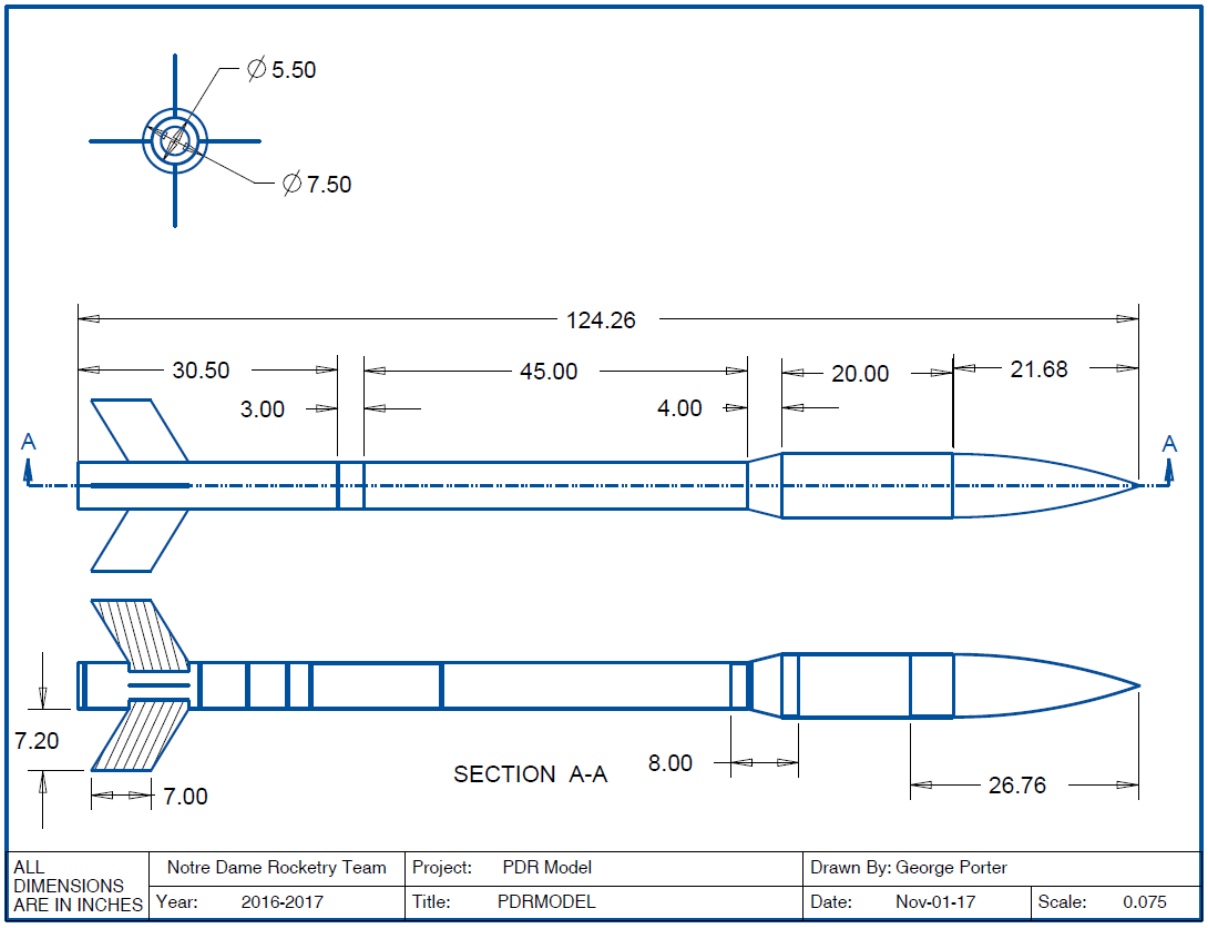

Balloon Number	Component
1	Bulkhead
2	Fin Can
3	ABP Coupler
4	Recovery Body Tube
5	Transition Section
6	Rover Body Tube
7	Nose Cone

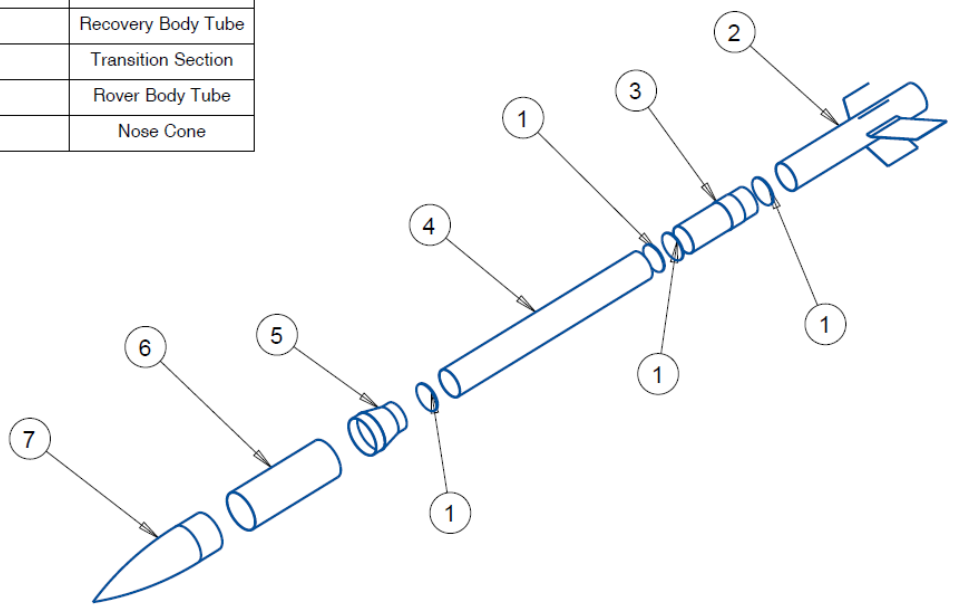

	Notre Dame Rocketry Team	Project: PDR Model	Drawn By: George Porter	
	Year: 2017-2018	Title: PDRMODEL	Date: Nov-01-17	Scale: 0.050

Appendix D: Launch Procedure Checklists

Prior to Departure for Launch Site: Vehicle Sub-team

- ❑ Personnel Safety Concerns
- ❑ Items to bring
- ❑ Safety goggles
- ❑ Gloves
- ❑ Ensure lids to epoxy bottles are appropriately
- ❑ Vehicle components
- ❑ Items to bring
- ❑ Nose cone
- ❑ Recovery body tube
- ❑ Fin can
- ❑ Communications coupler
- ❑ Shear pins
- ❑ Extra washers
- ❑ Extra nuts
- ❑ Extra screws
- ❑ Extra epoxy
    - ❑ Inspect the body tubes and couplers to ensure they have not been damaged during storage.
- ❑ Structural Integrity
- ❑ Ensure the items are stored in such manner as to not cause physical damage.
    - ❑ Ensure the fin can is stored on the rocket holder so as not to damage the fins during transportation.

Subteam Member: _____ Date: _____
Signature: _____
Team Lead: _____ Date: _____
Signature: _____

Prior to Launch: Vehicles Sub-team

❏ Personnel Safety Concerns
❏ Ensure everyone operating on the vehicle has proper safety equipment
❏ Safety goggles
❏ Prepare the vehicle for launch
❏ Insert payloads into the top-most body tube
❏ Insert nose cone into the top-most body tube
❏ Ensure that the screws on the nose cone are not loose
❏ Friction fit the nose cone with masking tape or scotch tape if necessary
❏ Ensure CRAM core is inside the CRAM body
❏ Process performed by the Recovery Sub-team
❏ Ensure the CRAM can be armed directly from the rocket's rail position
❏ Attach rocket sections
❏ Check that all interfaces are aligned correctly
❏ Insert shear pins to secure each section
❏ Ensure the screws are tight
❏ Perform Cg test to ensure the center of gravity matches the simulated center of gravity.
❏ Ballast as necessary to keep the stability margin.
❏ Prepare and insert the motor (Process performed by Team Mentor Dave Brunsting)
❏ Remove motor from packaging
❏ Check that motor is properly assembled according to manufacturer's instructions
❏ Remove pre-installed ejection charge
❏ Properly dispose of black powder
❏ Insert motor into casing
❏ Ensure two spacers precede motor
❏ Screw on rear closure
❏ Insert motor into rocket
❏ Attach motor retainer
❏ Check for secure fit
❏ Check rocket stability (at least 1-2 calibers) and final weight
❏ Register with LCO and RSO at launch site.
❏ Ignite motor right before launch (Process performed by Team Mentor Dave Brunsting)
❏ Remove igniter clips from igniter
❏ Remove igniter from rocket
❏ Ensure igniter has properly exposed ends which are split apart
❏ Insert igniter into motor
❏ Attach clips to igniter, ensuring good contact

Payload Member: _____ Date: _____
Signature: _____
Payload Member: _____ Date: _____
Signature: _____
Payload Member: _____ Date: _____
Signature: _____
Team Lead: _____ Date: _____
Signature: _____
Team Mentor: _____ Date: _____
Signature: _____

After Launch: Vehicle Sub-team

❏ Personnel Safety Concerns
❏ Instruct all personnel to get clearance before starting recovery process
❏ Assess there is no harmful physical damage before removal
❏ Ensure nothing is on fire
❏ Wait for at least 5 minutes before removing due to lingering motor heat
❏ Document state of rocket before removing
❏ Structural Integrity
❏ Check the physical state of the overall body tube
❏ Check the physical state of each payload
❏ Did the communication payload suffer damages to the electronic components
❏ Is the communication payload coupler structurally sound?
❏ Is the recovery body tube structurally sound?
❏ Ensure parachutes are re-usable

Subteam Member: _____ Date: _____
Signature: _____
Team Lead: _____ Date: _____
Signature: _____

Prior to Departure for Launch Site: Recovery

❏ Personnel Safety Concerns
❏ Items to bring
❏ Safety goggles
❏ Electronics
❏ Items to bring
❏ CRAM
❏ Main parachute
❏ Drogue Parachute
❏ Shock cords
❏ Shear pins
❏ Extra batteries
❏ Talcum powder
❏ Ensure the items are stored in safe boxes at a reasonable temperature.
❏ Ensure all applicable electronics are turned off.
❏ Structural Integrity
❏ Ensure the recovery body tube has not been damaged during storage.
❏ Ensure the holes in the recovery body tube are the appropriate size
❏ Ensure the recovery body tube is clear of electronics before storage.

Squad Member: _____ Date: _____
Signature: _____
Team Lead: _____ Date: _____
Signature: _____

Prior to Launch: Recovery

- ❑ Personnel Safety Concerns
- ❑ Ensure everyone operating on the payload has proper safety equipment
- ❑ Safety goggles
- ❑ Prepare CRAM
- ❑ Insert fresh batteries into CRAM core
    - ❑ Ensure batteries are connected to altimeters by listening for beeps from altimeters
- ❑ Insert CRAM core into CRAM body
- ❑ Put CRAM core cover on
- ❑ Tighten nuts down onto cover
- ❑ Insert long eyebolt through center of CRAM
- ❑ Place washer against both the bottom bulkhead and the CRAM cover
- ❑ Tighten nut against CRAM cover to hold bolt in place
- ❑ Connect the wires from CRAM core to screw terminals
- ❑ Attach short eyebolt to the long eyebolt with coupling nut
- ❑ Tighten nut on either side of coupling nut
- ❑ Electronics
- ❑ Prepare Avionics
- ❑ Mark the Primary Raven as official contest altimeter
- ❑ Ensure arming switch is “safe”
- ❑ Properly secure altimeters and batteries
- ❑ Install the CRAM until it locks
- ❑ Ensure the CRAM can be armed directly from the rocket’s rail position
- ❑ Structural Integrity
- ❑ Prepare ejection charges
- ❑ Ensure personnel are wearing safety glasses
- ❑ Move all non-essential personnel away from rocket
- ❑ Connect electric matches/ejection charges to altimeter
- ❑ Properly load and prepare parachutes
- ❑ Check that shroud lines are not tangled
- ❑ Apply talcum powder to each parachute
- ❑ Ensure that shock cord is not tangled
- ❑ Insert parachutes, chute protector, and shock cord into rocket
- ❑ Attach rocket sections
- ❑ Check that all interfaces are aligned correctly
- ❑ Insert shear pins to secure each section
- ❑ Ensure tight fit of all components
- ❑ Leave hatched door open
- ❑ Check shock cord for brittleness

❑ Replace shock cord that appears brittle

Squad Member: _____ Date: _____
Signature: _____
Team Lead: _____ Date: _____
Signature: _____

After Launch: Recovery

❏ Personnel Safety Concerns
❏ Instruct all personnel to get clearance before starting recovery process
❏ Assess there is no harmful physical damage before removal
❏ Ensure nothing is on fire
❏ Check that ejection charges have ignited
❏ Document state of rocket before removing
❏ Electronics
❏ Disarm altimeters
❏ Disconnect batteries
❏ Structural Integrity
❏ Check the physical state of the recovery body tube
❏ Is it re-usable?
❏ Check that components are safely inside the payload

Squad Member: _____ Date: _____
Signature: _____
Team Lead: _____ Date: _____
Signature: _____

Prior to Departure for Launch Site: Various Payloads

- ❑ Personnel Safety Concerns
- ❑ Items to bring:
- ❑ Safety Goggles
- ❑ Electronics
- ❑ Any Arduino connections must be soldered
- ❑ Any batteries must be unplugged to save power.
- ❑ Items to bring (as applicable):
- ❑ Soldering iron, with extra solder
- ❑ Spare batteries
- ❑ Electric tape
- ❑ Extra wire
- ❑ Wire crimpers
- ❑ Wireless Data Receiver
- ❑ GPS Receiver
- ❑ Ground Station
- ❑ Voltage Dividers
- ❑ Microcontroller
- ❑ Sensor Bay
- ❑ Transmitter
- ❑ Ensure the items are stored in safe boxes at a reasonable temperature.
- ❑ Ensure all applicable electronics are turned off.
- ❑ Structural Integrity
    - ❑ Perform visual inspection to make sure outer surface has not been damaged during storage.
- ❑ Shake the fin can to ensure the payload components do not wiggle when shaken

Squad Member: _____ Date: _____
Signature: _____
Team Lead: _____ Date: _____
Signature: _____

Prior to Launch: Various Payloads

- ❑ Personnel Safety Concerns
- ❑ Items to bring:
- ❑ Safety goggles
- ❑ Electronics (as applicable)
    - ❑ Before activating electronics, ensure that the time until launch does not exceed battery life.
- ❑ Ensure all connections are correctly soldered.
- ❑ Test all connections to verify there are no short circuits or faulty wiring.
- ❑ Turn on wireless data receiver
- ❑ Turn on GPS receiver
- ❑ Check that all wire connections are according to design
- ❑ Structural Integrity
    - ❑ Perform visual inspection to make sure outer surface has not been damaged during transportation.
- ❑ Ensure all connections are tight and secure.
- ❑ Double-check that the drogue bulkhead is secure.
- ❑ Tighten the nuts on the parachute eye bolt
- ❑ Ensure there are no loose wires or solder
- ❑ Ensure all payload hardware components properly secured to sleds
- ❑ Ensure that the main parachute eyebolt is tight and the screws do not unscrew
- ❑ Perform a shake test to ensure that payload materials do not shift

Squad Member: _____ Date: _____
Signature: _____
Team Lead: _____ Date: _____
Signature: _____

After Launch: Various Payloads

- ❏ Personnel Safety Concerns
- ❏ Instruct all personnel not let the fin can safely land before approaching.
    - ❏ Instruct all personnel not begin recovering the payload until given clearance by ground personnel.
- ❏ Ensure the fin can has adequately cooled before handling.
- ❏ Document the state in which the system is before any tampering
- ❏ Electronics
- ❏ Check that all electronics survived the flight intact.
- ❏ Structural Integrity
    - ❏ Perform visual inspection to make sure outer surface has not been damaged during flight.
- ❏ Assess any damages that may have occurred during operations.
    - ❏ Determine if the damages are severe enough to prevent additional launches. Repair any minor damages, where possible.
    - ❏ After recovery, re-perform component tests to ensure that operation has been uninhibited.

Squad Member: _____ Date: _____
Signature: _____
Team Lead: _____ Date: _____
Signature: _____

Appendix E: Personnel Hazard Analysis

Hazard	Cause	Effect(s)	Probability	Severity	Risk	Controls/Mitigations
Hand and power tools used in assembling systems	Improper use of tools due to lack of training; incorrect tool used for a job	Minor to severe injury to self and/or others	Remote	Critical	Moderate	Train all team members in proper tool use. Ensure the proximity of assistance in case of injury.
Flying sawdust chips or solder	Loose parts can fly some distance when using tools	Eye injury	Remote	Critical	Moderate	Ensure all team members working with power tools or soldering have eye protection.
Exposure to ammonium perchlorate	Handling rocket motor while ignited or hot from ignition	Risk of burn or fire	Remote	Critical	Moderate	Treat burns quickly and have fire safety equipment ready. Avoid handling motors.
Rocket launch ignition	Personnel being too close to rocket motor at ignition	Risk of burns	Improbable	Critical	Low	Ensure that personnel distance when launching rocket complies with NASA minimum distance table.
Exposure to lead	Ingesting solder	Lead poisoning	Improbable	Critical	Low	Wash hands after soldering. Avoid eating or drinking while soldering.
Exposure to detonated black powder charges or residue	Packing, handling, or cleaning black powder charges before or after launch	Risk of fire, burns, or irritation of respiratory system	Probable	Marginal	Moderate	Ensure proximity of fire safety equipment; ensure that eye and skin protection is used; wash exposed area thoroughly with water.
Exposure to fumes	Joining compo-nents with epoxy;	Nausea, light-headed-ness	Occasional	Marginal	Moderate	Ensure adequate ventilation and air flow when working with solder and epoxy.

	soldering; spray-painting					
Exposure to battery acid	Battery overheat-ing, event of crash	Potential chemical burns	Remote	Marginal	Low	Ensure batteries are properly maintained and operated, flush the affected area with either water or sodium bicarbonate solution depending on specific acid.
Soldering iron	Soldering irons reach very high temper-atures	First- or second-degree burns	Remote	Marginal	Low	Avoid contact with soldering iron. Tie back long hair.
Moving heavy objects	Transport-ing the ground station	Muscle strains; toe injury	Remote	Marginal	Low	Ensure the ground station is properly transported.
Exposure to epoxy hardener or resin	Using epoxy during assembly of rocket	Minor skin irritation	Frequent	Negligible	Low	Rinse area immediately with soap and water.
Electrical shock	Touching exposed wiring	Low level shock to person handling payload	Remote	Negligible	Minimal	Cover up exposed wires.

Appendix F: Failure Modes and Effects Analysis

Type	Failure Mode /Hazard	Cause	Effect	Probability	Severity	Risk	Controls/Mitigations
Payload 1: Deployable Rover	Solar Panel Malfunction: Solar Panels are adjusted to incorrect and insufficient position	Arduino/Control code error, calibration failure in servo motor and adjustment within the adjustment mechanism	Increases/decreased amount of solar power to recharge battery; fail to meet rechargeable battery requirements	Remote	Marginal	Moderate	Simulate and test control algorithm code, ground test solar panel adjustment mechanism
	Solar Panels breaking apart from rover body during flight and ground deployment	Excessive force applied on the sides of the rover during initial deployment or sustained pressure during flight	Uneven distribution of solar power on rover, loss of structural integrity, potential dead position into body of rover, loss of rover control	Remote	Critical	Moderate	Rover solar panels will be rigidly fixed to a desired orientation to provide more support and stability to the rover, solar panel deployment during ground testing
	Power Failure	Battery severely depleted during flight or on ground deployment due to temperature and pressure changes	Loss of controller function, no experimental data collected, underpowered servo motor	Remote	Critical	Moderate	Insure secondary batteries have sufficient charge to provide necessary power for the motor and sensors exceeding flight duration
	Nose cone ejection malfunction	Design lacks necessary robustness and stability to release it off rocket with gunpowder charge	Payload will not exit the vehicle and will remain there indefinitely	Remote	Critical	Moderate	Nose Cone will be flexible and durably sufficient to withstand outside forces during flight, nose cone will be ground tested before flight to ensure proper ejection

	Structural failure of polymers and aluminum metal during ground deployment	Design forcefully hits the ground at a very fast time response	Damage to payload, loss of data, failure of entire superstructure	Remote	Marginal	Moderate	Controller will be structurally and fully encased within the body of the rover, failure will not affect data, appropriate isolation from other payloads to be included in design
	Structural Failure of Tab	Improper calculations, higher-than-expected forces	Unbalanced drag system on rocket, possible tumble mid-flight	Remote	Catastrophic	Moderate	Run force calculations through multiple people, overcompensate strength of tabs.
ABP	Loss of Power	Dead Battery	Tabs lock in place, loss of control	Occasional	Critical	Moderate	Mark dead batteries during competition, don't turn on battery unnecessarily, keep batteries charged.
	Loss of Power Non-optimal flight adjustments	Faulty Wiring	Tabs lock in place, loss of control	Remote	Critical	Moderate	Use PCBs to decrease chance, double-check all solder points, make sure wiring diagram matches physical device.
		Weak control algorithm	Failure to meet precise height requirement	Frequent	Marginal	High	High volume of simulation and testing of code, physical ground tests, debugging.
	Non-optimal flight adjustments Jammed Tab System	Control algorithm with logic flaw	Tabs do not function as intended, possible mechanical failure from servo overextension	Occasional	Marginal	Moderate	High volume of simulation and testing of code, physical ground tests, debugging. Buy fast, strong servo, ensure actual speed matches expected speed.
		Servo cannot respond quick enough	Failure to meet precise height requirement	Remote	Marginal	Low	
		Unexpected physical friction /resistance	Failure to meet precise height requirement	Remote	Marginal	Low	Calculate expected values for speed, force, and other variables, record actual values from ground tests, compare and adjust accordingly.
		Fluid forces angle tabs, servo cannot contract tabs	Tabs lock in place, loss of control	Remote	Marginal	Low	Full mechanical analysis of physical tab system, obtain appropriate coefficient of friction.

	Structural Failure of Vertical Rail System	Experiencing too much acceleration coupled with weight of subsystems	Loss of rigidity of system components, possible inability of subsystems to function	Improbable	Marginal	Low	Ensure rails can bear maximum load of components, perform basic mechanical analysis

Appendix G: Environmental Effects on Rocket

Hazard	Cause	Effects	Probability	Severity	Risk	Mitigations
Bodies of Water	Launching near bodies of water	Landing in water can irrevocably damage electronics and the rocket can sink and become irretrievable	Remote	Catastrophic	Moderate	Being sure there are no bodies of water near the drift radius of the rocket
High Humidity	Launching in excessive humidity	The charges may become wet due to humidity and be unable to ignite	Improbable	Critical	Low	Motors and charges should be stored by certified personnel in a dry place
Lightning	Launching in a thunderstorm	Electrical shock to the rocket by lightning may ground the launch	Improbable	Catastrophic	Low	This will ground the launch; no rocket should be launched during a thunderstorm
Low Cloud Cover	Launching with low cloud cover	It can be difficult to keep track of the rocket and properly test rocket systems	Occasional	Critical	Moderate	Ow hanging clouds should be avoided during launch days, paying careful attention to the forecast
Low Temperature	Launching is extremely cold temperatures	Batteries can discharge at a faster rate and fiberglass parts can shrink.	Occasional	Critical	Moderate	Battery levels will be monitored by the ground station and battery life will be conserved by turning systems on at designated times

						and turning them off when not in use
Rain	Launching with risk of rain	Rain may damage electrical systems and ground the launch	Remote	Catastrophic	Moderate	This will ground the launch; rockets should not be launched in the rain
Trees	Launching near wooded areas	The rocket and parachute can be damaged if caught in a tree it may cause the rocket to be irretrievable	Occasional	Critical	Moderate	Ensuring that there are no trees near the drift radius of the rocket
UV Exposure	Rocket exposed to sun for long periods of time	This can weaken material adhesives if exposed for long durations of time	Improbable	Critical	Low	The rocket will not be exposed for a long period of time and extensive work on the rocket will be done indoors
High Winds	Launching in winds over 20mph	This can reduce altitude and send the rocket off course	Improbable	Catastrophic	Low	The launch will be grounded if the winds are too severe and there will be no obstructions in the estimate drift radius
Wildlife	Flying birds are large animals interfering with the launch	This can cause the rocket to be sent off course	Improbable	Catastrophic	Low	Ensuring the area is clear of wildlife

Appendix H: Safety Concerns for the Environment

Hazard	Cause	Effects	Probability	Severity	Risk	Mitigations
Battery Leakage	Improper disposal of damaged or used batteries	Contaminate groundwater	Remote	Critical	Moderate	Using proper battery disposal methods and ensuring batteries are not damaged
Carbon Emissions	Using cars to travel to launch sites	Damage the ozone layer with emissions	Occasional	Marginal	Low	Using carpooling as much as possible to minimize the amount of vehicles used
Epoxy Leakage	Improper use or disposal of epoxy resin in an uncontrolled environment	Contaminate drinking water, be ingested by wildlife, or pollute as solid waste	Improbable	Critical	Low	Using proper techniques in application to ensure the resin is properly dried and disposing of the resin in designated areas
Field Fire	Igniting rockets near dry grass and shrubs or motor CATO	Set the launch site or other nearby objects on fire	Remote	Critical	Moderate	Making sure that any field in use is not near any shrubs and using the proper launching pad to ensure the ignition doesn't affect the surrounding are

Harmful Gas Emissions	Motors emitting gases upon ignition into the environment	Pollute the atmosphere with harmful substances	Remote	Critical	Moderate	There will not be many launches done by the team so the emissions will not be to a concerning level
Harm to Wildlife	Launching a vehicle in a non-designated area around an animal's natural habitat	Destroy animal habitat and result in loss of food source, water source, or life	Improbable	Critical	Low	Ensuring that we only launch in predesignated areas that will have minimal effect on surrounding wildlife
Plastic/Wire Waste	Improperly disposing of the waste of stripping wires	If not properly disposed of, can cause solid waste or be ingested by an animal	Improbable	Critical	Low	Ensuring that any stripped wires have the waste properly collected and disposed of
Spray Paint Fumes	Spray painting the rocket	Can contaminate the water supply or atmosphere	Remote	Critical	Moderate	Painting the rocket in a painting booth that properly disposes of waste
Waste	Improper disposal or storage of rocket components	Can result in pollution of environment if improperly disposed or stored.	Improbable	Critical	Low	Correctly storing any piece of the rocket that is still waste and disposing off the rest in the proper fashion

Water/Ground Pollution	Leakage of motor chemicals into the ground and water	Pollute the water system with improper disposal	Improbable	Critical	Low	There will not be many launches done by the team so the pollution will not be to a concerning level

Appendix I: Project Risks

Likelihood - Rare, Unlikely, Even, Probable, Extremely Likely
Impact - Negligible, Low, Moderate, High, Critical

Risk	Likelihood	Impact	Mitigation
Time Possibility of falling behind schedule and/or missing deadlines	Probable	Low	All aspects of the project will be divided up among team members to reduce the chances of falling behind in work. Additionally, multiple team members will coordinate together to ensure that deadlines are met and to keep each other accountable.
Budget Failure to have enough funds to purchase rocket materials, cover transportation costs, and pay for other expenses	Rare	High	All material costs will be determined prior to construction. The team will determine how much material must be ordered in order to prevent overspending. Similarly, travel/transportation expenses will be planned out. Overall budget and spending plans will help ensure that this constraint is met.
Equipment and Facility Physical injury associated with on- and off-campus facilities and the material/equipment used to build and operate the rocket	Unlikely	High	Dangerous materials and equipment, including power tools, machinery, and rocket engines, will be used. Every team member will have proper knowledge and training before using laboratories, workshops, materials, and/or equipment. In addition, team members will use personal protective equipment when working with the rocket. The team safety officer, and subteam safety liaisons will communicate proper safety practices.

Personnel Potential issues involving team members leaving, which may impact time and budget	Unlikely	Negligible	In the case of someone leaving the team, their responsibilities will be spread among other members.
Payload Possibility of malfunctioning or inoperative payload(s)	Unlikely	High	The payload subteams will ensure that work is split among members and adequate time is spent on each step of payload design, construction, and testing. Payload functionality will be verified at the full-scale test launch.
Launch Launch errors and hazards, including defective launch component(s)	Unlikely	Critical	Prior to launch, the rocket will be thoroughly inspected, and all the launch checklists and procedures will be reviewed. Additionally, the team mentor, Dave Brunsting, will assist the team at every launch.
Recovery Failure of planned rocket recovery, which may result in physical injury or more likely, damage to the rocket and its components	Unlikely	High	The recovery subteam will ensure that the recovery system functions properly by thoroughly designing, constructing, and testing the system. On launch day, following the pre-launch procedures and checklists will reduce recovery system issues. Recovery system functionality will be verified at the full-scale test launch.
Resources Risk of lacking materials, equipment, and facilities to construct and operate the rocket	Rare	High	Each subteam will outline necessary materials, equipment, and facilities prior to construction. Budget and spending plans will also help ensure that all necessary materials are purchased/obtained.

Appendix J: General Requirement Verifications

Requirement	Requirement will be met by	Method of Verification
The launch vehicle will hit an apogee of 5280 ft.	- Choosing a motor that provides the launch vehicle with enough thrust to overcome its mass. - Constructing a launch vehicle that minimizes drag through a smooth surface	- The subscale test will verify the accuracy of the performance prediction software. - Full scale tests will verify predictions for the effect of the rover payload on the vehicle's apogee. - Wind tunnel tests will verify the accuracy of simulations for drag coefficients.
The launch vehicle shall carry one commercially available, barometric altimeter.	- Attaching the altimeter to the launch vehicle within the recovery system.	- The recovery sub-team lead will ensure that the recovery system of the launch vehicle includes a barometric altimeter.
The launch vehicle shall be recoverable and reusable.	- Ensuring the success of each sub-system through extensive testing that proves the system performs both individually and integrated - Designing the vehicle to launch safely more than once.	- The tests outlined Section XX will verify the performance of each subsystem individually. - Full scale tests will verify the performance of the vehicle as a whole; an evaluation of the vehicle following these tests will verify its ability to launch again successfully.
All recovery electronics shall be powered by	- Ensuring that the recovery system is designed to include	- Inspection will ensure that the vehicle includes the appropriate batteries.

commercially available batteries.	only commercially available batteries.	
The launch shall be limited to a single stage and four (4) independent sections	- Ensuring that the launch vehicle only requires one launch stage and that it includes the necessary amount of sections.	- Inspection will confirm that the launch vehicle is indeed a single stage launch vehicle. - The launch vehicle used during the full scale tests will be confirmed as having four (4) (or less) independent sections.
The launch vehicle shall be capable of being prepared for launch in 4 hours.	- Integrating all of the vehicle's subsystems in such a way that allows for assembly within the required time.	- During the full scale tests, the team will assemble the launch vehicle and have it prepared for launch within the proper time frame.
The launch vehicle shall be launched using a 12 V direct firing system.	- Ensuring that the vehicle design includes the required 12 V direct firing system.	- During the full scale tests, the team will use the required firing system to launch the vehicle.
The launch vehicle shall require no special ground equipment to initiate launch.	- Designing the launch vehicle to successfully launch without the aid of any special equipment.	- During the full scale tests, the team will launch the vehicle without utilizing any special equipment.
The launch vehicle shall use a commercially available motor.	- Choosing a motor in alignment with the NAR and TRA regulations. - Staying in contact with the team's mentor regarding any updates to motor choices as the vehicle design changes.	- During the full scale tests and on the day of the competition, the mentor of the team will handle all motors.
The minimum velocity off the rail shall not be below 52 ft/s.	- Selecting a motor with the right impulse to achieve the required velocity.	- Simulations using OpenRocket and RocketSim will verify that the vehicle

	- Meticulously calculating interruption angles for rail buttons to ensure that the launch vehicle's interaction with the launch pad is smooth and uninterrupted.	reaches the required minimum velocity. - Full scale tests will in turn verify the accuracy of the above simulations and confirm the velocity.
The team shall launch and recover a subscale.	- The team will construct and launch a subscale, the specifications and materials of which are outlined in Section XX and Section XX, respectively.	- The subscale test will verify the success of the subscale launch.
The launch vehicle shall have a static stability of at least 2.0 at rail exit.	- Placing the Air Braking System slightly above the center of pressure so that the deployment of tabs in flight does not cause over-stability when deployed - Ensuring that necessary ballasts are spread across the launch vehicle so as not to affect the stability margin	- The changes in the center of gravity and center of pressure over the course of the vehicle's flight will be determined using OpenRocket and RockSim simulations. - The subscale test and full scale tests will verify the accuracy of the simulations and ensure that the vehicle achieves the proper stability margin.
The launch vehicle shall have a sufficient thrust-to-weight ratio to achieve required apogee.	- Choosing a motor that provides the proper amount of thrust to overcome the weight of the launch vehicle.	- OpenRocket and RockSim simulations will verify the thrust-to-weight ratio provided by the motor choice. - Full Scale Tests will verify the accuracy of these simulations in reaching the required apogee.

The launch vehicle shall contain a remotely activated rover which will autonomously travel five ft and deploy a set of foldable solar panels.	- Designing, constructing, and deploying the Rover Payload system, the specifications of which are included in Section XXXX	- The subscale test and full scale tests will verify the ability of the Rover Payload system to deploy successfully.
Payload affecting flight shall be verified before launch at competitions	- Confirming the effect of Air Braking System's tabs on flight path compared to lack thereof - Confirming the structural strength of Payload Integration - Confirming the efficacy of Payload in a practical sense	- Subscale Flight - FEM Analysis and Load analysis - Full Scale Flights
Launch Vehicle performance shall be verified by wind tunnel testing	- By relating Reynolds number for fluid scaling and relating Reynolds number to the coefficient of drag of both subscale and full-scale	- The acquired coefficient of drag from wind tunnel testing shall be compared against all the performance predictions software and programs as well as subscale test results.
Launch Vehicle's subsystems shall have finished the design phase; Subscale will have been launched by CDR	- Ensuring each subsystem fits in with the overall system and can be edited at short notice. - Designing and launching a subscale that will verify the accuracy of our software prediction for confidence.	- *In Process:* Subsystems independent of payloads almost complete; subsystems dependent on payload such as Deployable Rover Integration advancing - Altimeter on subscale shall contain the data needed to verify its efficiency.

Appendix K: Vehicle Design Requirement Verifications

TBC – To be completed

Requirement	Verification Method	Status
Airframe Strength and Structural Stability	- Conduct finite element analysis. FEM Analysis in ANSYS through Notre Dame's Center for Research Computing (CRC) - Inspect airframe after full-scale test to identify any damage. Inspection after full-scale test launch	- Ongoing, TBC Nov 2017 - TBC Feb/Mar 2018
Accuracy of Center of Mass Calculations	- Estimations of individual masses and center of mass location using Openrocket and RockSim simulations - Measurement of individual masses and center of mass by weighing each component with scale and balance assembled rocket at center of mass	- Complete, updated constantly with changes to rocket - Construction TBC Jan/Feb 2018 and during test launch in Feb/Mar 2018
Effectiveness of Air Braking Payload	- Drag estimation using computational fluid dynamics analysis in ANSYS Fluent through Notre Dame's Center for Research Computing - Subscale wind tunnel testing force measurements at different wind speeds using a force balance - Full scale testing measurements. Comparison between altitude data with payload deactivated and activated	- Ongoing, TBC Nov 2017 - Ongoing, Nov 2017 - TBC Feb/Mar 2018
Aerodynamic effect of variable diameter rocket geometry	- Computational fluid dynamics simulation to ensure no boundary layer separation or shock over the length of the rocket.	- Preliminary modeling in Sep 2017, comprehensive modeling ongoing, TBC Nov 2017

	Analysis in ANSYS Fluent through Notre Dame's Center for Research Computing - Subscale wind tunnel testing to verify computer simulations. Force measurements taken at different wind speeds to ensure no significant increases in drag due to these effects.	- Ongoing, TBC Nov 2017
Fin Strength and Alignment	- Creating finite element models and analyzing potential loads in ADINA. - Analyzing fins prior and after each launch for damage. - Ensuring proper alignment during construction with laser cut fin alignment mechanism. Visual inspection and angle verification with protractor.	- TBC Nov 2017 - TBC Feb/Mar 2018 - TBC Jan /Feb 2018
Air Braking System Integration	- Ensuring the payload tabs do not endanger the structural integrity of the launch vehicle. Verified in Full Scale Test.	- TBC Feb/Mar 2018
Deployable Payload Integration	- Ensuring rail system for rover is secured to body tube, and that the rover is secured to the rail system. Verified with shake tests.	- TBC Jan/Feb 2018
Recovery Integration	- Shear pins shear as predicted. Verified during black powder charge tests. - Ensuring that the bulkheads and eye-bolts supporting the system are robust. Verified by both shake tests and inspection of system after Full Scale Test.	- TBC Feb/Mar 2018 - TBC Feb/Mar 2018
Motor Integration and Retention	- Verifying the sizes of purchased material prior to construction. Inspection and measurements using calipers and rulers.	- TBC Dec 2017/Jan 2018 - TBC Nov 2017

	- Performing load analysis on chosen system using FEM analysis in ADINA. - Launching full scale rocket with the chosen motor. Inspection of motor retention after full scale test flight.	- TBC Feb/Mar 2018
Motor Performance	- Simulations using RockSim and OpenRocket to predict apogee of rocket with chosen motor - Full scale flight to measure apogee of rocket with chosen motor. Gather and analyze altimeter data of full scale test flight.	- Complete Oct 2017, updated constantly with changes to rocket or motor - TBC Feb/Mar 2018
Ballast will not move throughout flight.	- Proper retention of ballast within ballast container, and proper retention container in the body tube. Verified through shake tests of ballast container with ballast loaded and body tube with container loaded. - Full scale flight to ensure that ballast and ballast container does not puncture or move during flight. Inspection after full scale test flight.	- TBC Feb 2018 - TBC Feb/Mar 2018

Appendix L: Recovery System Requirement Verifications

Requirement:	Verification method	Status
Staged recovery deployment: drogue at apogee, main at a lower altitude	- The recovery system will contain a drogue parachute and main parachute, which will be deployed at apogee and 600 AGL respectively	- Complete
Ground ejection tests performed before full-scale launches	- Black powder will be prepared and then ignited remotely while shear pins secure the body tubes to test the amount/number combination	- Pending further system development
Independent sections of launch vehicle with less than 75 ft-lbf kinetic energy	- The rocket will descend at 12.57 ft/s, limiting the KE of the heaviest section (the fin can) to 57.41 ft-lbf	- Complete
Recovery system circuits independent of any others	- No wires will or transmitters will connect the recovery circuitry to that of any other part of the rocket	- Complete
Recovery electronics powered by commercially available batteries	- The recovery electronics will be be powered by three independent 9V Duracell batteries	- Complete
Recovery system contains redundant, commercially available altimeters	- The recovery system will contain *triple* redundant commercial Featherweight brand *Raven3* altimeters	- Complete
Removable shear pins used for main and drogue	- Four-five shear pins at each junction will secure the launch vehicle sections until they are separated by the recovery ejection charges	- Pending further system development
Recovery area limited to 2550 ft radius	- The parachute sizes and deployment altitudes will be selected to limit wind drift to within the given radius, as confirmed by multiple simulations	- Complete
Recovery system electronics not affected by other on-board electronic devices	- The recovery system electronics will be shielded from outside interference by a protective layer of copper tape	- Pending further system development

Appendix M: Deployable Rover Requirement Verifications

Requirements	Verification Method(s)	Status
Rover: House deployable solar panels, exit rocket fuselage, and travel specified distance	- Inspection and demonstration through ground testing and full scale flight test	- TBC Feb/Mar 2018
Solar Panels System: Deploy solar panels and generate power	- Demonstration and analysis through ground testing	- TBC Jan 2018
Internal Vibration Limitation System: Lock rover in place within the fuselage during flight	- Demonstration through ground testing and full scale test flight	- TBC Feb/Mar 2018
Deployment System: Enable rover to exit the rocket fuselage	- Demonstration through ground testing and full scale test flight	- TBC Feb/Mar 2018
Electronic Control System: Initiate payload deployment and communicate between payload components	- Demonstration through ground testing and full scale test flight	- TBC Feb/Mar 2018
Rover Algorithm: Track rover displacement and provide object avoidance	- Demonstration through ground testing and full scale test flight	- TBC Feb/Mar 2018
Power Control System: Provide power to components of the payload that require it	- Inspection and ground testing	- TBC Jan 2018

Sensors: Record and store data	- Test and analysis through ground testing and full scale flight test	- TBC Feb/Mar 2018

Appendix N: Air Braking System Requirement Verifications

Requirement	Verification Method	Status
The drag tabs have enough area to induce the required amount of drag to reach 5280 ft	- Wind Tunnel Testing - ANSYS Fluent Simulation - Full-Scale Flight Test	- In Progress - In Progress - TBC Feb 2018
The drag tabs are strong enough to withstand the forces they will experience	- FEM Analysis - Full-Scale Flight Test	- In Progress - TBC Feb 2018
The mechanism is powerful and fast enough to provide a quick tab extension	- Mechanical Analysis - Ground Test - Full-Scale Flight Test	- Complete - TBC Feb 2018 - TBC Feb 2018
The control code is fast and accurate enough to process the data and calculate the necessary tab extension	- Preliminary Simulation - Ground Test - Full-Scale Flight Test	- Complete - TBC Feb 2018 - TBC Feb 2018
The tabs will not be extended during motor burn and during descent	- Ground Test - Full-Scale Flight Test	- TBC Feb 2018 - TBC Feb 2018
The extension of the tabs will not induce any additional moments or create instabilities in the rocket	- OpenRocket Simulation - Full-Scale Flight Test	- In Progress, TBC Nov 2018 - TBC Feb 2018

Appendix O: Budget Breakdown

Vehicle Design Line Item Budget				
	Material	**Quantity**	**Price per Unit**	**Total Cost**
Subscale	Polypropylene Nose Cone	1	$20.74	$20.74
	Phenolic Body Tube	4	Previously Bought	$0.00
	Bulkheads, Centering Rings, Fins (cut from same material)	1	$13.29	$13.29
	Couplers, Motor Mount	1	$8.38	$8.38
	Transition Section Material	1	$8.11	$8.11
	Motor	2	$27.99	$55.98
	Screws	3	$5.00	$15.00
	Motor Retainer	1	$24.61	$24.61
	Subtotal			**$146.11**
Full Scale	Carbon Fiber Body Tube	10 ft	$97.79	$977.90
	Carbon Fiber Motor Mount	21 in	$133.58	$133.58
	Carbon Fiber Plates, 0.127”	1	$550.39	$550.39
	Carbon Fiber Couplers	1	$100.00	$100.00

	Fiberglass Transition Section	1	$150.00	$150.00
	Fiberglass Body Tube	4 ft	$100.00	$400.00
	Fiberglass Plates	2	$28.99	$57.98
	Motors	4	$190.00	$760.00
	Quick Links	6	$1.50	$9.00
	Eye bolts	4	$1.50	$6.00
	Motor Retention	1	$45.00	$45.00
	Nose Cone	1	$45.00	$45.00
	Flat Head Wood Screws	10	$1.00	$10.00
	Hex Nuts and Bolts	10	$0.50	$5.00
	Subtotal			**$3249.85**
Multipurpose Material	JB Weld	1	$10.00	$10.00
	RocketPoxy	6	$12.00	$72.00
	15 Minute Mid Cure Epoxy	6	$13.00	$78.00
	30 Minute Slow Cure Epoxy	6	$13.00	$78.00
	Subtotal			**$238.00**
	TOTAL			**$3633.96**

Recovery System Line Item Budget			
Material	**Quantity**	**Price per Unit**	**Total Cost**
Main parachute	1	$620	$620
Nomex (tubular)	2	$15	$30
Nomex (square)	4	$3.75	$15
PVC	1	$5	$5
Acrylic	1	$15	$15
Copper plating	1	$12	$12
Altimeter	1	$155	$155
Shock cords	1	$70	$70
9V battery boxes	3	$3	$9
9V batteries	3	$6	$18
Wire	1	$6	$6
Wire connectors	20	$1	$20
TOTAL			**$975**

Deployable Rover Line Item Budget			
Material	**Quantity**	**Price per Unit**	**Total Cost**
Aluminum Block	1	$60	$60
Microcontroller	1	$10	$10
Altimeter	1	$5	$5
Gyroscope	1	$7	$7
Lidar	1	$150	$150

Batteries	2	$30	$60
PCB Boards	6	$13.33	$80
Wheels	4	$8	$32
Solar Panels	12	$5.75	$69
Wheel Hardware	1	$100	$100
Servomotor	1	$40	$40
Brushless Motors	4	$30	$120
Ejection System	1	$50	$50
Miscellaneous	1	$200	$200
TOTAL			**$983**

Air Braking System Line Item Budget			
Material	**Quantity**	**Price per Unit**	**Total Cost**
Air braking Tab Material (Aluminum)	1	$27.53	$27.53
Servo Motor	2	$60.00	$120.00
Accelerometer	1	$24.95	$24.95
Barometer	1	$9.95	$9.95
PCB	3	$5/in^2	$93.75
Circuit Components	1	$170.00	$170.00
Microcontroller	1	$24.95	$24.95
Batteries	2	$15.95	$31.90
Mechanism components	1	$150.00	$150.00
Integration components	1	$19.66	$19.66

TOTAL			**$672.69**

Educational Outreach Line Item Budget			
Material	**Quantity**	**Price per Unit**	**Total Cost**
Scissors	3 (2 pairs each)	$5.99	$17.97
Tape Rolls	10	$1.00	$10.00
Colored Pencils	3 packs	$2.77	$8.31
Estes Wizard Rocket Bulk Pack	1 (12 rockets each)	$76.29	$76.29
Estes Motors	4 (3 engines each)	$10.29	$41.16
Super Glue	2 (3 each)	$2.49	$4.98
Poster Board	2	$0.97	$1.94
Wiffle Balls	1 (6 ball pack)	$4.49	$4.49
Embroidery Floss	1	$0.52	$0.52
Felt Squares	1 (12 pack)	$2.47	$2.47
TOTAL			**$168.13**

Appendix P: Timeline